The Institute of Paper Science and Technology

Atlanta, Georgia

Doctor's Dissertation

Selectivity of Iron-Based Catalysts in a Polymeric Model System for Biomimetic Bleaching

Colleen C. Walker

September 1994

SELECTIVITY OF IRON-BASED CATALYSTS IN A POLYMERIC MODEL SYSTEM FOR BIOMIMETIC BLEACHING

A Dissertation Submitted by

Colleen C. Walker

B. S. 1987, University of Delaware

M. S. 1989, Lawrence University

in partial fulfillment of the requirements
from the Institute of Paper Science and Technology
for the degree of Doctor of Philosophy
Atlanta, Georgia

September 1994

TABLE OF CONTENTS

LIST OF FIGURES

LIST OF TABLES

ABSTRACT

Discovery and characterization of fungal enzymes capable of degrading lignin have suggested the study of simpler compounds to mimic these enzymes. Use of these so-called biomimetic compounds has been extended to applications in bleaching wood pulp. Attempts to bleach pulp with biomimetic compounds have so far failed to demonstrate that these compounds are selective catalysts for pulp delignification.

To be feasible as bleaching agents, such compounds must be selective, i.e. demonstrate high reactivity toward lignin without severely damaging carbohydrates. The goal of this thesis was to evaluate the selectivity of three biomimetic systems. The systems investigated were ferrous sulfate, ferrous ion chelated with ethylenediaminetetraacetic acid (EDTA), and hemoglobin, all in the presence of hydrogen peroxide. A polymeric, homogeneous model system has been used to represent wood pulp. Lignosulfonate and hydroxyethyl cellulose (HEC) were chosen as water-soluble, polymeric models for lignin and carbohydrate. Molecular weight changes of these substrates were measured by High Performance Size-Exclusion Chromatography (HPSEC) and viscometry, respectively.

When these substrates were individually exposed to each biomimetic compound in the presence of hydrogen peroxide, substantial degradation of both lignin and carbohydrate model compounds was observed. Rates of lignosulfonate and HEC degradation were separately determined and compared for each biomimetic catalyst. Hemoglobin was found to be the most selective for lignosulfonate degradation over HEC degradation. In addition, hemoglobin was found to be the most effective for catalyzing the oxidation of lignosulfonate versus decomposition of hydrogen peroxide to oxygen.

During these reactions the production of hydroxyl radicals was measured using a chemiluminescence assay. Although hemoglobin interfered with this assay, results from the

ferrous sulfate and chelated ferrous catalyzed reactions were obtained. Rates of hydroxyl radical production in the ferrous system were directly related to bond cleavage of lignosulfonate.

When lignosulfonate and HEC were simultaneous exposed to hydrogen peroxide and these catalysts, a high molecular weight product was formed. This product is the result of condensation reactions between the lignin and cellulose models. Its formation is significant as it represents a counterproductive process that may be responsible for the limited effectiveness of biomimetic delignification systems.

INTRODUCTION

Government regulations and increased environmental awareness have provided a strong impetus for the pulp and paper industry to replace chlorine-containing chemicals used to produce fully bleached wood pulp. Delignification with oxygen-containing agents, such as oxygen, hydrogen peroxide, and ozone has necessarily become a more attractive bleaching technology. Biotechnological applications are also receiving increased attention as viable adjuncts to traditional chlorine bleaching.[1,2,3,4,5,6]

The isolation and subsequent characterization of enzymes which are capable of degrading wood components have greatly advanced technologies for enzymatic delignification and bleaching. Key areas of interest have been pulp bleaching with enzymes which degrade lignin (ligninolytic enzymes) or hemicelluloses, xylan in particular.[4,7]

Pulp bleaching with ligninolytic enzymes has not been very successful. This has been attributed to substrate inaccessibility: others argue that the correct lignin-degrading enzymes have not been identified. Biomimetics, the use of synthetic compounds to mimic biological functions, may be more promising. Enzymes perform only specific functions and are often large molecules. Biomimetic compounds can be designed to be smaller, more stable and perform specific functions.

Lignin peroxidase, originally isolated from the white-rot fungus Phanerochaete chrysosporium, is a lignin-degrading enzyme which has been widely studied.[8,9] This enzyme possesses an iron porphyrin group as cofactor. In addition, lignin peroxidase is dependent on hydrogen peroxide for activity. Researchers have used various iron complexes to mimic the action of lignin peroxidase, both to obtain a better understanding of the enzymatic mechanisms involved in lignin biodegradation, and to investigate their potential as bleaching agents.[10,11,12,13]

For biomimetic bleaching systems to be considered as a feasible alternative to chlorine bleaching, they must demonstrate a selectivity which favors lignin degradation over that of carbohydrate. The selectivity of biomimetic systems has not been fully evaluated. In addition, many of the compounds used in these studies are known to generate hydroxyl radicals in solution (in the presence of an oxidant, typically hydrogen peroxide). The hydroxyl radical is highly reactive and not known to be a selective oxidant. If, however, these catalysts can be used to direct the unspecific hydroxyl radicals towards lignin, their utility as bleaching agents would be great.

This dissertation presents the results of an evaluation of three biomimetic compounds for their selectivity for lignin degradation relative to that of carbohydrate. The degradation of a lignin and a carbohydrate model compound were compared. Hydroxyl radicals produced during these reactions were measured using a chemiluminescence assay, and their role in selectivity discussed.

When the lignin and carbohydrate polymeric models were combined in reaction solutions, a high molecular weight condensation product formed. This product is believed to limit the effectiveness of delignification using biomimetic systems. It is likely that this condensation product forms during other acid oxidative bleaching stages, i.e., ozone, and its role in these processes should be investigated.

LITERATURE REVIEW

This section contains a review of the literature pertinent to this work. First, a detailed discussion of the enzymatic degradation of lignin is presented, describing the major enzymes and mechanisms involved. Degradation of lignin model compounds, wood, and pulp by lignin-degrading enzymes are also discussed. Next, the ability of biomimetic compounds to degrade lignin model compounds and pulp is reviewed. Then the chemistry of acidic hydrogen peroxide delignification of pulp is presented, with particular emphasis on the chemistry of peroxide decomposition in the presence of iron.

ENZYMATIC DEGRADATION OF LIGNIN

The natural decay of wood and lignin by a variety of fungi has been extensively studied.[8,9,14] Under the appropriate environmental conditions, white-rot fungi will completely degrade all of the structural components of wood, producing carbon dioxide, humic substances and water.[14] The mechanism by which fungi degrade lignin has been an area of active research.[8,9,14] Phanerochaete chrysosporium has been the most widely studied of the white-rot fungi; hence, enzymes discussed in the following section will be for the most part those isolated from Phanerochaete chrysosporium cultures.

Ligninolytic Enzymes

Phanerochaete chrysosporium is a white-rot fungus which preferentially degrades lignin. When starved of nitrogen, Phanerochaete chrysosporium exhibits high ligninolytic activity.[8,9] In 1983, two independent laboratories announced the discovery of an extracellular enzyme from the white-rot fungus Phanerochaete chrysosporium [15,16] This enzyme was called ligninase for its ability to degrade lignin. Since that time much work has been done to elucidate the role of ligninase (or more appropriately, lignin peroxidase) in the enzymatic degradation of lignin.

The isolated enzyme was found to be dependent on hydrogen peroxide for activity, and it catalytically contributed to degradation of various lignin-like compounds. Recent studies have confirmed that there are about ten different isomers of lignin peroxidase.[17] Four exhibit an additional dependence on manganese,[17] and are, therefore, referred to as manganese-dependent peroxidases.

In an effort to establish a system of nomenclature for these enzymes, Farrell and coworkers[17] have proposed to refer to lignin peroxidase as LiP and manganese-dependent peroxidases as MnP. The most abundantly-produced isozyme under nitrogen-limited conditions has an isoelectric point (pI) of 3.5. (The isoelectric point is the pH at which the charge on the protein is zero.[18]) This isozyme is referred to as LiP1 (previously called H8). The second most abundant isozyme (pI = 4.4, or H2) is referred to as LiP2. As LiP1 is most commonly isolated and used in experiments, LiP will be used to indicate LiP1 throughout this document. Similarly, MnP will be used to refer to the main isozyme of manganese peroxidase.

A review of the literature suggests that LiP and MnP are not the only enzymes involved in the enzymatic degradation of the lignin polymer. Other enzymes believed to participate in this process are briefly discussed.

Lignin Peroxidase

It has been determined that LiP contains a heme structure, an iron protoporphyrin IX (Figure 1), as a prosthetic group. LiP has a molecular mass of about 42,000 - 43,000 daltons and a carbohydrate content averaging about 15 - 21%.[19] LiP has been crystallized and yields an orthorhombic, brown crystal with four LiP molecules per unit cell.[20]

A catalytic cycle for LiP has been identified from spectral characterization of LiP and its oxidized forms.[21] Figure 2 diagrams the role of the organic substrate, enzyme, and hydrogen peroxide in a single catalytic cycle of the enzyme. This schematic shows how the enzyme is first oxidized by the hydrogen peroxide and then reduced by organic substrates. The

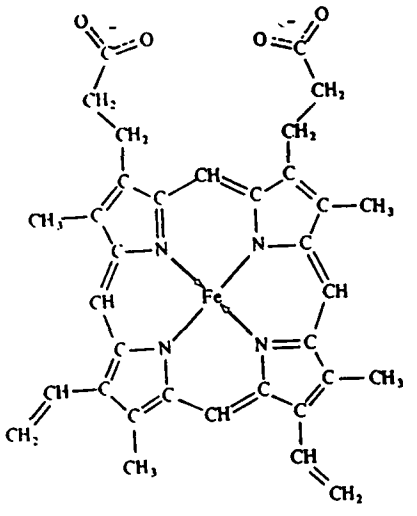

Figure 1. Heme structure showing iron protoporphyrin IX.

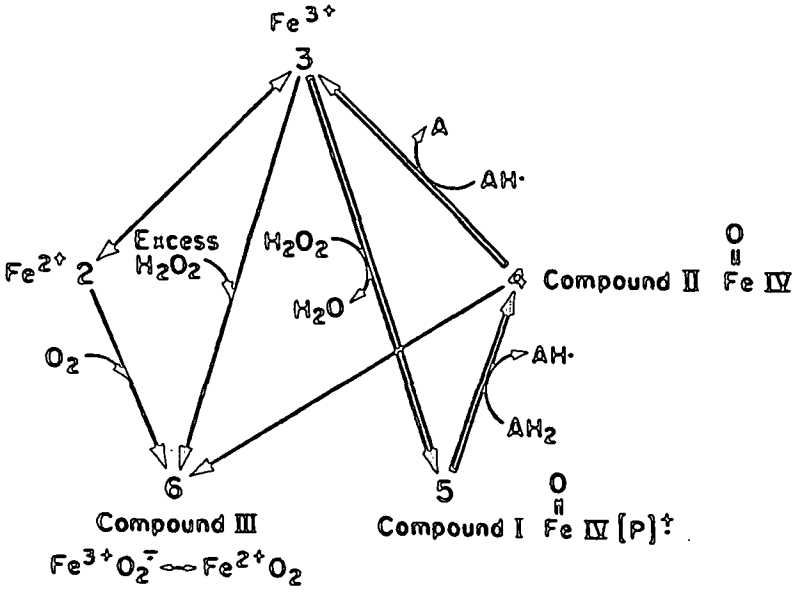

Figure 2. Catalytic cycle of lignin peroxidase (taken from Ref. 20).

reduction of LiP by the organic substrate causes a radical cation to form within the organic substrate.

Manganese Peroxidase

MnP has also been isolated and characterized.[22,23,24] MnP has a molecular mass averaging 45,000 - 47,000 daltons with a carbohydrate content of about 17%.[23] It is believed that

MnP is localized on the mycelium in fungal cultures.[23] This was discovered by examining extracellular media from cultures of Phanerochaete chrysosporium for MnP activity. Little activity was present in the culture media, but increased activity was observed when the mycelium was extracted with 0.5 M NaCl to recover the enzyme.

The unique feature of MnP is its dependence on manganese for activity. The catalytic cycle of MnP is shown in Figure 3, and is adapted from Gold, et al.[25] Oxidation of the native enzyme by hydrogen peroxide produces MnP Compound I. Subsequent oxidation achieved via electron abstraction from MnP Compound I produces MnP Compound II. MnP Compound II is then reduced to the native enzyme as Mn(II) is oxidized to Mn(III). This final reduction of MnP Compound II to the native enzyme is only effectively carried out when Mn(II) is the substrate. MnP Compound II can be reduced to the native enzyme MnP by organic substrates, but the reaction rate is very slow.

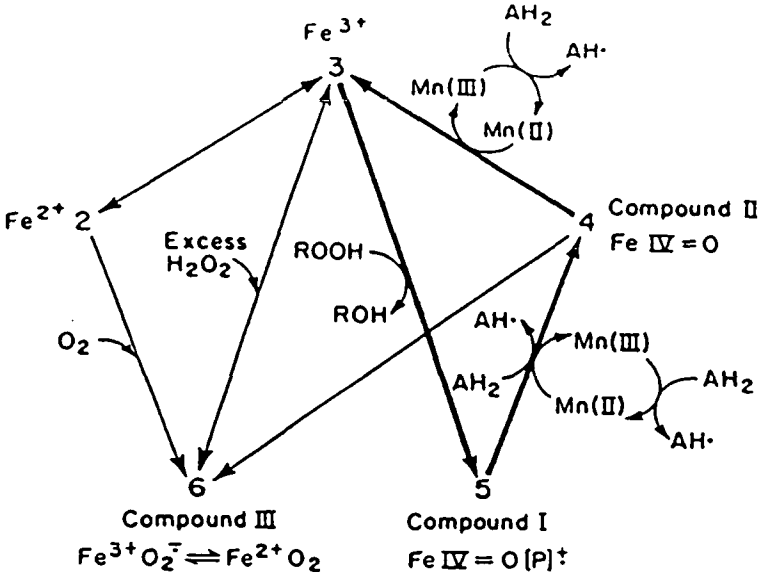

Figure 3. Catalytic cycle of Mn-peroxidase (taken from Ref. 24).

Laccases and Other Lignin-Degrading Enzymes

LiP and MnP are phenoloxidases, enzymes which catalyze the removal of one electron from phenolic hydroxyl groups. Laccase, also a phenoloxidase, has been isolated in ligninolytic cultures of several white-rot fungi.[8] Several different types of laccases have been isolated, usually containing 4 copper atoms per enzyme molecule, with average molecular weights ranging from 62,000 to 210,000 daltons.[26]

Little laccase is produced by Phanerochaete chrysosporium as compared to lignin and manganese-dependent peroxidases; therefore, the importance of laccase in the enzymatic degradation of lignin was originally questioned.[8] It has been reported that a laccase, isolated from Coriolus versicolor (a white-rot fungi), is able to degrade ß-O-4 and ß-1 phenolic lignin model compounds. Aromatic ring cleavage of 4,6-di(tert-butyl)guaiacol has also been reported.[27] Laccase reportedly causes polymerization of lignin as well as depolymerization.[8]

Enzymes other than phenoloxidases have been found to be involved in lignin degradation. The enzymatic degradation of lignin is part of the complex enzymatic system which degrades all wood components. In this complex process it is highly probable that enzymes involved in lignin degradation act synergistically with other enzymes to achieve complete breakdown of lignin.

Cellobiose: quinone oxidoreductase (CBQ) is an enzyme which requires both phenols and carbohydrates for activity. CBQ utilizes quinones and phenoxy radicals from lignin. It has been suggested that CBQ is able to prevent repolymerization of lignin degradation products by reducing these species to phenols.[28,29] A combined enzymatic system, utilizing several different enzymes, may be required to achieve full depolymerization of lignin.

Dioxygenases are enzymes which catalyze the incorporation of O_2 into organic substrates, utilizing both oxygen atoms in the oxidation. These enzymes catalyze ring cleavage of aromatic compounds (i.e. catechol).[30] Immobilized protocatechuate 3,4-dioxygenase isolated from

fungal cultures causes ring cleavage in lignosulfonate fractions.[31] Dioxygenases, although mostly produced intracellularly, have been reported to depolymerize and polymerize lignin and lignin-like compounds.[8,32,33]

Mechanism for Enzymatic Lignin Degradation

Most of the information on the mechanisms of enzymatic degradation of lignin has resulted from studies of LiP. Numerous studies using lignin model compounds have shown that LiP is able to break the C_α-C_β bond of diarylpropane units. LiP is capable of catalyzing the oxidation of many lignin model compounds. The mechanisms involved have recently been reviewed for ß-O-4, ß-1 and ß-5 lignin model compounds.[34] LiP is able to catalyze both phenolic and non-phenolic models.

It has been established that one-electron oxidation of a phenolic ring leads to aryl cation radical formation which begins lignin degradation reactions.[35,36,37] A generally accepted mechanism for the initiation of lignin degradation by lignin peroxidase is shown in Figure 4.

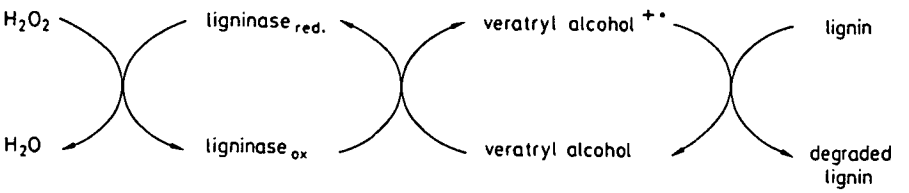

Figure 4. Proposed mechanism for the enzymatic degradation of lignin (from Ref. 8).

This simplistic view has been questioned by various researchers. In two recent reviews on lignin biodegradation, the role of lignin peroxidase as a lignin-degrading enzyme is debated.[38,39] These authors suggest that the true enzyme(s) involved in lignin degradation has not been isolated.

The involvement of a secondary metabolite, veratryl alcohol (Figure 5), has been debated for some time. The exact role of veratryl alcohol in lignin degradation by Phanerochaete chrysosporium is not clear. It is believed that veratryl alcohol protects ligninases from degradation by radicals which are produced during the decomposition of hydrogen peroxide.[40] Fungal cultures supplemented with veratryl alcohol have been observed to produce more LiP.[41,42] Other researchers propose that veratryl alcohol acts as a mediator between LiP and lignin.[43] Veratryl alcohol may be protecting LiP from inactivation by hydrogen peroxide; however, the mechanism by which this inactivation occurs is not known.[40]

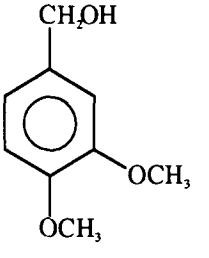

Figure 5. Veratryl alcohol, believed to be involved in the enzymatic degradation of lignin.

Involvement of the Hydroxyl Radical

The involvement of the hydroxyl radical in the fungal and enzymatic degradation of lignin has been a subject of debate. Numerous investigations have been made in which hydroxyl radicals were measured in ligninolytic cultures or during enzymatic treatments, concomitant with controls using Fenton's reagent, a known hydroxyl radical producer.

The earliest investigation into the involvement of the hydroxyl radical was performed prior to the discovery of lignin peroxidase. Hydroxyl radicals were measured in fungal ligninolytic cultures using a variety of methods for their detection.[44,45,46,47] Results from these studies agree hydroxyl radicals are formed during lignin degradation by Phanerochaete chrysosporium.

Once the enzyme lignin peroxidase had been isolated in 1983, attempts were made to measure hydroxyl radicals produced during enzymatic degradations of lignin model compounds. Kirk, et al.[48] investigated the presence of hydroxyl radicals in degradation of ß-1 and ß-O-4 lignin model compounds by Phanerochaete chrysosporium, isolated LiP and Fenton's reagent. A comparison of degradation products from these systems showed that similar products were formed by the fungus and isolated LiP. Different products were obtained when Fenton's reagent was used.

Electron Spin Resonance (ESR) spectroscopy of reaction samples indicated that hydroxyl radicals were not produced in either the fungal or enzymatic systems; however, hydroxyl radicals were detected in the reaction mixture containing Fenton's reagent. Kirk and coworkers concluded that hydroxyl radicals were not involved in the C_α-C_β cleavage of the selected models, and by extension, in the enzymatic degradation of lignin.

In a recent publication, Barr and coworkers[49] provide evidence for the production of hydroxyl radicals by LiP in solutions containing hydrogen peroxide, veratryl alcohol, oxalate, and ferric ions. It is known that ferric ions catalyze the decomposition of hydrogen peroxide and generate hydroxyl radicals through the Fe(III)-Fe(II) redox cycle.[50] Barr and coworkers concluded that hydroxyl radicals are involved in the fungal degradation of lignin, but are not produced directly by LiP.

Most data in the literature indicates that the hydroxyl radical is not generated directly by the enzyme LiP, but that this radical is involved in the degradation of lignin by white-rot fungi. The ubiquitous nature of the hydroxyl radical makes it seem rather likely that hydroxyl radicals are involved in some manner in the biodegradation of wood by fungi.

In these published studies different methods were used to detect hydroxyl radicals during lignin degradation. No analytical technique is completely selective for hydroxyl radicals. Hydroxyl radicals are extremely difficult to detect due to their high reactivity.

Aromatic hydroxylation reactions are generally specific for hydroxyl radicals; however, not all reagents have been shown to be specific for hydroxyl radicals, or appropriate for the conditions used in this study. For example, hydroxyl radicals can be detected by measuring the hydroxylation of salicylate.[51] However, once hydroxylated, salicylate can bind free iron to form chelated catechols. Once iron becomes bound the catalytic environment is altered.

In 1988, Reitberger and Gierer[52] introduced a unique assay for measuring hydroxyl radicals in situ. This assay uses an inexpensive and easily obtained reagent. The chemiluminescence assay has been used to measure hydroxyl radicals in white-rot[53] and brown-rot[54] fungal cultures, as well as in oxygen,[52] ozone,[55] and hydrogen peroxide bleaching of wood pulp.[52]

The active reagent in the chemiluminescence assay is phthalic hydrazide. Phthalic hydrazide does not chemiluminesce upon oxidation. Once added to reaction solutions, phthalic hydrazide becomes hydroxylated by hydroxyl radicals. Hydroxylated phthalic hydrazide (HPH) does exhibit chemiluminescence upon subsequent oxidation. Reaction samples can then be removed and the amount of HPH determined by photometric analysis. The concentration of hydroxyl radicals formed is, therefore, proportional to the amount of chemiluminescence observed.

The two major chemical reactions involved in the chemiluminescence assay are shown in Figure 6. Phthalic hydrazide is hydroxylated by hydroxyl radicals during the reaction. A sample is then removed for oxidation in a light-detecting apparatus. Oxidation is performed using hydrogen peroxide and ammonium persulfate. The amount of light emitted during this reaction is proportional to the concentration of hydroxylated phthalic hydrazide, and therefore the amount of hydroxyl radicals generated in solution.

Pulp Delignification with Ligninolytic Enzymes

Pulp delignification with ligninolytic enzymes was evaluated immediately after these enzymes were isolated and characterized.[15] Kirk, et al.[56] found that LiP polymerizes lignin

IN THE REACTION:

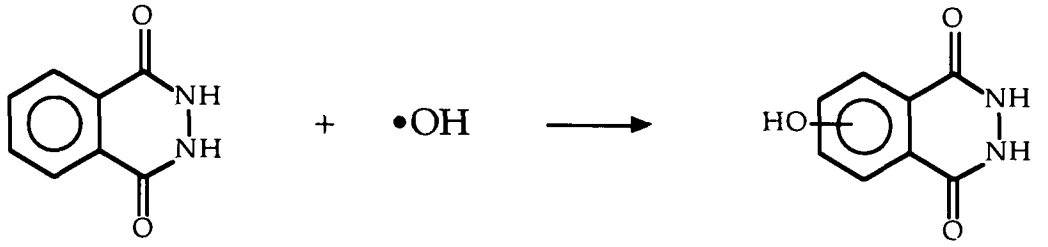

Phthalic hydrazide

IN THE PHOTOMETER:

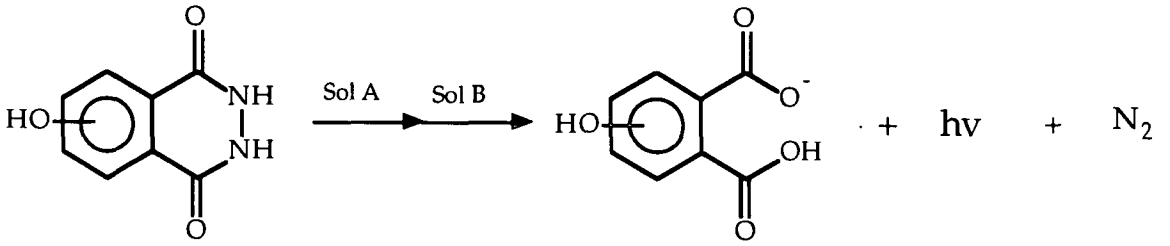

Hydroxylated Phthalic Hydrazide
(HPH)

Figure 6. The two major reactions involved in the chemiluminescence assay. Solution A: Na_2CO_3 and EDTA, Solution B: H_2O_2 and $(NH_4)_2S_2O_8$.

fragments as well as causing depolymerization. Reductions in kappa number were not significant, although significant loss of color was noted. As LiP was not able to completely depolymerize lignin, Kirk suggested that other enzymes were needed to fully degrade the lignin polymer.

Several patents using lignin peroxidases to bleach pulps have been issued.[57, 58] In a recent investigation of the ability of lignin peroxidases to bleach pulp,[59] several factors were manipulated to achieve optimum results. These included hydrogen peroxide addition rate (as opposed to a batch charge), addition of veratryl alcohol, and pH. It was observed that the presence of veratryl alcohol improved the enzymatic treatment. The slow addition of hydrogen peroxide

was also found to obtain improved delignification. The optimum pH was found to be between 4.5 and 5.5, where the enzyme exhibited greater efficiency.

Ligninolytic enzymatic bleaching treatments have met with limited success, despite early promises of a process specific for lignin removal.[60,61] The failure of this process has been attributed to the inability of these enzymes to reach the lignin within the pulp fiber. Biomimetic compounds, which mimic the action of these enzymes and are not as large as enzymes, are more suitable for pulp delignification.

BIOMIMETIC COMPOUNDS

Biomimetic compounds mimic a more complex biological function. Biomimetics have been an active area of research for several years. Biomimetics have been used to investigate new ways of obtaining methanol from methane by mimicking methane monooxygenases and cytochrome P-450.[62] Other active areas involve mimicking oxidases and dioxygenases for oxidative degradation of many organic compounds.[63]

Once the prosthetic group of lignin peroxidase was identified as an iron porphyrin, biomimetic compounds resembling this structure were used to facilitate studies of the reaction mechanisms in enzymatic systems. Porphyrins containing iron or other transition metals as the complexed metal were used to mimic the action of lignin peroxidase. Other systems which do not possess the porphyrin group have also been found to mimic the action of LiP. These include chelated metals, and simple systems containing just a transition metal. In all cases an oxidant must be present; hydrogen peroxide is most commonly used.

Applications of biomimetic compounds to commercial processes were later attempted as their potential for commercial viability improved. Pulp bleaching using biomimetic compounds has produced promising results as discussed below.

Model Compound Studies

Shimada, et al.[64] used several compounds which contained a porphyrin structure, namely hemin, Fe(III)- and Mn(II)- tetraphenylporphyrins (TPP). All structures were found to cleave the C-C bond in a 1,2-diarylpropane-1,3-diol lignin model compound. Habe, et al.[65] used an iron porphyrin with an imidazole complex to study bond cleavage in lignin model compounds. This structure was also found to cleave the C-C bond. Additionally, several other metalloporphyrins were evaluated in this study [including TPPs, octaethylporphyrins, and phthalocyanins with Fe(III), Mn(III), Co(II) and Cu(II)], but iron porphyrins were reported to give the best results (no quantitative data was presented).

A subsequent article published by Shimada, et al. also examined the utility of using the iron porphyrin as a mimic of LiP.[66] Two iron porphyrins, hemin and tetraphenylporphyrin (TPP), were evaluated for their ability to degrade several lignin model compounds. Hemin was found to be more reactive, cleaving the C-C bond more rapidly than TPP.

The linkages investigated in this study were ß-1, ß-0-4 and ß-5. Two model compounds were used to represent the ß-1 linkage; one possessed a hydroxyl group at the α-carbon, while the other contained a methoxyl group. In both cases the hemin catalyst was able to cleave the C_α-C_β bond, showing no discrimination between the two α-carbon substituents. For the ß-0-4 and ß-5 models, the same carbon-carbon linkage was broken. This paper confirmed that a single, one-electron transfer reaction was performed, catalyzed by the metalloporphyrin.

Huynh[67] used simple inorganic complexes to determine their ability to mimic the LiP enzyme. Complexes of peroxydisulfate with Cu(II), Co(II), Fe(II), Mn(II), Mn(III), and Co(III) were used. It was found that the Cu(II) peroxydisulfate complex mimicked the enzyme LiP most closely. A ß-1 lignin model compound was used in this study with the C-C linkage being the predominant bond broken.

Although researchers inferred the use of these catalysts for pulp delignification, their studies were not directed towards achieving this goal. These studies have shown that biomimetic catalysts are able to break common linkages which are found in native lignin. If these biomimetic compounds are to be used as bleaching catalysts, detailed studies using residual lignin model compounds would provide better information.

In addition, the studies above focused on the ability of the biomimetic compound to break certain linkages connecting lignin-like components. The effect of these biomimetic compounds on carbohydrate alone, or carbohydrate in the presence of lignin, were not investigated. These biomimetic compounds may cleave the glycosidic linkages found in carbohydrates as readily as linkages in lignin substructures. In the following section, the use of biomimetic compounds on wood pulp are presented. Although these studies are in most cases not aimed at discriminating between lignin and carbohydrate degradation, some information on the selectivity of these compounds is gained.

Pulp Delignification with Biomimetic Systems

Paszczynski, et al.[11] used a variety of natural and synthetic compounds to delignify pulp and wood chips. This study included analyses of wood component losses as well as morphological changes. Table 1 below shows the amount of component losses for several different biomimetic treatments of wood chips and pulp.

From the data presented in Table 1, hydrogen peroxide alone removed more lignin than tert-butyl hydroperoxide (TBH). The addition of hemin as catalyst increased losses in all components for the TBH experiment. Hemin with hydrogen peroxide did not significantly increase degradation of any wood components over that achieved with hydrogen peroxide alone. These results indicate that careful selection of oxidant as well as catalyst is essential for optimum bleaching results.

Table 1. Wood component losses following several bleaching treatments of birch chips and a single treatment on a softwood pulp.[11]

Treatment (hours)	Weight	% Loss In Lignin	Glucose	Xylose	Mannose
Wood Chips					
Hemin Only (24)	4.0	7.5	6.9	2.2	12.7
TBH[a] Only (24)	10.1	15.8	6.9	10.8	40.1
Hemin and TBH (24)	23.4	25.6	9.8	21.6	44.6
H_2O_2 only (24)	45.7	40.6	35.9	55.9	77.9
Hemin and H_2O_2 (24)	48.7	42.5	37.5	63.0	77.9
Softwood Kraft Pulp					
Hemin + TBH (24)	19.0	100.0	9.8	36.2	41.8

[a] TBH = tert-butyl hydroperoxide

When the biomimetic treatment was used on pulp, essentially all lignin was removed. Although the sugar content was measured, the viscosity of the pulp was not reported. The strength of paper can be related to the viscosity, and would, therefore, have provided more useful information than the glucose content. High carbohydrate losses make this process very unattractive for use in pulp bleaching.

Paszczynski, et al. also investigated the effect of pH on their chosen biomimetic bleaching systems. Both hemin and iron porphyrin increased delignification over the pH range studied, as shown in Table 2. Results from these experiments show a slight decrease in the kappa number (a measure of lignin content in pulp) with increasing pH for all conditions.

Table 2. Degree of delignification as a function of three different pH levels on softwood pulp.[11]

TREATMENT[a]	Kappa Number at pH 5.5	7.0	9.5
None	35.4	35.4	35.4
TBH	12.5	11.3	10.5
TBH plus Hemin	1.9	1.8	1.6
TBH plus porphyrin iron chloride	1.8	1.6	1.5

[a] Samples were refluxed for 24 hours.

Paszczynski, et al. felt that their results showed delignification equal to that of peroxide bleaching. Of the many organometallic complexes used in this study, the authors felt that the iron porphyrins showed the best activity and resulting pulp bleaching.

Many biomimetic compounds are insoluble in aqueous solutions and suffer from chemical instabilities. Dolphin and coworkers[68] synthesized a sulfonated and chlorinated porphyrin (Figure 7) to overcome these limitations. Sulfonation of the porphyrin increased water-solubility, and chlorination of the porphyrin stabilized it from self-deactivation.

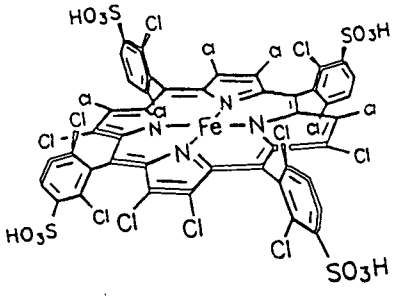

Figure 7. Synthesized porphyrin, sulfonated and chlorinated, used by Skerker and Dolphin.[68]

Skerker and coworkers[12] used this porphyrin for biomimetic bleaching studies. The oxidant used in this system was tert-butyl hydroperoxide. Reactions were run at 60°C for 15 minutes with 2.5% pulp consistency, 0.1 - 3.0 % t-butyl hydroperoxide (w/v) on pulp. Bleaching experiments with this compound indicated a direct dependence of kappa number on the bleaching temperature and oxidant concentration. Large viscosity losses were also noted in this system. In an attempt to minimize cellulose degradation, magnesium sulfate, known for its protective behavior in oxygen bleaching,[69] was added. However, cellulose damage was not prevented.

Skerker and coworkers also changed the metal in the porphyrin from iron to manganese and found that this made no significant difference in kappa number reduction or

viscosity losses. As previously noted, the work by Habe[65] found that iron porphyrins worked better than manganese porphyrins. This conflicted with results obtained by Skerker and coworkers. The metal in the porphyrin structure affects the reduction potential of that compound; however, degradation of lignin or lignin model compounds was not studied as a function of the redox potential of these biomimetic compounds.

Crawford, et al.[13] examined the ability of several inexpensive chelated iron compounds to bleach pulp. These compounds included EDTA, NTA, DTPA, 2,2'-dipyridyl, and Tiron. Good delignification and subsequent brightness increases were observed with all of the compounds (data not available). However, significant viscosity losses were observed during the treatment of softwood pulps.[70]

A study of another class of biomimetic catalysts was published by Shimada, et al.[71] Peracetic acid with Mn(II) and Co(II) catalysts were used to bleach pulp. This system does not possess the caged metal as found in porphyrins or chelated metals. Degradation of ß-O-4 model compounds was achieved in the initial work performed. Significant brightness increases were obtained with this biomimetic system in studies performed on an unbleached kraft pulp. No information on carbohydrate losses or kappa number reductions were presented. These researchers feel their results show that the peracetic acid and Mn/Co system mimics the enzyme MnP.

Pettersson, et al.[10] used hemoglobin to bleach both softwood and hardwood pulps. Significant delignification was achieved when the pulp samples were exposed to this biomimetic treatment. Results obtained from the treatment of the softwood (pine) pulp are shown in Table 3. For the unbleached pulp, equal reductions in the kappa number and viscosity were obtained with both the biomimetic and conventional oxygen treatments. This demonstrates that the selectivity for lignin removal over carbohydrate degradation (i.e., viscosity loss) in the biomimetic system is acceptable.

For the oxygen bleached pulp, additional delignification was obtained with a concomitant loss in viscosity. Biomimetic treatment of the oxygen bleached pulp was not compared to other conventional bleaching treatments.

Table 3. Kappa number and viscosity reductions of a softwood kraft pulp (pine) after treatment with hemoglobin and hydrogen peroxide.[10]

	KAPPA NUMBER		VISCOSITY (dm^3 / kg)	
TREATMENT	Before	After	Before	After
Unbleached Pulp				
Oxygen	30.0	22.5	1180	1050
Hemoglobin	30.0	22.0	1180	1051
Oxygen Bleached Pulp				
Hemoglobin	22.5	13.5	1050	876

The hemoglobin used in these treatments was derivatized with palmitoyl chloride [$CH_3(CH_2)_{14}COCl$]. Pettersson and coworkers believe that the addition of palmitoyl chloride increases the specificity of the hemoglobin treatment.

For biomimetic bleaching systems to be effective, they must be selective (i.e., demonstrate a high reactivity towards lignin degradation without severely damaging the carbohydrates). Metal ions in the presence of hydrogen peroxide are known to generate hydroxyl radicals. The behavior of hydrogen peroxide in biomimetic systems has not been well characterized. The formation of hydroxyl radicals has not been investigated. In addition, these studies have not shown how much of the added peroxide is directly involved in oxidation of the substrate by the biomimetic compound versus how much is lost in conversion to oxygen.

DELIGNIFICATION WITH HYDROGEN PEROXIDE

Hydrogen peroxide has been studied as a bleaching agent for both mechanical and chemical pulps.[69, 72] Pulp delignification is most commonly performed in strongly alkaline

aqueous solutions (pH > 11). Transition metals are removed in a chelation stage, as these metals are believed to be detrimental to bleaching efficiency. Metal ions are known to catalyze the decomposition of hydrogen peroxide.[73] Hydroxyl radicals and other radical species produced are also believed to be responsible for the viscosity loss (carbohydrate degradation) observed during pulp bleaching.[74]

A substantial body of literature exists which has investigated the major reactive species involved in alkaline hydrogen peroxide delignification of pulp. Hydrogen peroxide is a weak acid (pKa = 11.8) and dissociates at high pH. The resulting perhydroxyl ion, HOO^-, was initially believed to be the predominant reaction species. The transition metal catalyzed decomposition products of H_2O_2 (i.e., $O_2^{-}\bullet$, $HO\bullet$) are also believed to play an active role in bleaching.[75,76]

The presence of transition metals was initially believed to be detrimental to pulp bleaching with alkaline hydrogen peroxide. Excessive decomposition of hydrogen peroxide to oxygen was noted. Later investigations revealed that decomposition of hydrogen peroxide was a necessary step. Smith and McDonough[75] have provided evidence that the oxidation of a lignin model compound is related to the amount of hydrogen peroxide decomposed. In addition, metal ions are believed to catalyze phenoxy radical formation.[77,78]

Acid Hydrogen Peroxide Delignification

Bleaching with hydrogen peroxide in acidic media has been attempted with moderate success.[79,80] In the limited studies reported, a chelation stage often precedes the peroxide stage to remove any transition metals. Suss and Helmling found that a slight gain could be achieved when an acidic hydrogen peroxide pretreatment was used prior to oxygen bleaching.[80] These researchers also found that increasing the acid strength in their bleaching media increased delignification; they attributed this to increased acid hydrolysis.

Delignification with acidic hydrogen peroxide has been attributed to the formation of the hydroxonium ion (OH+),[81] occurring through protonation and subsequent dissociation of hydrogen peroxide as follows:

$$H_2O_2 + H^+ \text{ --> } OH^+ + H_2O,$$

and not to lignin degradation occurring through radical reactions.[80] However, it is very likely that hydrogen peroxide is catalytically decomposed to form radical species at these conditions. Lignin degrading reactions are, therefore, initiated either through direct attack by hydrogen peroxide, or possibly protonated hydrogen peroxide,[82] or by radicals produced from the catalyzed decomposition of hydrogen peroxide.[83]

Concentrated solutions (18 - 70 %) of hydrogen peroxide are relatively stable; however, as the pH deviates in either direction from 4.0 ± 0.5, decomposition increases.[84] This decomposition, although measurable, is very small. It has been attributed to the difficulty of obtaining contaminant-free reagents. Even under carefully prepared conditions, decomposition does occur.

Catalyzed Decomposition of Hydrogen Peroxide

Iron is present in both the enzyme LiP and compounds used to mimic this enzyme; therefore, the catalytic effect of iron on the behavior of hydrogen peroxide must be considered. The decomposition of hydrogen peroxide to oxygen has been extensively studied, especially the effect of catalytic quantities of transition metals.[73]

It has been known for nearly a century that iron catalyzes the decomposition of hydrogen peroxide. It is believed that decomposition occurs via a complex radical mechanism. The main reactions occurring during iron-catalyzed decomposition of hydrogen peroxide are: [50, 73]

$$Fe^{++} + H_2O_2 \rightarrow Fe^{+++} + OH^- + \bullet OH \quad [1]$$

$$\bullet OH + Fe^{++} \rightarrow Fe^{+++} + OH^- \quad [2]$$

$$\bullet OH + H_2O_2 \rightarrow HO_2\bullet + H_2O \quad [3]$$

$$HO_2\bullet + Fe^{++} \rightarrow HO_2^- + Fe^{+++} \quad [4]$$

$$HO_2\bullet + Fe^{+++} \rightarrow H^+ + O_2 + Fe^{++} \quad [5]$$

$$Fe^{+++} + H_2O_2 \rightarrow Fe^{++} + H^+ + HO_2\bullet \quad [6]$$

Chelated iron complexes are known to generate hydroxyl radicals through the above outlined steps.[85, 86] Hydroxyl radicals have also been observed in solutions containing hemoglobin and hydrogen peroxide.[87] Biomimetic compounds must, therefore, participate in the catalytic decomposition of hydrogen peroxide to produce radicals.

The hydroxyl radical is not selective, due to its high reactivity. However, in a recent study with model compounds, it was found that hydroxyl radicals react 5 - 6 times faster with aromatic compounds (lignin-like) than with sugars (carbohydrates).[88] The key to using hydroxyl-radical generating systems to delignify pulps may be in achieving close association between reactant and substrate. This may be achieved by selecting the correct biomimetic compound or additives.

Hydroxylation of aromatic compounds by Fenton's reagent is reported to proceed via a homolytic cleavage of hydrogen peroxide. The resulting radicals either add to the aromatic ring to form hydroxylated radicals, or abstract carbon-bound hydrogen atoms. These radicals either decompose, or couple to form dimers, depending on reaction conditions and chemical structure.

Apart from LiP's dependence on hydrogen peroxide for activity, the role of hydrogen peroxide in the previously discussed lignin-degrading systems has not been thoroughly addressed in the literature. However, its inhibitory effect on enzyme activity has been noted.[18,89] Further investigation of the role of the hydrogen peroxide in this environment is necessary to

obtain a better understanding of delignification mechanisms and of ways to optimize its behavior. This is especially important if biomimetic systems are to be applied to industrial pulp bleaching.

SUMMARY

It is apparent from the preceding discussion that the exact mechanisms of enzymatic lignin degradation by fungi have not been clearly established. In fact, the role of lignin peroxidase, the proposed key enzyme in lignin degradation, has been questioned. Limited success in pulp bleaching with lignin peroxidases seems to support this claim.

Biomimetic compounds were initially used to help elucidate mechanisms for the enzymatic degradation of lignin. A biomimetic approach to pulp bleaching was also evaluated using these compounds. In these systems biomimetic compounds catalyze the decomposition of hydrogen peroxide via a chain mechanism which generates hydroxyl radicals These radicals are most likely responsible for degradation reactions.

The efficiency of these catalysts to oxidize substrate versus decompose hydrogen peroxide to oxygen has not been evaluated. During both of these processes, hydroxyl radicals are generated. These radicals, and other types produced, will contribute to carbohydrate degradation as well as that of lignin. The selectivity of biomimetic systems has only been given passing attention. This thesis is an attempt to further understand the selectivity and efficiency of biomimetic systems.

OBJECTIVES AND EXPERIMENTAL APPROACH

OBJECTIVES

The main thrust for this work was to evaluate the potential of particular biomimetic compounds as catalysts for hydrogen peroxide delignification of pulp. To be suitable for pulp delignification, biomimetic compounds must demonstrate selectivity for lignin degradation relative to that of carbohydrate. As these compounds are supposed to mimic a lignin-degrading enzyme, lignin degradation would be expected to predominate.

Objectives of this dissertation were to:

- evaluate the selectivity of three biomimetic compounds for lignin degradation relative to that of carbohydrate, when substrates are individually exposed to these systems,
- evaluate the selectivity of these biomimetic compounds when these substrates are simultaneously combined in solution,
- measure hydroxyl radicals generated by each of the biomimetic compounds in these systems, and assess their role in the degradation of the model compounds.

EXPERIMENTAL APPROACH

To limit the scope of this work, iron was the only metal considered for investigation. Three different types of biomimetic, iron-based catalysts were chosen for evaluation: $FeSO_4$, Fe-EDTA, and hemoglobin. These three compounds resemble the enzyme lignin peroxidase to different degrees. $FeSO_4$ mimics only the metal present in the enzyme. The iron in Fe-EDTA is sequestered by a relatively small but strong chelator. Hemoglobin resembles the enzyme the most because the iron is surrounded by protein.

Water-soluble model compounds representing the two major constituents of wood pulp, i.e. lignin and cellulose, were chosen. Water solubility was desired so that homogeneous reaction mixtures in aqueous solution were maintained. An acidic pH was used, as the enzyme (LiP and MnP) functions optimally under acidic conditions.[8] Polymeric, as opposed to monomeric and dimeric, model compounds were sought as these more closely represent the natural polymers.

Few residual lignin model compounds are appreciably soluble in acidic aqueous solution. For this reason, lignosulfonate was chosen as a residual lignin model compound, since it is highly soluble in acidic aqueous solution. Although not really representative of the residual lignin found in chemical pulps, lignosulfonate incurs structural changes in chemical pulping.[90] Refer to Figure 8 for an illustration of a generalized structure of a water-soluble lignosulfonate.

Hydroxyethyl cellulose (HEC) was selected as the carbohydrate model compound. HEC (obtained from Aqualon, Wilmington, DE) possesses attributes which make it ideal for this project. The viscosity of HEC solutions is independent of pH, which allows intrinsic viscosity measurements to be made without correction for changing pH with dilution. HEC is highly water soluble, and a wide range of molecular weight samples are available.

As ethyl-oxo groups can form long side chains, the degree of substitution is ambiguous. Moles of substitution more clearly indicate the extent of substitution on the HEC molecule. For this particular product (Natrosol), 2.5 moles of ethylene oxide reacted with 1 mole of cellobiose. Figure 9 shows a schematic of HEC.

A chemiluminescence assay (as described in the Literature Review section) was used to detect the generation of hydroxyl radicals in reactions. Modifications of this assay, discussed in detail in the Results and Discussion section, were made so that minor problems were eliminated.

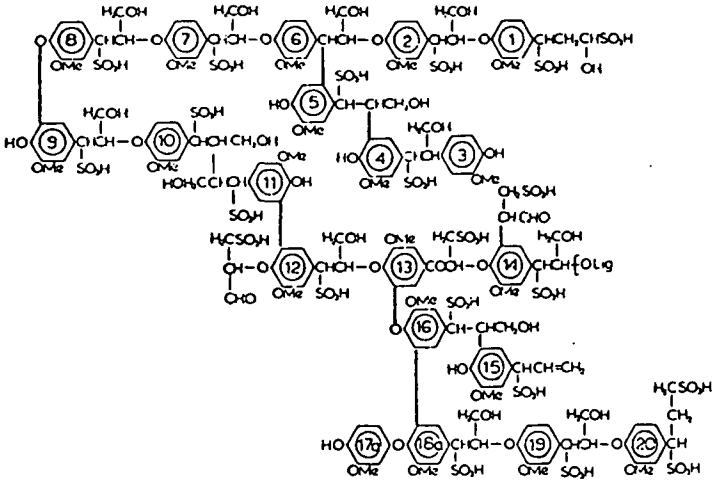

Figure 8. Generalized structure of a water-soluble lignosulfonate (taken from Ref. 90).

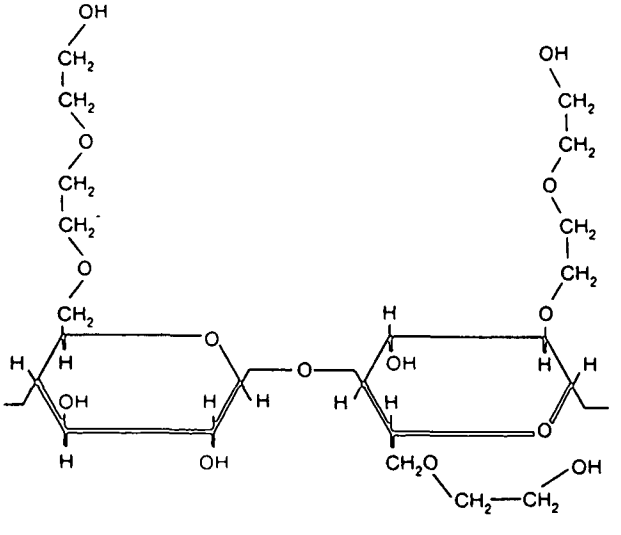

Figure 9. Generalized structure of HEC with 2.5 moles of substitution (taken from Natrosol product literature).

Lignosulfonate and HEC were individually exposed to each of the three biomimetic compounds in the presence of hydrogen peroxide. Empirical rate laws were developed for each of these systems. Rates of chain scission were also determined, and selectivities were calculated using these rates.

Lignosulfonate and HEC were also combined in reaction solutions and then exposed to the same three catalysts. During these experiments the formation of a high molecular weight product was observed. The rate and extent of formation and degradation of this product was evaluated.

All reactions were performed in a teflon-lined, magnetically stirred reactor. The amount of hydrogen peroxide decomposed to oxygen was measured independently of that which was consumed in reactions. Deionized-distilled water and ultrapure chemicals were used to minimize effects due to extraneous metals.

MATERIALS AND METHODS

SOLUTIONS AND REAGENTS

Water

Water was obtained from a Barnestead Water Purifier configured to provide Type I reagent grade water. (Specific resistance of output water: 18.3 MΩ-cm).

Hydrogen Peroxide

Ultrapure hydrogen peroxide (30%) was obtained from J. T. Baker. A stock solution was prepared (approx. 3%) from this concentrated solution and stored in a polypropylene bottle at 4°C. Concentration was determined prior to use. This solution was made as needed.

Ferrous Sulfate

A 0.5 M solution of ferrous sulfate was made according to procedures outlined in the CRC Handbook of Chemistry and Physics for standard solutions.[91] To prepare 100 ml, 1.0 ml of concentrated sulfuric acid was first added to a 100 ml volumetric flask. The predetermined amount of $FeSO_4$ (13.90 g) was then added. After the $FeSO_4$ had dissolved, water was added to the final dilution. This solution was stored in a glass volumetric flask at 4°C in the dark. A fresh solution was prepared once every two months.

Fe-EDTA

A 25 mM stock solution of Fe-EDTA was made according to the following procedure. The predetermined amount of $FeSO_4$ was added to 1 mL of concentrated sulfuric acid. Once the $FeSO_4$ dissolved, ~200 mL of water was then added. The required amount of ethylenediaminetetraacetic acid (EDTA) was then added (in a 1:1 molar ratio with $FeSO_4$). Sodium

hydroxide was added until all EDTA was dissolved (3 - 5 mL). This solution was diluted to 250 mL, and then stored at 4°C in a glass volumetric flask.

Hemoglobin

Hemoglobin was obtained from Sigma Chemical Co. as purified from bovine red blood cells. A 20.0 g/l hemoglobin solution was prepared the day before use. 2.0 g of hemoglobin was weighed into a 150 mL beaker. 100.0 mL of water was then slowly added. This solution was stirred until all hemoglobin had dissolved. It was then stored at 4°C overnight.

PURIFICATION AND PREPARATION OF SUBSTRATES

Lignosulfonate

Partially purified lignosulfonate (Lot # D-442-14, softwood cook) was obtained from Daishowa Chem. Inc., (Lignotech) Rothschild, Wisconsin. Approximately one liter of solution (at ~50 % solids) was obtained and split into 50 ml aliquots and stored in polyethylene bottles. These bottles were purged with nitrogen and then frozen at - 20°C. Solutions were thawed at 4°C before use.

Solutions were first diluted to approximately 30 g/l (1.0 liter total volume) and passed through a 0.22 μm Whatman filter. Ultrafiltration was then performed to obtain a sample with a narrow molecular weight distribution. This was accomplished using an Amicon Stirred Filtration Cell (Model 345) with a 200 ml capacity. Solutions were slowly added to the filtration cell which was fitted with an Amicon 30,000 dalton PM (inert, non-ionic) filter. The filtrate (< 30,000 daltons) was collected for further ultrafiltration. The retentate (> 30,000 daltons) was washed with water until the filtrate was clear, indicating nearly complete removal of material < 30,000 daltons.

The filtrate collected (< 30,000 daltons) was passed through the filtration cell, but now fitted with an Amicon 10,000 PM filter. The filtrate from this step (< 10,000 daltons) was

discarded. The retentate (10,000 - 30,000 daltons) was washed with copious amounts of water until the filtrate was clear. The retentate was removed from the filtration cell, placed into a glass reagent bottle, purged with nitrogen, and stored at 4°C in the dark.

The final concentration of ultrafiltered solutions of lignosulfonate was determined by absorbance at 280 nm. This was accomplished by preparing an absorbance versus concentration curve from several dilutions of a lignosulfonate preparation at a known concentration. The solids content of a diluted sample of the original lignosulfonate was obtained, using the standard procedure for black liquor solids content determination.[92] Several dilutions of this solution were made, and the absorbance at 280 nm recorded. The resulting curve of absorbance versus concentration was used to determined the concentration of all lignosulfonate preparations.

Hydroxyethyl Cellulose (HEC)

Hydroxyethyl cellulose samples were obtained from Aqualon, a division of Hercules Chemical Co., in Wilmington DE. Three samples were obtained, having approximate molecular weights of 90,000 (Natrosol 250 LR), 720,000 (Natrosol 250 MR), and 1,300,000 (Natrosol 250 HHR).

HEC solutions were prepared by dissolving the required amount of HEC into the necessary premeasured volume of water. HEC was slowly added to the water on a magnetic stirrer at the vortex. The solution was allowed to stir at room temperature for one hour. The solution was then placed in a 4°C cold room to continue stirring overnight (a minimum of 14 hours).

All three HEC samples were used to evaluate the calibration system (see below) for determination of HEC molecular weights. HEC 250 HHR (M_w = 1,300,000) was used for all HEC degradation experiments with hydrogen peroxide and catalysts.

REACTOR

All experiments were performed using a 300 ml teflon-lined, magnetically stirred batch reactor (Figure 10) used from a previous study.[77] Reaction pH was measured using a Sensorex combination pH probe connected to a Chemcadet pH Meter. The reactor was placed in a magnetically stirred water bath maintained at 45°C by a CRC thermoregulator.

Evolved gas was captured and measured in a water-jacketed buret (Figure 11). This entire system was gas tight once reactions were initiated. Reaction pressure was maintained at atmospheric, as indicated by the water manometer, by adjusting the pulley system. The evolved oxygen expanded into the buret and could be measured in milliliters.

REACTION PROCEDURES

Reactor Preparation

The reactor, a 100 ml graduate cylinder, and a 50 ml polypropylene bottle were washed with distilled water, alconox, rinsed with distilled water again and dried. These items were then washed with acetone, allowed to dry, then rinsed with 35 % nitric acid. A final thorough wash was performed with deionized distilled water. These items were allowed to dry completely before each use. The pH probe was standardized at pH 4.0 and 45°C prior to use.

Experiments in which hydroxyethyl cellulose was used, HEC solutions were prepared the night before the experiment, in accordance with the procedures outlined in the section on preparation of HEC solutions. For all other experiments, solutions were prepared that day.

For reactions containing lignosulfonate or no substrates, water was first added to the reactor (usually 80 to 250 mls, depending on total reaction volume). The reactor was then placed in the 45°C water bath. The solution was continuously purged with prepurified nitrogen for an hour. Lignosulfonate (if present) was then added to the reactor. The catalyst (if present) was then added.

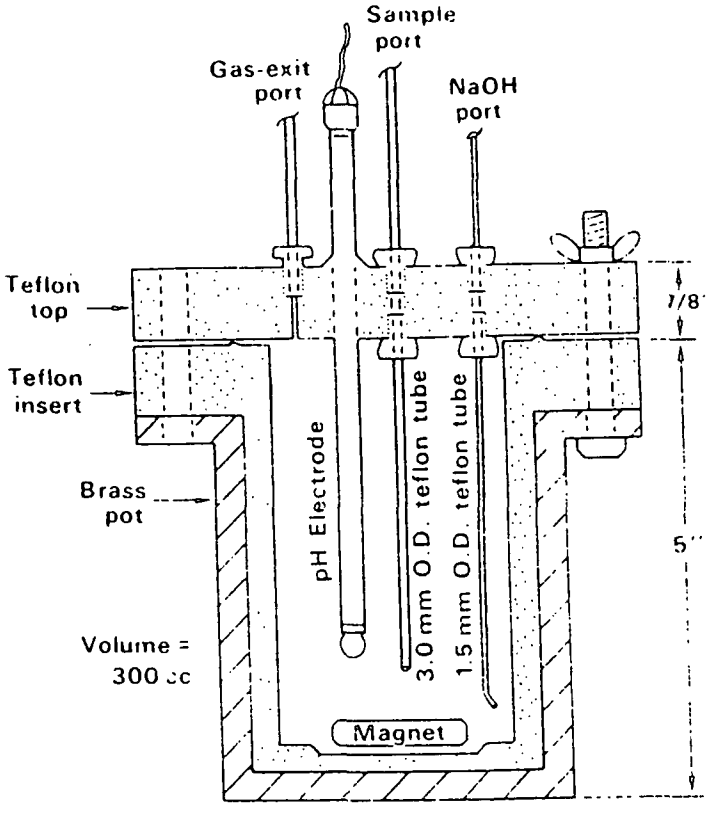

Figure 10. Reactor used for experiments (taken from Ref. 77).

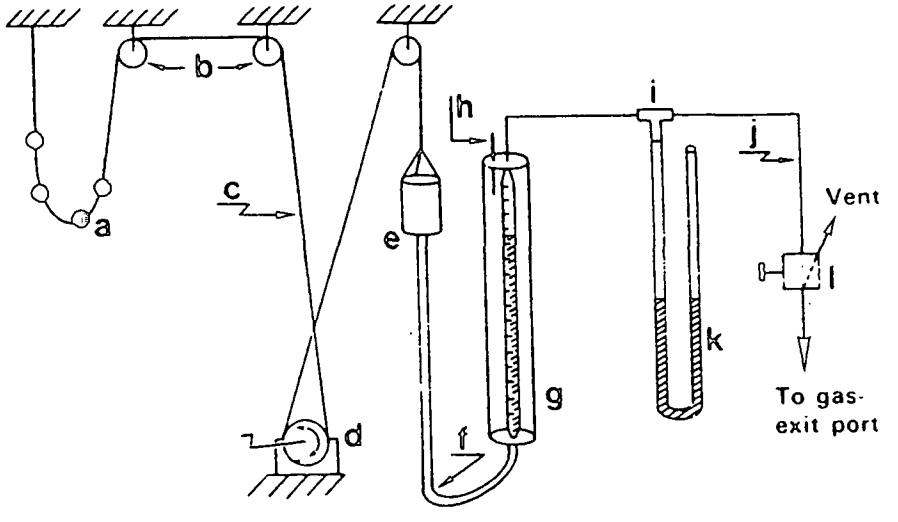

Figure 11. System used to measure gas evolution (taken from Ref. 77): (a) counterweights, (b) pulleys, (c) nylon cord, (d) rotatable shaft, (e) water reservoir made of PVC, (f) thick-walled rubber tubing, (g) water-jacketed 100 mL gas buret, (h) thermometer, (i) tee connector, (j) Teflon tubing, (k) water manometer, (l) 3-way slide valve.

For reaction solutions containing hydroxyethyl cellulose, 200 ml of water was added to the reactor. The predetermined amount of HEC was then added to reactor in accordance with the procedures described above in the Preparation and Purification of Substrates Section for HEC solutions. The reactor was capped with a teflon lid and then placed in the cold room for overnight stirring. The following morning the reactor was removed from the cold room and placed in the 45°C water bath. Lignosulfonate (for combined substrate experiments) was then added. The catalyst (if present) was added next.

Once substrate and catalysts were added to the reactor, the pH was adjusted (usually to pH 3.0) by addition of 15 % ultrapure HCl (usually 10 - 50 µl was required).

Initiation of Reactions

Reaction solutions were equilibrated in the 45°C water bath for one hour (clocked from when the reactor was first placed in the bath). It was previously determined that one hour was required for 300 ml of water to reach 45°C.

Reactions were initiated by the addition of hydrogen peroxide. Hydrogen peroxide and makeup water were added to a polyethylene bottle and preheated to 45°C. At time zero this solution was added to the reactor via syringe. The nitrogen purge was discontinued and the reactor sealed immediately after the addition of hydrogen peroxide.

Sampling

Samples were usually taken at 15 - 20 minute intervals during the first hour of reaction. For fast reactions, samples were taken more frequently during the initial phases. Times between samples were increased as the reaction slowed. Samples were removed via the sample line, placed in 15 ml glass sample bottles, and immediately placed on ice. Aliquots from this sample were removed immediately for chromatography and viscometry measurements; hydrogen

peroxide was removed from these aliquots using sodium bisulfite. Hydrogen peroxide was not removed from aliquots used in the chemiluminescence assay.

ANALYTICAL PROCEDURES

High Performance Size Exclusion Chromatography

Bio-Rad Bio-Sil SEC 125 and 250 Size Exclusion Columns were used on a Varian 5060 High Performance Liquid Chromatograph. It was equipped with a Varian UV-50 Variable Wavelength Detector and a Hewlett-Packard Integrator.

Data from the detector was also acquired via a data acquisition system. The output from the detector was first passed through a signal amplifier. This amplified signal was then collected using a 286 CompuAdd computer equipped with a data acquisition board. LabTech Notebook® was used to collect and manipulate the signal. A 20 Hz sampling rate was used; one-second averages were computed and saved to files.

The mobile phase used was 50 mM citric acid-disodium hydrogen phosphate (CA-DHP) buffer[93] at pH 3.0 and flowed at 0.8 ml/min. Lignosulfonate samples were diluted in CA-DHP buffer to achieve concentrations of 0.05 to 0.10 g/l; 250 µL of this sample was injected.

Calibration

Sodium polystyrene sulfonates (SPS) were obtained from Scientific Polymer Products, Inc. in five different molecular weight sizes (see Table 4). 1.5 g/l solutions in CA-DHP were made from each standard and analyzed by HPSEC. 5-Sulfosalicylic acid, dihydroxy-benzene sulfonic acid, and phthalic hydrazide were also used and similarly prepared in CA-DHP. Standards and corresponding molecular weights are shown in Table 4. The calibration curve used for the SEC 250 column is shown in Figure 12 (a similar curve was obtained using the SEC 125 column).

A linear region for molecular weight estimation is present between 250 and 100,000 molecular weight units. This provides a good operating range to measure molecular weight changes in the lignosulfonate. From this calibration curve lignosulfonate has an apparent molecular weight of 4300. Lignosulfonates of characterized molecular weights could not be obtained to check the calibration.

Table 4. Molecular weight standards used for the calibration curve shown in Figure 12.

Standard	Molecular Weight
SPS	1,118,000
SPS	400,000
SPS	178,000
SPS	104,000
SPS	8,000
SPS	1,620
5-Sulfosalicylic acid	254.22
Phthalic hydrazide	162.15

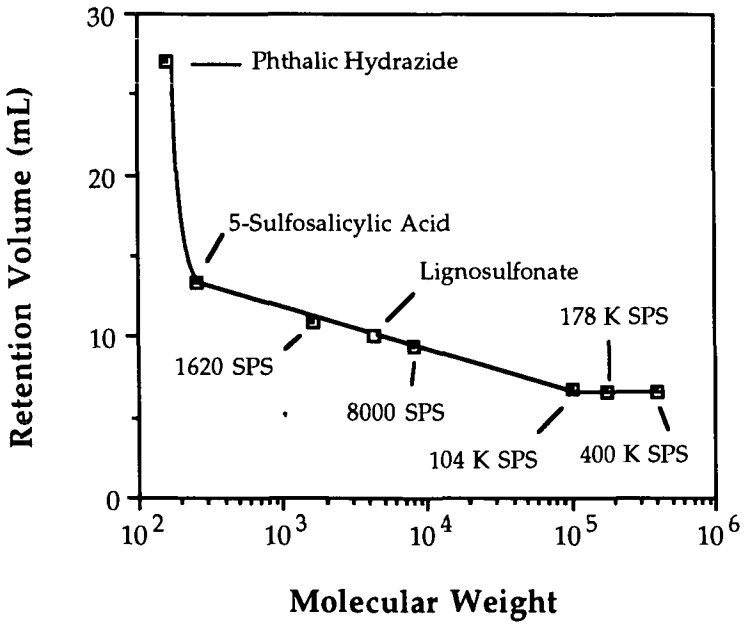

Figure 12. Calibration curve used for determination of molecular weights from HPSEC (data shown for the Bio-Rad SEC 250 column). Mobile phase: 50 mM citric acid-disodium hydrogen phosphate buffer, pH 3.0.

Although sodium polystyrene sulfonates were used to calibrate this column, it has been shown that commercially available proteins can be used to calibrate size-exclusion columns for use with lignosulfonates.[94] It has also been demonstrated that calibration with polystyrenes is not indicative of true lignin molecular weights, although similar slopes are obtained.[95]

Determination of Molecular Weights

LabCalc®, a software program for analysis of spectra, was used to calculate areas of collected peaks. Raw data collected using the data acquisition system was imported into this program. An integration program, INTGAUTO, developed and written by Dr. Michael Friese,[96] was used to break the chromatograph into equally spaced sections. The area of these sections were then determined using a trapezoid approximation technique. Data from this analysis was exported to files.

This data was then imported into Lotus 1-2-3 worksheets for the final determination of molecular weights. The weight- and number-average molecular weights were determined using typical procedures.[97]

Viscometric Determinations

The most accurate technique is to observe the change in the molecular weight distribution during reaction. Another method is to measure the change in the viscosity-average molecular weight. This is done by measuring the intrinsic viscosity of a sample and using an established relationship to determine molecular weight. It must be noted that this latter method only gives relative differences providing no information on the molecular weight distribution.

Molecular weight changes of the HEC polymer were determined by using the Mark-Houwink relationship. The Mark-Houwink equation relates intrinsic viscosity, $[\eta]$, to molecular weight, Mv:[98]

$$[\eta] = KM_v^a$$

The intrinsic viscosity, [η], of a polymer solution is obtained by measuring the specific viscosity, η_{sp}, at several concentrations, c. Plots of η_{sp}/c versus c yield straight lines with intercept equal to the intrinsic viscosity, [η].[98]

Mark-Houwink parameters were found in the literature for HEC in water at 25°C. Brown, et al.[99] reported these values, determined from light scattering measurements, to be: $K = 9.53 \times 10^{-3}$ and $a = 0.87$. Weight-average molecular weights, as determined by light scattering, were used to establish these parameters. HEC samples used by Brown had the following molecular weights (M_W): 625,000, 570,000, 515,000, 190,000, and 80,000.

Intrinsic viscosity measurements were made using a Cannon-Ubbelholde 100 viscometer. The viscometer was placed in a large water bath maintained at 25 ± 0.5°C. A minimum of 1.0 to a maximum of 10.0 mL of sample were added to the viscometer via pipette. Water was then added as needed to obtain a reading (a minimum of 8.0 mL is required for this viscometer).

After each sample measurement was completed, the viscometer was rinsed thoroughly with distilled water and then acetone. The viscometer was then dried completely under vacuum before other samples were tested.

Calibration

The calibration of the Mark-Houwink equation was checked using three samples of HEC obtained from Aqualon. The molecular weights of these standards are only approximate values provided in the product literature. Figure 13 shows the Mark-Houwink equation (straight line) obtained from the literature. The solid circles represent experimentally determined intrinsic viscosities plotted versus the manufacturer's estimate of molecular weight.

Samples obtained from Aqualon, Inc. were reported to have the following molecular weights: 1,300,000, 720,000, and 90,000. These molecular weights reported by

Aqualon for HEC were determined by intrinsic viscosities; consequently, these values are viscosity-average molecular weights and should agree well with the experimental values. However, Aqualon reported that these listed values were only estimates.

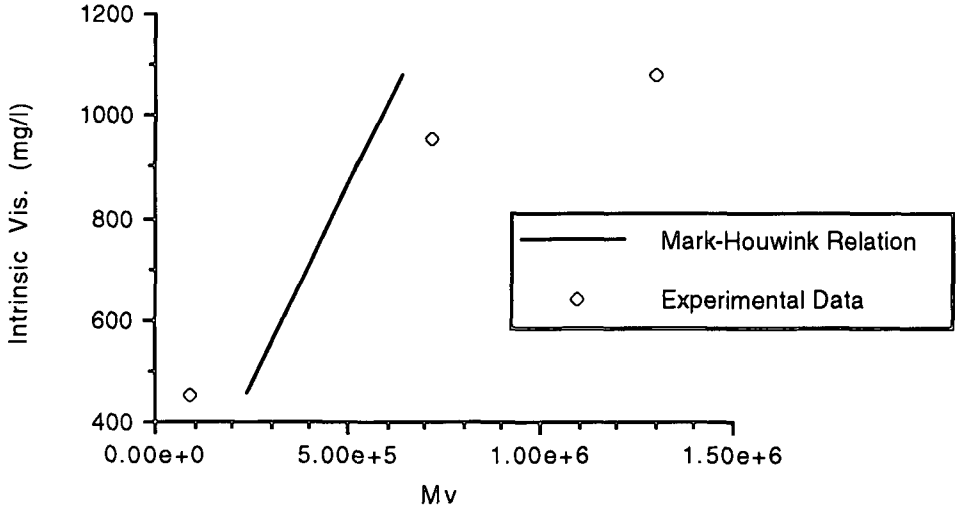

Figure 13. The Mark-Houwink relationship and the experimentally determined intrinsic viscosities plotted versus the molecular weights from the product literature for the three HEC samples.

DETERMINATION OF HYDROGEN PEROXIDE CONCENTRATION

Residual hydrogen peroxide was determined by iodometric titration. 1.0 or 2.0 mL of sample (depending on the original concentration) was added to a freshly prepared solution containing 50 mL distilled water, 10 mL 1 N KI, 10 mL 4 N H_2SO_4, and 3 drops of a saturated solution of $(NH_4)_2MoO_4$. This solution was then titrated with 0.01 N (or 0.001N) $Na_2S_2O_3$ to a starch endpoint. Three determinations were made for most samples, with a minimum of two always performed.

The following formula was used to calculate the concentration of residual hydrogen peroxide:

$$N_{H_2O_2} = \frac{N_{Thio} V_{Thio}}{V_{H_2O_2}}$$

The amount of hydrogen peroxide decomposed was determined by measuring the amount of oxygen evolved. The following formula[77] was used to calculate the number of mmoles of oxygen evolved:

$$O_2\,(\text{mmoles}) = \frac{V_g}{22.4} \times \frac{273}{273+T} \times \frac{P - P_v}{760} + D$$

where V_g is the volume of oxygen evolved (ml), T is the temperature of water jacket (°C), P is the atmospheric pressure (mm of Hg), Pv is the vapor pressure of water (mm of Hg) and

$$D = a\frac{V_i}{22.4}\frac{P}{760}$$

where a is 0.02 and V_i is the initial reaction solution volume (ml). As the decomposition of hydrogen peroxide follows the reaction:

$$2H_2O_2 \text{ --> } O_2 + 2H_2O$$

the amount of hydrogen peroxide decomposed can be calculated from:

$$[H_2O_2]_d = 2000 \times \frac{O_2 \text{ mmoles}}{V_s}$$

where V_S is the reactor solution volume. The amount of hydrogen peroxide consumed during reaction was determined by difference:

$$[H_2O_2] \text{ consumed} = [H_2O_2] \text{ original} - \{ [H_2O_2] \text{ residual} + [H_2O_2] \text{ decomposed} \}.$$

THE CHEMILUMINESCENCE ASSAY

An Amincon ChemGlow Photometer was used for all chemiluminescence measurements. Samples were placed in to 6 x 50 mm borosilicate test tubes (Kimble Glass). A data acquisition system was used to capture the signal from the photometer. Data was collected for

90 seconds at a rate of 20 Hz (20 samples per second); one-second averages were then calculated and saved on disk. Area under the light intensity curve for each sample, up to 60.0 seconds, was determined from this averaged data.

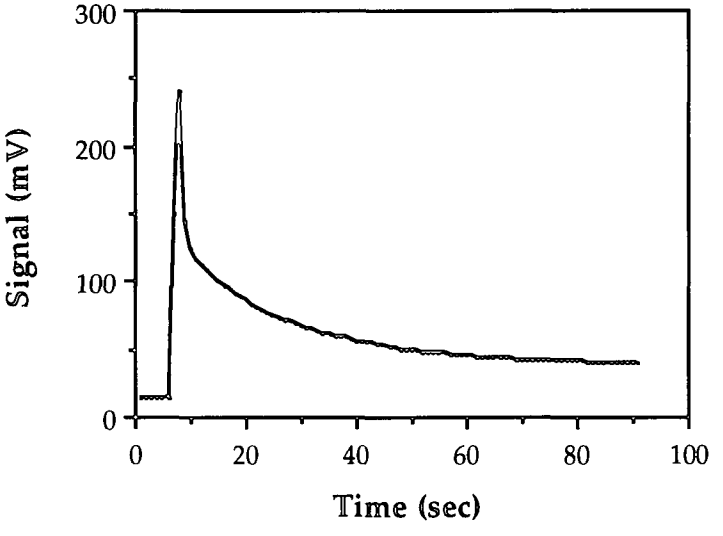

Figure 14. Light intensity curve for a typical sample showing millivolts emitted per sec for a time span of 90 seconds.

The area under the light intensity curve (Figure 14) was, therefore, measured for all samples. Following the suggestion of Reitberger and Gierer, the value obtained sixty seconds after reaction initiation was tabulated and compared between samples. This value has been termed the chemiluminescence, with corresponding units of millivolts-seconds. For all samples, at least three determinations were made.

Solutions

Phthalic hydrazide was prepared as a concentrated solution (5.5 mM) in water. Solutions A and B are required for this assay. The ratio of components suggested by Reitberger and Gierer are: 1.0 mL Solution A (1 M Na_2CO_3 and 25 mM EDTA), 0.2 mL Solution B [50 mM

H_2O_2 and 50 mM $(NH_4)_2S_2O_8$], and 0.1 mL of sample. For best results it has been recommended[100] that sample volumes in the photometer should not exceed 100 µl. Volumes of solution and sample were reduced to meet this 100 µl volume constraint while maintaining ratios of components as suggested by Reitberger and Gierer. Unless specified otherwise 127 µl of sample containing 0.5 mM phthalic hydrazide was placed into 1.0 mL of Solution A. 25 µL of this solution was then added to each of three test tubes. 5 µl of Solution B was then injected into the test tube once inside the photometer.

Original Method

For the original assay, as described by Reitberger and Gierer, phthalic hydrazide was added directly to reaction solutions. A 5.5 mM stock solution of phthalic hydrazide was prepared (pH ~ 6.0 was needed to achieve complete solubility). The necessary volume of phthalic hydrazide required for the planned reaction was measured out via pipette and added directly to the reactor.

The reactor at this point, depending on which experiment was being performed, contained water and substrate (lignosulfonate or HEC, if present). Catalyst was then added after the addition of phthalic hydrazide. Hydrogen peroxide was added last, to initiate the reaction as described in a previous section. Reaction procedures were as for other reactions and have also been described previously.

Sampling was performed as outlined earlier for all reactions. From each reaction sample withdrawn from the reactor, a predetermined amount of sample was added to 1.0 mL of Solution A for a duration of one or five minutes, as specified in the text. Hydrogen peroxide was not removed from these samples. After the one to five minutes incubation time in Solution A, 115 µl (for samples containing 0.5 mM phthalic hydrazide) was added to each of three to six 6 x 50 mm borosilicate test tubes (Kimble Glass). For samples containing 0.25 mM phthalic hydrazide, 279 µl of sample was added to 1.0 ml of Solution A.

Each test tube was individually placed in the ChemGlow Photometer for analysis. The data acquisition system was started for 5 to 7 seconds before the addition of Solution B, to obtain a baseline from the photometer. After a suitable baseline was collected, 5 µl of Solution B was added. Data was collected for 90 seconds after the initiation of the data acquisition system.

External Method

Reaction solutions were prepared as described for the Original Method, omitting the addition of phthalic hydrazide. When reaction samples were removed, 1.0 mL of sample was added to 0.1 mL of a 5.5 mM stock solution of phthalic hydrazide. The sample was held in the phthalic hydrazide solution for 1 to 5 minutes after which 0.127 mL of this solution was added to 1.0 mL Solution A. Samples were then treated in the usual manner.

UV-Irradiation of Hydrogen Peroxide

UV-irradiation of hydrogen peroxide solutions was performed to produce hydroxyl radicals to calibrate the chemiluminescence assay. As a solution of hydrogen peroxide is exposed to UV-irradiation, the concentration of hydroxyl radicals produced increases.

A Spectroline Transilluminator (Model TR-302, 302 nm Ultraviolet) was used as the UV-source for these experiments. A 50 mL solution containing 100 mM H_2O_2 and 0.5 mM phthalic hydrazide was prepared. This solution was poured into a 150 mL beaker which was placed directly over the UV source. The reaction was initiated by turning on the UV-light source.

Samples (2 - 8 mL) were withdrawn from the beaker by pipette. Samples were taken frequently during the initial 50 minutes of the reaction. As the reaction slowed, the time between samples increased.

PULP BLEACHING

Pulp bleaching was performed in plastic bags. Kappa numbers and viscosities were measured using standard test methods.[101,102]

RESULTS AND DISCUSSION

This section, which is divided into five parts, contains a complete summary of all experimental results. The first part describes a modified chemiluminescence assay used for detection of hydroxyl radicals. The second and third parts contain results from reactions with lignosulfonate and hydroxyethyl cellulose, respectively. This is followed by a discussion of selectivity based on these reactions. The final section describes results obtained when these substrates were combined in reaction solution.

DETECTION OF HYDROXYL RADICALS

The chemiluminescence assay is described in the Literature Review section. This assay measures the production of hydroxyl radicals (•OH) by monitoring the chemiluminescence produced from the oxidation of a hydroxylated compound. This assay uses a reagent which is readily available and does not require expensive analytical equipment. The calibration of this assay, an evaluation of its sensitivity, and a modification made to the originally published procedure are described in the following sections.

Calibration

The chemiluminescence assay was calibrated using UV-irradiation of hydrogen peroxide solutions to produce hydroxyl radicals.[103] The chemiluminescence from UV-irradiation of a solution containing 100 mM H_2O_2 and 0.5 mM phthalic hydrazide was measured (Figure 15). Data points in Figure 15 represent the area under the light intensity curve (see Materials and Methods section) for each sample taken at the designated UV-exposure time.

Maximum chemiluminescence is achieved after only 90 minutes of exposure. After this point the chemiluminescence begins to decrease. Phthalic hydrazide is continually hydroxylated during this experiment. For the chemiluminescence to decrease, the amount of

hydroxylated phthalic hydrazide must decrease. This indicates that phthalic hydrazide is degraded in the reactive environment.

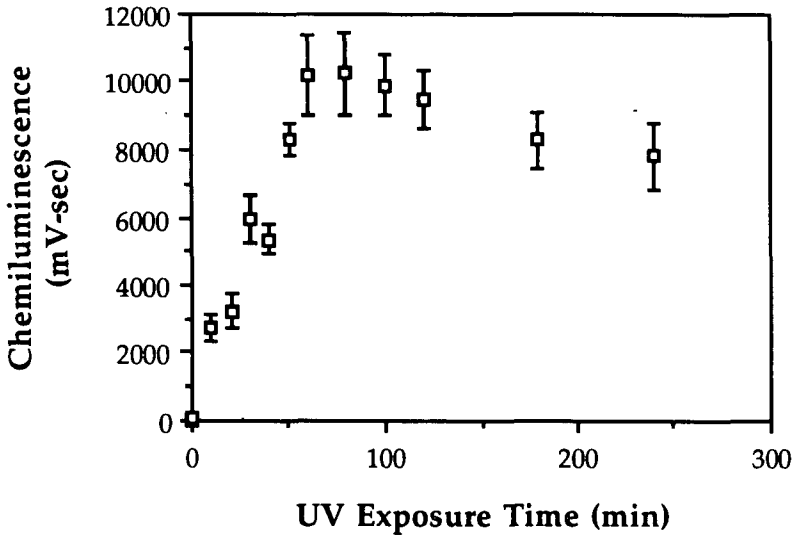

Figure 15. Chemiluminescence versus UV exposure time for a solution containing 100 mM H_2O_2 and 0.5 mM phthalic hydrazide in water. Error bars represent ± 95% confidence intervals determined from six replicates of each sample.

A rough calibration of the chemiluminescence assay can be obtained from this method. At the maximum chemiluminescence observed at 90 minutes, it can be assumed that all phthalic hydrazide has been hydroxylated. Assuming that no phthalic hydrazide has degraded in the reaction at this point, and that one mole of hydroxyl radicals reacts with one mole of phthalic hydrazide, 0.5 mM of hydroxyl radicals have been produced after 90 minutes. Therefore, 200 mV-sec correspond to 0.01 mM (10 μM) of hydroxyl radicals produced.

Sensitivity

For the chemiluminescence assay to be suitable for measuring •OH formation, it must be sensitive as well as unobtrusive. To test the sensitivity of the chemiluminescence assay, hydroxyl radicals were measured in solutions which were known to generate hydroxyl radicals. Fe-EDTA in the presence of hydrogen peroxide is known to produce hydroxyl radicals.[86]

Solutions containing 100 mM H_2O_2 and various levels of Fe-EDTA were therefore chosen for evaluation.

The chemiluminescence from reactions of H_2O_2 with 0.1, 0.25, 0.5 and 10.0 mM Fe-EDTA were measured (Figure 16). For all reactions containing Fe-EDTA and hydrogen peroxide, an initial increase in the chemiluminescence was observed, which was followed by a decline. Rates of this initial increase are dependent on Fe-EDTA concentration. For the 10.0 mM Fe-EDTA run, this initial increase was extremely rapid. As the Fe-EDTA concentration was decreased, the rate at which chemiluminescence was initially produced decreases.

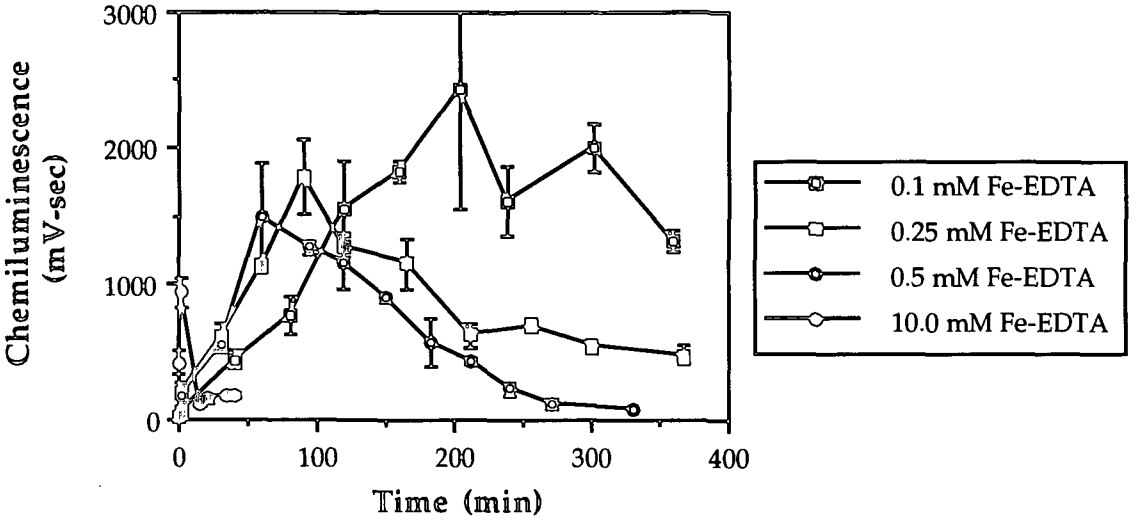

Figure 16. Chemiluminescence versus reaction time obtained for reactions containing 100 mM H_2O_2, 0.5 mM phthalic hydrazide, and various concentrations of Fe-EDTA at pH 3.0 and 45°C.

For the blank runs (no H_2O_2 or Fe-EDTA), no chemiluminescence was observed (data not shown, see Appendix I). This is expected as few radicals will be produced in the presence of hydrogen peroxide alone. And, of course, when no hydrogen peroxide is present, no hydroxyl radicals are formed.

At different Fe-EDTA concentrations, the amount of chemiluminescence produced (i.e., hydroxyl radical concentration) varied. The sensitivity of the assay to hydroxyl radical concentration is apparent in Figure 16 (the times of maximum chemiluminescence can be clearly distinguished). However, the decline in chemiluminescence for all reactions suggest hydroxylated phthalic hydrazide is participating in other reactions.

As the phthalic hydrazide present in reaction solutions was continually hydroxylated, the reduction in chemiluminescence during these reactions must therefore be due to the destruction of the hydroxylated phthalic hydrazide. This decrease in chemiluminescence was also observed in the UV-irradiation experiment (Figure 15). This is a serious drawback of the technique; destruction of phthalic hydrazide precludes accurate determination of hydroxyl radical production.

In addition, the concentration of phthalic hydrazide in these solutions was found to affect reaction rates. As the concentration of phthalic hydrazide was increased, the rate at which hydrogen peroxide reacts decreased (Figure 17). This verifies that phthalic hydrazide scavenges hydroxyl radicals, slowing the radical-driven decomposition of H_2O_2.[50,73]

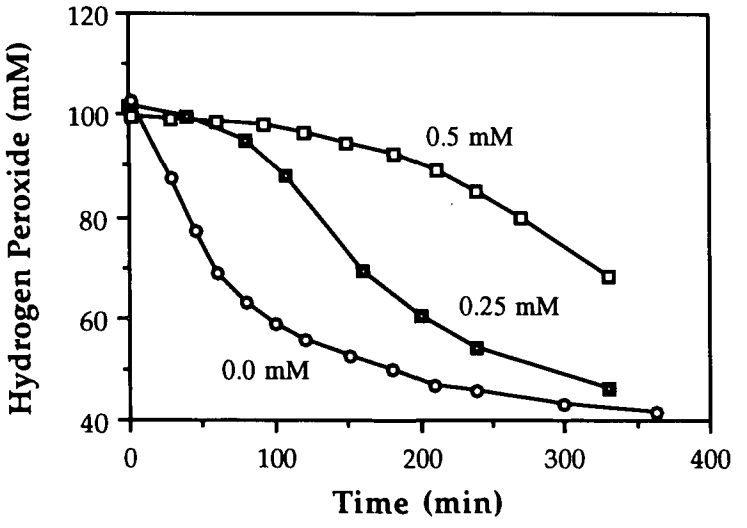

Figure 17. Residual hydrogen peroxide concentration versus reaction time for a control reaction and reactions containing 0.25 and 0.5 mM phthalic hydrazide. Reaction conditions: 100 mM H_2O_2, 0.5 mM Fe-EDTA, pH 3.0 and 45°C.

The above results indicate that the chemiluminescence assay can measure the production of hydroxyl radicals. However, as the phthalic hydrazide in reaction solutions is degraded and affects reaction rates, accurate determination of the amount of hydroxyl radicals produced is not possible. The following section presents a modification made to the chemiluminescence assay to alleviate this problem.

The External Method of the Chemiluminescence Assay

As the chemiluminescence method was originally described, phthalic hydrazide was added directly to reaction solutions.[52] In the external method of the chemiluminescence assay, developed during this work, phthalic hydrazide was not added in situ. Samples were periodically removed from the reactor and exposed to phthalic hydrazide for a predetermined time. A portion of this sample was then placed in the photometer for measurement of chemiluminescence.

The duration which a sample was exposed to phthalic hydrazide was evaluated in the Fe-EDTA + H_2O_2 system. Two incubation times were chosen, one and five minutes. The five minute incubation gave a slight increase in chemiluminescence as compared to the one minute period (Figure 18).

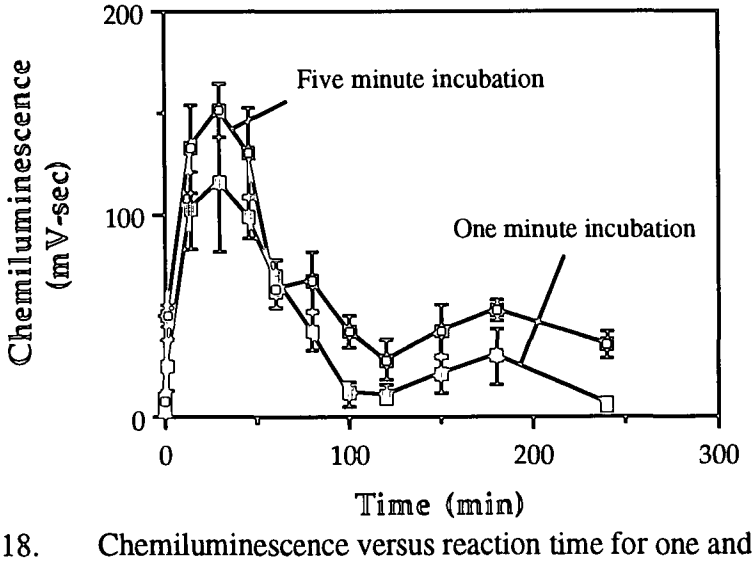

Figure 18. Chemiluminescence versus reaction time for one and five minute incubation times using the external method of the chemiluminescence assay. Reaction conditions: 100 mM H_2O_2, 0.5 mM Fe-EDTA, pH 3.0, and 45°C. Error bars represent ± 95% confidence intervals determined from four replicates.

During this incubation period, H_2O_2 continued to react, producing hydroxyl radicals (reaction samples were not cooled). As the incubation time of five minutes gave only a slight increase in chemiluminescence, it is better to use the shorter incubation period of one minute. After five minutes exposure to the reaction system, phthalic hydrazide degradation is likely to occur. It is assumed that no degradation of the phthalic hydrazide occured during the one minute incubation time.

The chemiluminescence for solutions containing 100 mM H_2O_2 and 0.1, 0.25, 0.5 and 10.0 mM Fe-EDTA was measured using this modified procedure. The chemiluminescence obtained using the external method (Figure 19) was substantially reduced from that obtained with the original method (Figure 16). This is due to the non-cumulative nature of this method. The external method provides an estimate of the instantaneous hydroxyl radical concentration at the time which the measurement is made. The original method measured the total concentration of hydroxyl radicals produced.

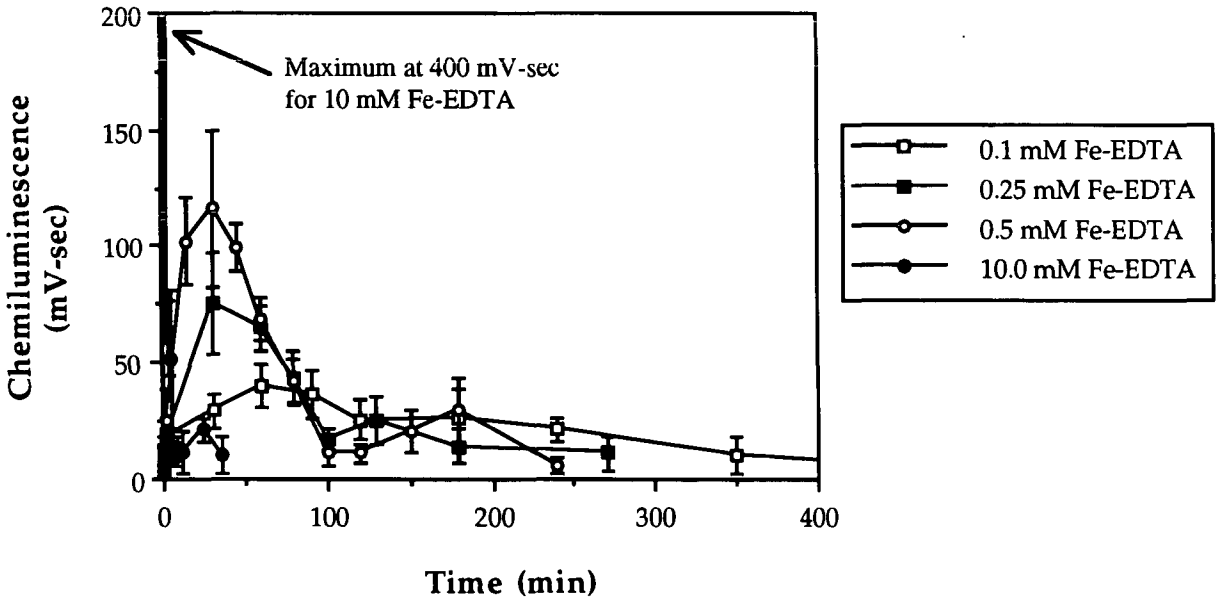

Figure 19. Chemiluminescence versus reaction time, obtained using the external method of the chemiluminescence assay. Reactions conditions: 100 mM H_2O_2 and 0.1, 0.25, 0.5, and 10.0 mM Fe-EDTA at pH 3.0 and 45°C. Error bars represent ± 95% confidence intervals for three replicates.

The trend in chemiluminescence production for the H_2O_2 + Fe-EDTA reactions was similar for all concentrations of Fe-EDTA. During the initial phase of each reaction, the chemiluminescence (or ∘OH concentration) was relatively high. As the reaction proceeds (and slows), the chemiluminescence decreased although H_2O_2 continued to react (Figure 20).

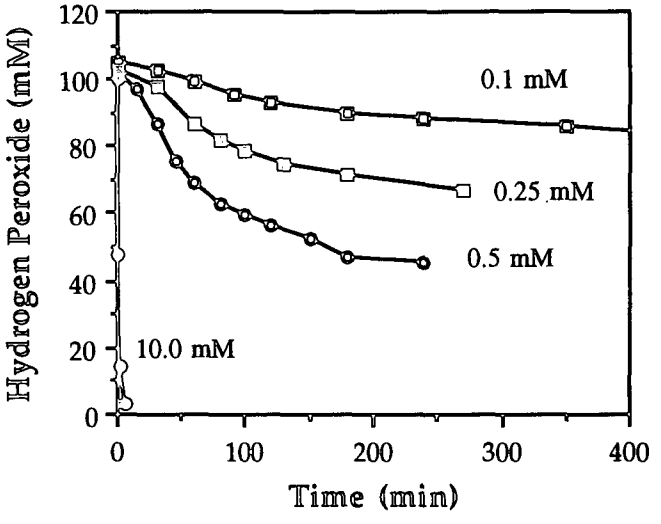

Figure 20. Residual hydrogen peroxide versus reaction time for those reactions shown in Figure 18. Reaction conditions: 100 mM H_2O_2 and 0.1, 0.25, 0.5, and 10.0 mM Fe-EDTA at pH 3.0 and 45°C.

The level of chemiluminescence was lower using the external method; however, differences in chemiluminescence are still distinguishable for several concentrations of Fe-EDTA (Figure 19). For 0.1 mM Fe-EDTA, the maximum chemiluminescence achieved was 38 mV-sec (3.8 μM ∘OH) at 60 minutes. For the 0.25 mM Fe-EDTA reaction, maximum chemiluminescence is observed at 40 minutes to be 75 mV-sec (1.9 μM ∘OH). The difference between these two maxima, 37 mV-sec or 1.9 μM ∘OH, is readily observed.

Summary

The chemiluminescence assay is an adequate technique for measuring hydroxyl radicals generated in solutions. This method is relatively simple, does not require expensive equipment or exotic reagents which require synthesis. This assay, however, does suffer from

some drawbacks. The presence of phthalic hydrazide in reaction solutions affects reaction rates. In addition, hydroxylated phthalic hydrazide is degraded when exposed to systems which rapidly produce hydroxyl radicals.

An improvement was made to this assay which eliminates the effect of phthalic hydrazide on reaction rates. This modification also prevents the eventual destruction of phthalic hydrazide by reactive systems. The chemiluminescence obtained from samples analyzed using this method is low. This is due to the small sample volume required for measurement of chemiluminescence in the photometer. Additional modifications can be made to improve this assay, and are discussed in the Recommendations section.

The external method of the chemiluminescence assay can detect differences in chemiluminescence of approximately 40 mV-sec, or 2 μM •OH. For this study, only relative differences in the hydroxyl-radical generating ability of biomimetic systems is of interest. Chemiluminescence measurements will therefore be expressed in mV-sec, and not converted to μM of hydroxyl radicals produced.

CATALYZED OXIDATION OF LIGNOSULFONATE

Lignosulfonate was reacted with hydrogen peroxide alone and with each of the three biomimetic catalysts. For each reaction, the molecular weight distribution of lignosulfonate, hydrogen peroxide concentration, and production of hydroxyl radicals were measured.

Concentrations of substrates and reactants (Table 5) were selected to resemble those commonly found in typical bleaching applications, while remaining within the constraints required by the analytical techniques. A pH of 3.0 was selected, that at which the mimicked enzyme, lignin peroxidase, exhibits maximum activity.[89] Data from all experiments are tabulated in Appendix III.

Table 5. Reaction conditions for the catalytic oxidation of lignosulfonate by hydrogen peroxide.

Lignosulfonate	3.4 g/l
H_2O_2	50 mM
Catalyst	
$FeSO_4$ and Fe-EDTA	0.5 mM
Hemoglobin (as Fe)	0.062 mM
Temperature	45°C
pH	3.0

Hemoglobin has a molecular weight of 64,500 daltons with each molecule possessing four iron atoms. An extremely large concentration of hemoglobin (8.1 g/l) would be needed to match the 0.5 mM iron concentration used in the $FeSO_4$ and Fe-EDTA experiments. Consequently, the concentration of hemoglobin used in these experiments was arbitrarily selected, using as large a concentration as was practical (1.0 g/l), but not to exceed the concentration of lignosulfonate (3.4 g/l).

Lignosulfonate Degradation

Chromatograms from a $FeSO_4$ catalyzed reaction are shown in Figure 21. The absorbance at 280 nm was continuously measured as samples eluted from the column. A clear, increase in retention time of the molecular weight distribution of lignosulfonate is observed. Chromatograms of reactions samples from experiments with the other catalysts are similar (see Appendix III).

In size-exclusion chromatography, molecular mass determines elution time. Large molecules elute earlier, as they are too large to penetrate the pores of the gel which make up the column packing. Small molecules can penetrate these pores and are therefore retained. The rightward shift in the molecular weight distribution of lignosulfonate observed during reaction (Figure 21), showing an overall decrease in the molecular weight of lignosulfonate, is indicative of depolymerization.

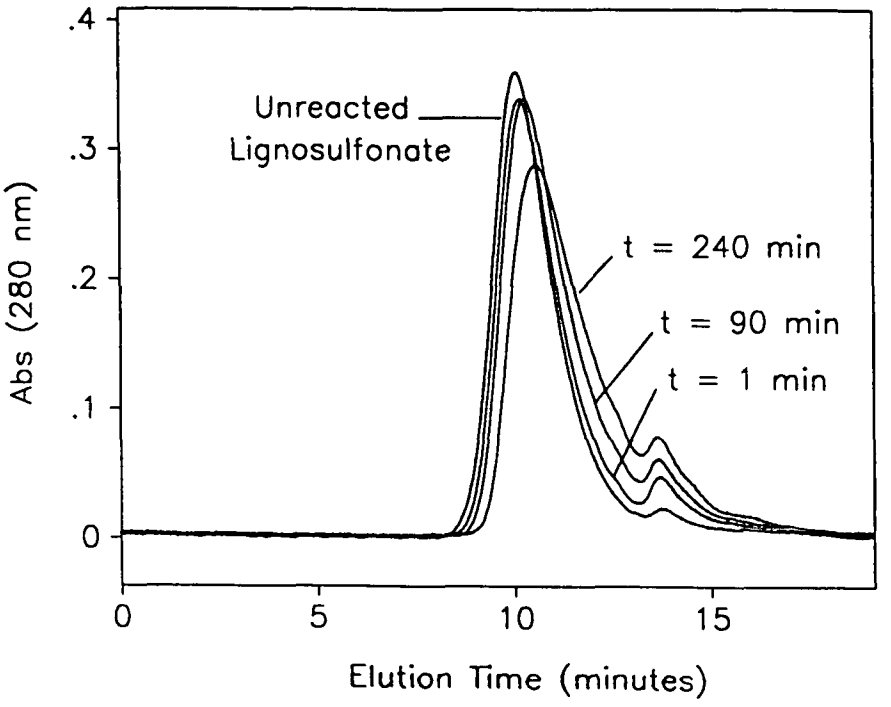

Figure 21. Size-exclusion chromatograms of several samples from the $FeSO_4$ catalyzed oxidation of lignosulfonate. See Table 5 for reaction conditions.

Weight-average molecular weights (M_w) of lignosulfonate were determined from the distribution profiles obtained from duplicate injections of each sample. All biomimetic compounds were able to catalyze bond cleavage in lignosulfonate (Figures 22 and 23). In the $FeSO_4$ and hemoglobin catalyzed reactions, substantial depolymerization of lignosulfonate as compared to the control was achieved. The Fe-EDTA catalyzed reaction showed only a slight overall decrease in lignosulfonate M_w. Rates of lignosulfonate degradation are compared in the section on kinetics.

Depolymerization of lignosulfonate during these reactions is apparent from the decrease in M_w. As discussed in the Literature Review, hydroxyl radicals are produced in solutions of hydrogen peroxide and iron,[50,73] chelated iron,[85,86] and hemoglobin.[87] Hydroxyl radicals add to aromatic rings in lignin, forming hydroxycyclohexadienyl radicals.[104] These radicals then decay, resulting in chain cleavage.

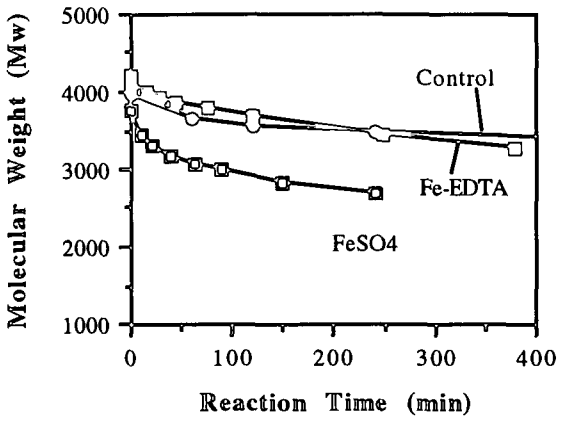

Figure 22. Weight-average molecular weights of lignosulfonate versus reaction time for control, $FeSO_4$ and Fe-EDTA catalyzed reactions. See Table 5 for reaction conditions.

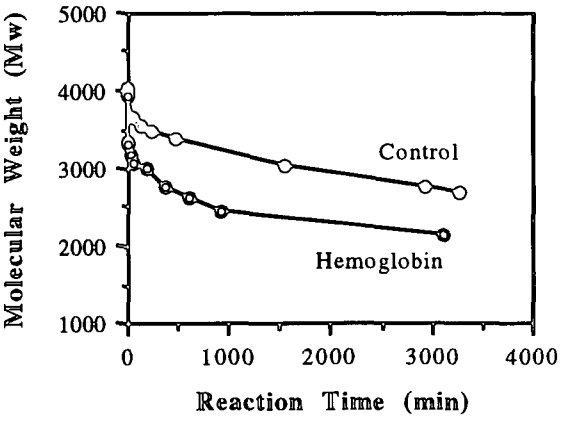

Figure 23. Weight-average molecular weights of lignosulfonate versus reaction time for the control and hemoglobin catalyzed reactions. See Table 5 for reaction conditions.

Although not clearly visible in Figure 23, when hemoglobin is added to solutions containing lignosulfonate, prior to the addition of hydrogen peroxide, a reduction in the weight-average molecular weight of lignosulfonate is observed (Table 6). This contributes to the larger overall reduction in lignosulfonate molecular weight observed for this reaction.

Table 6. Molecular weight of lignosulfonate before and after addition of hemoglobin (no H_2O_2 present). (3.4 g/l Lignosulfonate, 1.0 g/l hemoglobin.)

Sample	Lignosulfonate (M_w)
Before addition of hemoglobin	4300
After addition of hemoglobin	3300

Experiments with hemoglobin and lignosulfonate, in the absence of hydrogen peroxide, showed that no significant degradation of the lignosulfonate occurred after the initial drop (see Appendix III). This initial decrease in molecular weight was not observed in either the $FeSO_4$ or Fe-EDTA catalyzed control reactions (no H_2O_2) (see data in Appendix III).

The initial decrease in the M_w of lignosulfonate observed upon addition of hemoglobin (Table 6), indicates that hemoglobin is able to catalyze some chain cleavage in the absence of hydrogen peroxide. Aqueous solutions of hemoglobin contain mostly methemoglobin,[105] where the iron is in the +3 oxidation state and unable to bind oxygen.[106]

When hemoglobin solutions were prepared for use in these experiments, solutions were not deoxygenated. The lignosulfonate solution in the reactor was purged with nitrogen (see Materials and Methods section) prior to addition of the hemoglobin. The dissolved oxygen in the hemoglobin solution may participate in a slight oxidative degradation of lignosulfonate. The elevated temperature and acidic pH provide a sufficient environment for this limited reaction to occur.

Hydrogen Peroxide Consumption Versus Decomposition

During lignosulfonate degradation reactions, reacted hydrogen peroxide was either consumed through oxidation of lignosulfonate or decomposed to oxygen. The net effect of these two reactions is reflected by the change in the residual hydrogen peroxide concentration over time (Figures 24 and 25). The addition of $FeSO_4$ results in the largest overall reaction of hydrogen peroxide. Fe-EDTA and hemoglobin both catalyze the disappearance of hydrogen peroxide, but not to the same extent as $FeSO_4$.

The reactor used for these experiments (see Materials and Methods section) was equipped with a device to measure oxygen as it was produced. Hydrogen peroxide decomposes to

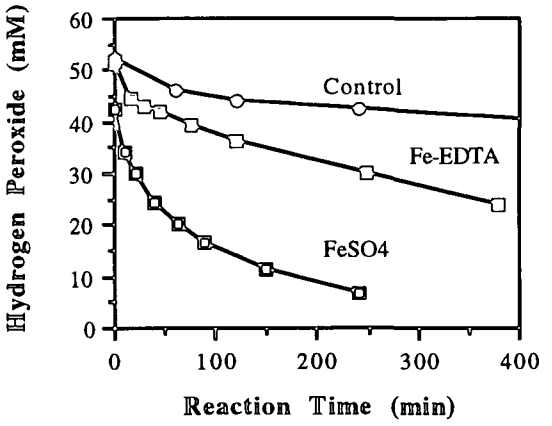

Figure 24. Residual hydrogen peroxide concentration versus reaction time for the control, $FeSO_4$, and Fe-EDTA reactions with hydrogen peroxide and lignosulfonate.

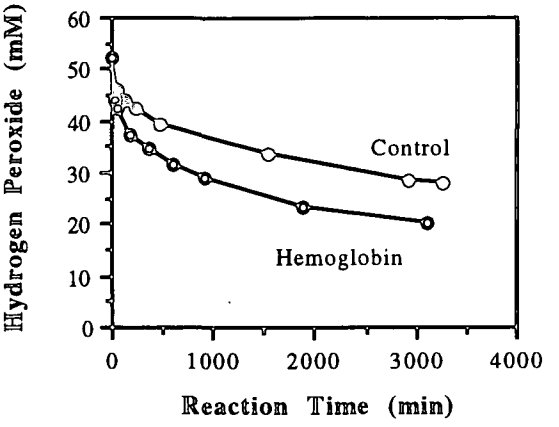

Figure 25. Residual hydrogen peroxide concentration versus reaction time for the hemoglobin and control reactions with hydrogen peroxide and lignosulfonate.

oxygen via a complex radical mechanism,[73] which can be summarized as:

$$2H_2O_2 \text{ --> } 2H_2O + O_2$$

Knowing the amount of peroxide converted to oxygen and the residual peroxide concentration, the amount of peroxide consumed by reaction could be determined.

There are substantial differences between the three catalysts in the amount of hydrogen peroxide which was decomposed to oxygen (Figure 26). For the control reaction, when no iron catalyst was present, there was an initial increase in the amount of peroxide decomposed to oxygen. This levels off as most peroxide was then consumed in the reaction.

The initial increase in the amount of H_2O_2 decomposed to oxygen in the control reaction may be due to the presence of trace metals, although the system has been carefully prepared to be metal-free. As lignosulfonate is degraded, phenolic products formed may chelate

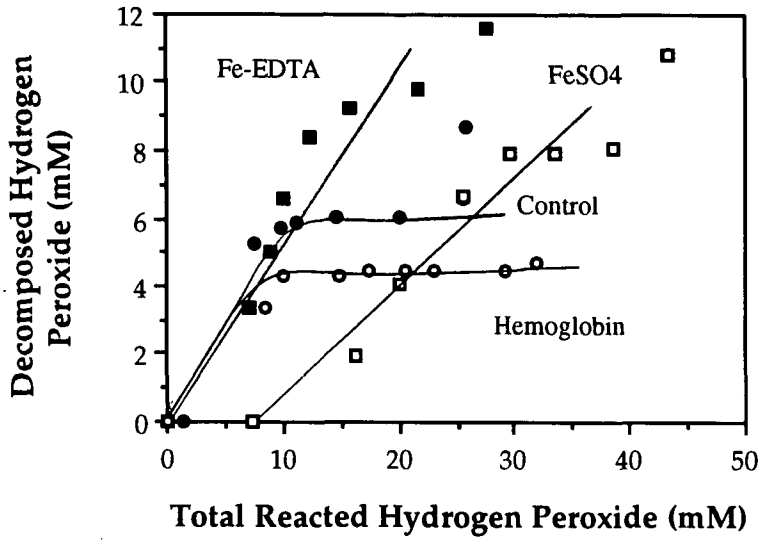

Figure 26. Amount of hydrogen peroxide decomposed to oxygen versus the total amount of hydrogen peroxide reacted during the oxidation of lignosulfonate. Reaction conditions as in Table 5.

these metals and render them inactive. This slows down the decomposition to result in more peroxide being consumed in oxidation of lignosulfonate. It is also possible that certain lignosulfonate degradation products may catalyze the decomposition of hydrogen peroxide. As these products are degraded or altered, the decomposition of peroxide is slowed.

The hemoglobin catalyzed reaction exhibits a trend similar to that of the control. After an initial increase, the amount of hydrogen peroxide which was decomposed to oxygen levels off. The presence of hemoglobin decreased the amount of hydrogen peroxide decomposed to oxygen. Hemoglobin, which is known for its ability to transport oxygen, is obviously superior to the other catalysts in this regard.

The addition of $FeSO_4$ to reaction solutions caused a substantial decrease in the decomposition of hydrogen peroxide (or an increase in the oxidation of substrate). In the $FeSO_4$ catalyzed reaction, Figure 26 shows that for the first ~8 mM of H_2O_2 reacted, all H_2O_2 was consumed by reaction. Alternatively, the addition of Fe-EDTA resulted in a substantial increase in

the amount of decomposed hydrogen peroxide. These results explain why little degradation of lignosulfonate was seen in the Fe-EDTA catalyzed reaction (Figure 22). Most of the hydrogen peroxide was lost in conversion to oxygen and not utilized in oxidative degradation of lignosulfonate as catalyzed by Fe-EDTA.

Significant differences in the amount of hydrogen peroxide which was decomposed to oxygen is observed for each catalyst. Reproducibility of the $FeSO_4$ and Fe-EDTA reactions show some scatter (Figure 27), but the trends for each catalyst are clearly different. These differences are related to the Fe(II) --> Fe(III) catalytic cycle.

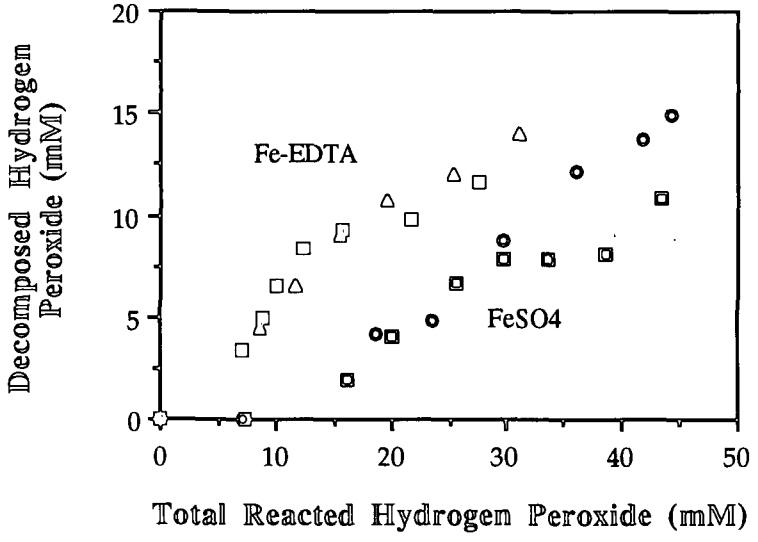

Figure 27. Amount of hydrogen peroxide decomposed to oxygen versus the total amount of hydrogen peroxide reacted during the oxidation of lignosulfonate for two replicates of the $FeSO_4$ and Fe-EDTA catalyzed reactions.

$FeSO_4$, Fe-EDTA, and hemoglobin participate in the Fenton radical chain reaction. Fe(II) is initially oxidized by H_2O_2 to Fe(III). Fe(III) is then reduced to Fe(II) by HO_2° or H_2O_2, producing O_2 in reaction with the latter (see Equations 5 and 6 in the Literature Review section). For the $FeSO_4$ reaction, less H_2O_2 was decomposed to oxygen. This indicates that decrease in O_2 evolution may be due to decreased reduction of Fe(III) to Fe(II).

For Fe-EDTA, the presence of the chelated iron alters the catalytic cycle from that of unchelated iron. In this case, the reduction of Fe(III)-EDTA to Fe(II)-EDTA with concomitant production of oxygen predominates.

For the conditions evaluated in this study, the presence of chelated iron causes a substantial increase in this decomposition. Hemoglobin is obviously the most efficient catalyst as it results in the least amount of hydrogen peroxide lost as oxygen.

Excessive decomposition of hydrogen peroxide to oxygen is not an efficient use of oxidant. Trace quantities of iron present in commercial hydrogen peroxide bleaching systems typically has been thought to be detrimental to bleaching, resulting in an increased decomposition of hydrogen peroxide to oxygen.[74] The choice of appropriate catalysts can minimize this decomposition.

Kinetics of Lignosulfonate Degradation

Lignosulfonate degradation reactions were characterized in two ways. First, a kinetic analysis was performed to determine empirical rate laws. Degradation of lignosulfonate was also characterized by comparing rates of chain scission at specific concentrations of hydrogen peroxide.

Empirical Rate Laws

Rate laws for chemical reactions are written as a function of the disappearance of reactant. The analogous relationship for polymer degradation can be written in terms of the concentration of intact bonds. The change in the concentration of bonds with time will be dependent on the number of bonds present and the concentration of reactant. The rate equation applicable to all of the catalyzed reactions is therefore:

$$-\frac{d\,[\text{bonds}]}{dt} = k_1\,[\text{bonds}]^{a}\,[C_H]^{b} \qquad [7]$$

where k_1 represents the overall rate constant, a the reaction order in bonds, b the reaction order in hydrogen peroxide, and C_H the concentration of hydrogen peroxide.

The number of intact bonds can be determined from the number-average degree of polymerization, DP_n, as follows:[107]

$$[\text{bonds}] = \frac{m}{u}\,\frac{(DP_n - 1)}{(DP_n)} \qquad [8]$$

where m is the mass of the polymer and u the mass of the monomer. This equation can be rearranged to give the following proportionality:

$$[\text{bonds}] \propto 1 - \left(\frac{1}{DP_n}\right) \qquad [9]$$

As DP_n is proportional to M_n, and M_n is related to M_w, Equation 9 can be rewritten as:

$$[\text{bonds}] \propto 1 - \left(\frac{1}{M_w}\right) \qquad [10]$$

For these systems, it is most likely that bonds are broken randomly, therefore, the decrease in the concentration of bonds will exhibit a first order dependence on the concentration of bonds present.[108] However, evaluation of rate data according to Equation 7 (with a = 1) showed that the rate is independent of the concentration of bonds. Although the change in the concentration of bonds is measurable, this change is relatively small compared to the change in hydrogen peroxide concentration. Equation 10 can then be simplified to give:

$$-\frac{d\,[\text{bonds}]}{dt} = k_1' \left[C_H\right]^b \qquad [11]$$

where k_1' is a modified rate constant equal to [bonds] x k_1.

The differential method was used to evaluate the reaction order **b** for the dependence of the rate on hydrogen peroxide in Equation 11. Reaction rates were determined by calculating slopes from [bonds] versus time plots. A log-log plot of the reaction rate versus hydrogen peroxide concentration yields a line of slope **b**.

Once the reaction order **b** was determined, the rate constant **k_1'** was calculated using the integration method. In this method, the rate equation was integrated over time and plotted to give a line with a slope equal to the rate constant (plots are shown in Appendix IV). Values of parameters obtained for each catalyst are summarized in Table 7.

For the $FeSO_4$, Fe-EDTA, and control reactions, there is a change in the reaction order with H_2O_2 concentration (Figure 28). At high H_2O_2 concentrations, the reaction rate exhibits a significant dependence on hydrogen peroxide. Once the concentration of peroxide drops below a certain value, the rate becomes substantially less dependent on hydrogen peroxide. The data for the hemoglobin reaction is slightly curved, exhibiting only a slight change in slope.

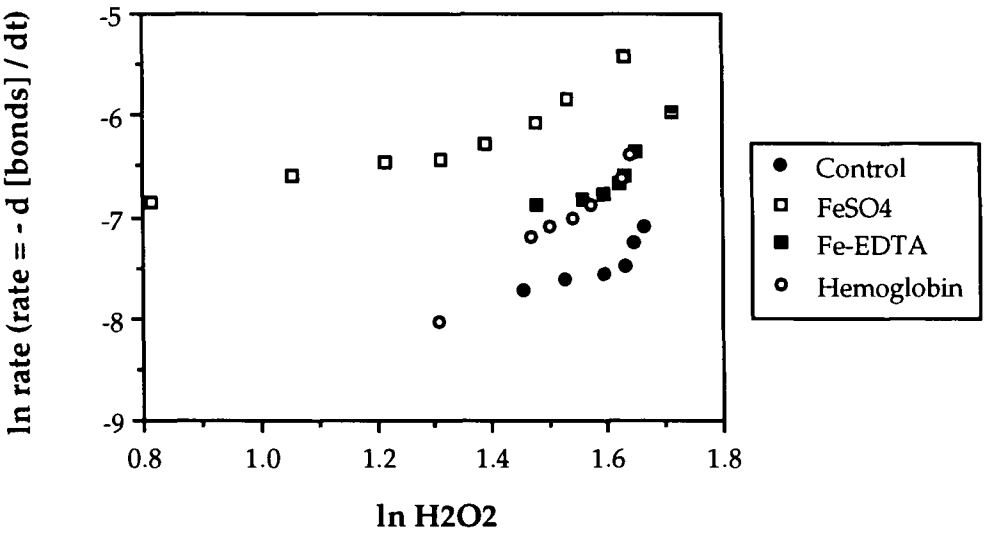

Figure 28. Kinetic plot for the control and the three catalyzed reactions of lignosulfonate. Slopes of line are equal to the dependence of the rate on hydrogen peroxide, or **b** of Equation 11.

Table 7. Rate laws for the catalyzed hydrogen peroxide depolymerization of lignosulfonate.

CATALYST	H_2O_2 RANGE (mM)	Reaction Order, b	Rate Constant, k_1' [a]
Control	40 - 50	6.7	3.92×10^{-17}
Control	< 40	1.9	2.13×10^{-9}
$FeSO_4$	20 - 50	3.1	2.35×10^{-11}
$FeSO_4$	< 20	0.86	2.90×10^{-8}
Fe-EDTA	40 - 50	6.9	1.47×10^{-18}
Fe-EDTA	< 40	0.88	7.07×10^{-9}
Hemoglobin	20 - 50	4.4	$1,15 \times 10^{-12}$

[a] units (order): $mM^{-6.7}\ min^{-1}$ (6.7), $mM^{-1.9}\ min^{-1}$ (1.9) $mM^{-3.1}\ min^{-1}$ (3.1), $mM^{-0.86}\ min^{-1}$ (0.86), $mM^{-6.9}\ min^{-1}$ (6.9), $mM^{-0.88}\ min^{-1}$ (0.88), $mM^{-4.4}\ min^{-1}$ (4.4).

The shift in reaction order reflects either changes in the substrate or changes in the catalytic system. For the control reaction, where no catalyst is present, this change is still evident. Consequently, this shift is not dependent on the Fe(II) --> Fe(III) oxidation cycle.

Smith noted similar shifts in reaction order for iron- and manganese-catalyzed H_2O_2 oxidations of a lignin model compound under alkaline conditions (pH 11.0 - 11.4).[77] These changes were attributed to changes in the catalysts. Under alkaline conditions, Fe and Mn are most likely present as insoluble hydroxides and/or oxyhydroxides. As the reaction proceeded, these metals may have become chelated by degradation products and catalyzed the reaction. The decreased dependence of the rate on hydrogen peroxide was attributed to the catalytic effect of these chelates.

For results obtained from this study (Figure 28), it seems most likely that the observed change in reaction order is a result of a change in the substrate. Certain bonds in the lignosulfonate polymer are more easily broken than others. The differing reactivities of each system would perhaps alter the definition of easy bonds. It would seem more plausible that the

ability of hydrogen peroxide to aggressively degrade lignosulfonate is limited to the availability of certain bonds which are easier to break than others.

From Figure 28 it is evident that $FeSO_4$ catalyzes the greatest rate in bond breakage at a given hydrogen peroxide concentration. A change in the rate of chain scission, the inflection point in the curves, occurs at the same place for the control and Fe-EDTA reactions.

The data for the Fe-EDTA and hemoglobin reactions are very close, although the molar iron concentration in the hemoglobin reaction (0.062 mM) was considerably less than that used for the $FeSO_4$ and Fe-EDTA reactions (0.5 mM).

To compare the efficiency of Fe-EDTA and hemoglobin at equal concentrations, the Fe-EDTA reaction was performed using 0.062 mM of iron. The kinetic plot from this and the 0.5 mM experiment (Figure 29) shows that the concentration of catalyst does not significantly affect the rate of reaction. The dependence of the rate of bond breakage on hydrogen peroxide, particularly at the beginning of the reaction (ln H_2O_2 = ~1.73), is nearly identical at both Fe-EDTA concentrations.

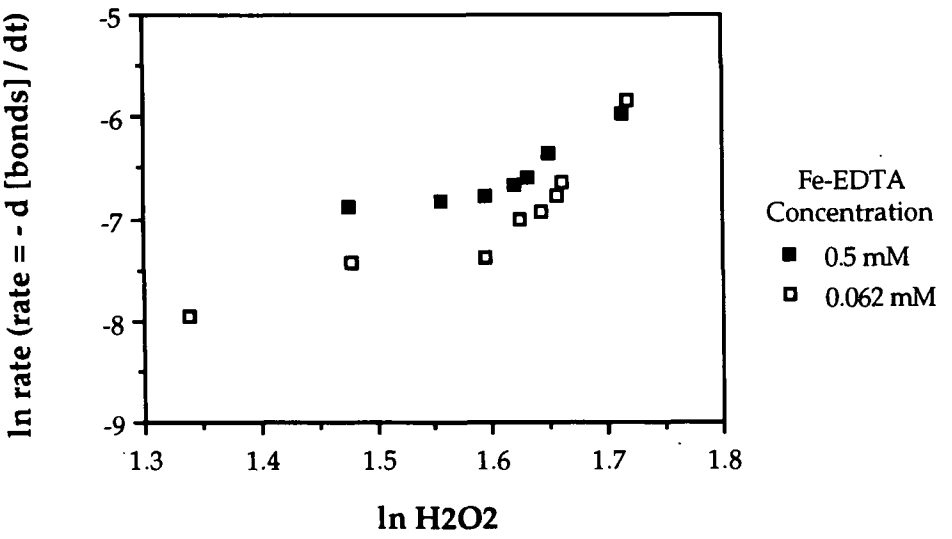

Figure 29. Kinetic plot from the Fe-EDTA catalyzed reaction of lignosulfonate with 0.062 and 0.5 mM Fe-EDTA and 50 mM H_2O_2.

From Figure 29 it can be concluded that when the concentration of hydrogen peroxide is high, the concentration of catalyst is not as important as at lower concentrations of peroxide. This information suggests that the reactions which predominate at high H_2O_2 concentrations are those reactions which consume H_2O_2:

$$Fe^{++} + H_2O_2 \text{ --> } Fe^{+++} + OH^- + {}^\circ OH \qquad [1]$$

$${}^\circ OH + H_2O_2 \text{ --> } HO_2{}^\circ + H_2O \qquad [3]$$

These reactions set up the radical-driven chain reaction described by Equations 1 - 6 in the Literature Review section. As the concentration of hydrogen peroxide decreases, the role of the iron catalyst becomes more important, hence the higher rate of reaction at higher catalysts concentration.

The above kinetic analysis provides an indication of the complexity of these reactions. Rate laws were evaluated without considering the changing oxidation state of the iron (this was not measured during reactions). The ferrous-catalyzed decomposition of hydrogen peroxide is known to exhibit a second order dependence on the ferrous ion concentration in the absence of organic substrates.[50] As the oxidation state of iron is changing throughout the reaction, it is very difficult to accurately determine the prevailing rate law using the approach taken here.

Rates of Chain Scission

It can be shown[109] that the number of chain scissions, $\mathbb{N}$, is proportional to the difference in the reciprocal degree of polymerization, $\mathbb{DP}$:

$$N \propto \frac{1}{DP_t} - \frac{1}{DP_0} \qquad [12]$$

where $\mathbb{DP}_t$ is the DP at time t, and $\mathbb{DP}_o$ is the DP at t = 0 minutes. As the DP is proportional to the molecular weight, $\mathbb{M}_w$, Equation 12 can be rewritten as:

$$N \propto \frac{1}{Mw_t} - \frac{1}{Mw_0} \qquad [13]$$

The number of chain scissions plotted against reaction time yields a straight line when the rate of chain scission is constant throughout the reaction. In all reactions, the rate of chain scission varies with time during the initial phases of reaction. As the reaction proceeds, the rate of chain scission becomes more nearly constant (Figures 30 and 31). For the control and Fe-EDTA catalyzed reaction, the rate of chain scission decreases only slightly with respect to reaction time. For the $FeSO_4$ and hemoglobin reactions, the initial rate of chain scission is somewhat higher.

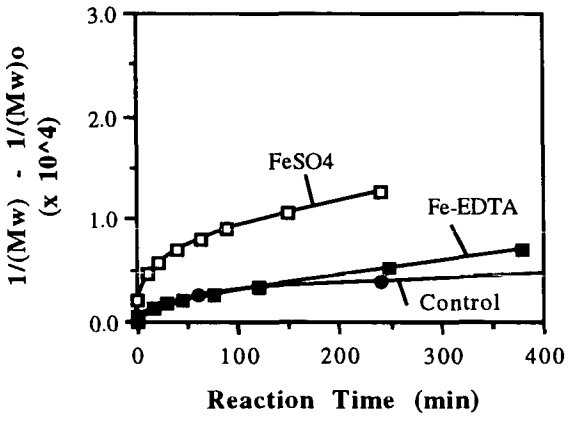

Figure 30. Number of chain scissions in lignosulfonate versus reaction time for the control, $FeSO_4$, and Fe-EDTA reactions with hydrogen peroxide.

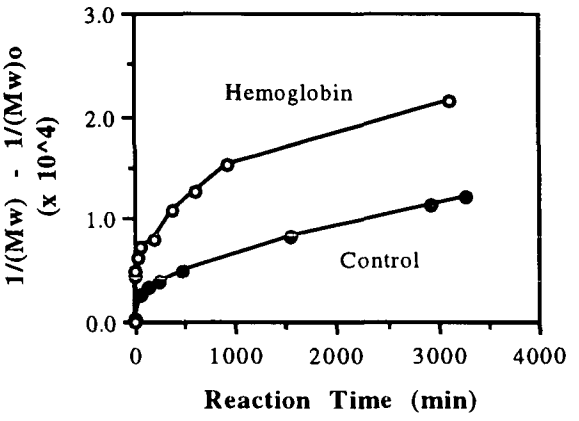

Figure 31. Number of chain scissions in lignosulfonate versus reaction time for the hemoglobin and control reactions with hydrogen peroxide.

For a typical chemical reaction where:

$$A + B \rightarrow C$$

the rate of disappearance of A is equal to the rate of disappearance of B:

$$\text{rate} = -\frac{dA}{dt} = -\frac{dB}{dt}$$

For the hydrogen peroxide oxidation of lignosulfonate, where the proposed reaction can be generally expressed as:

$$\text{intact bond} + H_2O_2 \text{ --> broken bonds} + O_2$$

the rate of bond breakage (or the decrease in bond concentration) should equal the rate of H_2O_2 disappearance. For all catalysts and the control, the rate of chain scission is proportional to the rate of hydrogen peroxide disappearance (Figure 32). This important result verifies that the chain scission analysis used to measure reaction rates is valid.

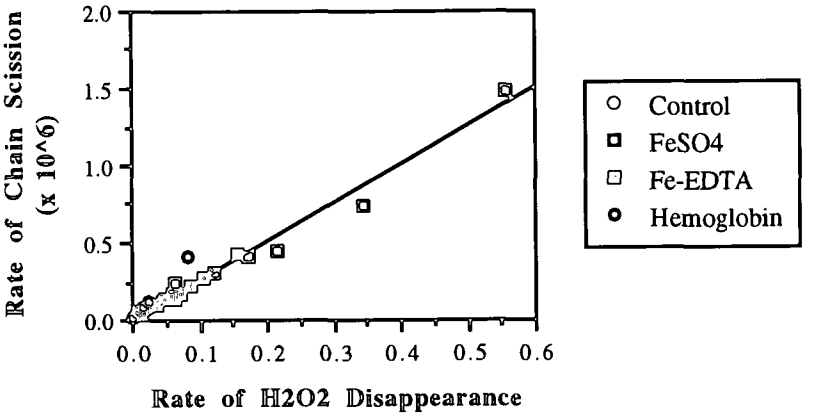

Figure 32. Rate of chain scission plotted against the rate of hydrogen peroxide disappearance for the control and catalyzed reactions of lignosulfonate.

As shown in Figure 32, rates of chain scission are related to the reactivity of hydrogen peroxide. As hydrogen peroxide reacts, it is either reduced to oxygen or combined with lignosulfonate. All peroxide consumed by lignosulfonate should result in chain cleavage. The amount of hydrogen peroxide consumed by reaction is directly proportional to the number of chain scissions (Figure 33). Although $FeSO_4$ catalyzed more H_2O_2 consumption than the other catalyst, the data in Figure 33 indicate that to break a given number of chains, $FeSO_4$ consumed more H_2O_2.

A linear correlation is not evident for the amount of H_2O_2 decomposed to oxygen (Figure 34). In fact, results differ greatly between the three biomimetic compounds and the control. Data from this figure indicate that Fe-EDTA is a poor catalyst for hydrogen peroxide

oxidation of lignosulfonate. Much of the hydrogen peroxide is lost through decomposition to oxygen. $FeSO_4$ is more efficient than the control initially, but as the amount of hydrogen peroxide reacted increases, more oxidizing power is lost through decomposition. Results in Figure 34 are very similar to those in Figure 26. This is expected as the rate of chain scission is dependent on the hydrogen peroxide concentration.

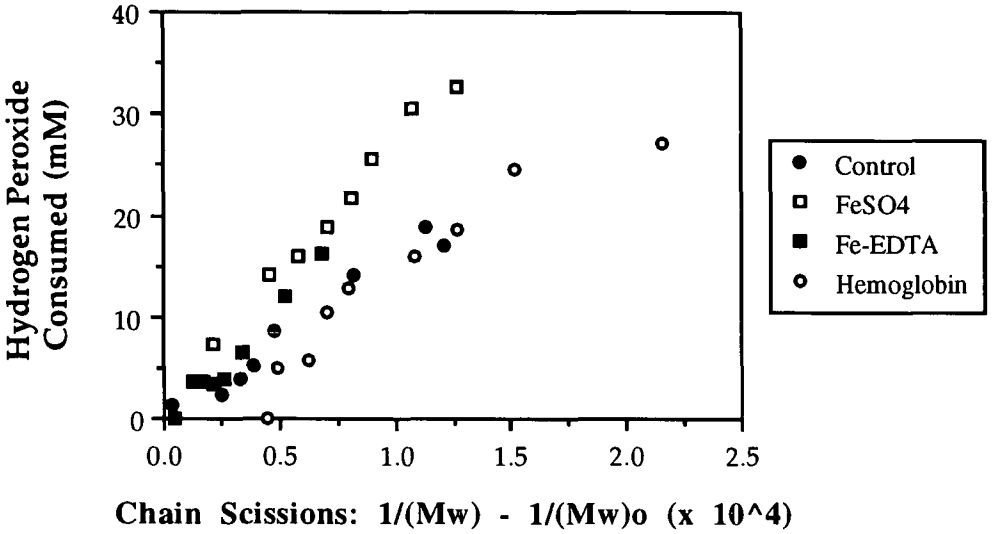

Figure 33. Amount of hydrogen peroxide consumed in reaction versus the number of chain scissions in lignosulfonate.

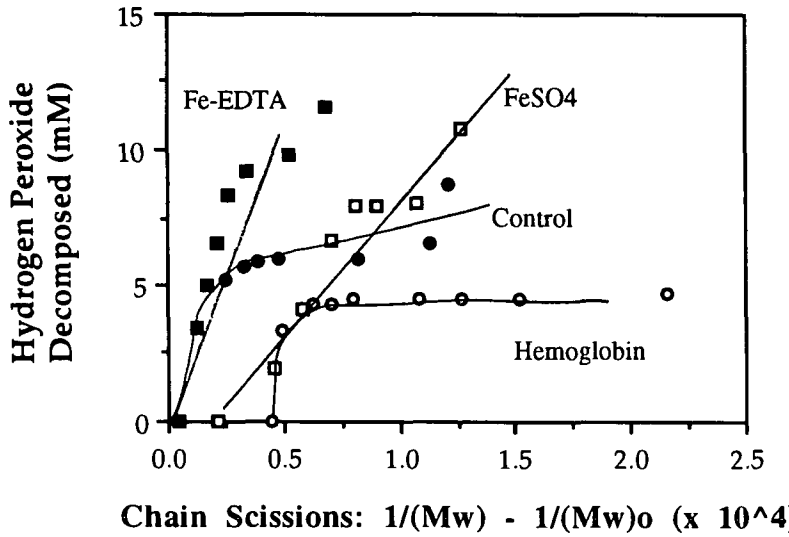

Figure 34. Amount of hydrogen peroxide decomposed versus the number of chain scissions in lignosulfonate.

Another way to compare the behavior of these catalysts is to determine the rate of chain scission occurring at specific hydrogen peroxide concentrations. Table 8 shows the rate of chain scission occurring at 40 and 20 mM hydrogen peroxide. These values are taken from the same experiment with an initial H_2O_2 concentration of 50 mM. The rate of chain scission, as evidenced by the slope from the curves in Figures 30 and 31, is steepest for the $FeSO_4$ catalyzed run.

Table 8. Rate of chain scission for the catalyzed hydrogen peroxide depolymerization of lignosulfonate at 20 and 40 mM H_2O_2.

	RATE OF CHAIN SCISSION ($\times 10^{-7}$)	
CATALYST	20 mM H_2O_2	40 mM H_2O_2
Control	0.17	0.36
$FeSO_4$	4.10	20.0
Fe-EDTA	1.10	1.90
Hemoglobin	0.09	1.73

The differences between the rate of chain scission at 40 and 20 mM H_2O_2 may not be due to the hydrogen peroxide concentration alone. At 20 mM H_2O_2, a substantial number of bonds have been broken in the lignosulfonate polymer. The slower rate at 20 mM H_2O_2 may be a result of all "easy" bonds having been broken.

Generation of Hydroxyl Radicals

The external method of the chemiluminescence assay was used to measure hydroxyl radicals formed during lignosulfonate degradation reactions. Hemoglobin was found to interfere with this assay. The problems encountered and results obtained from hemoglobin reactions are discussed in Appendix VII.

The chemiluminescence obtained from a sample analysis is proportional to the concentration of hydroxyl radicals in solution. For the external method, samples were exposed to

the reagent for one minute; therefore, the chemiluminescence produced is proportional to the concentration of hydroxyl radicals produced during that one minute.

Figure 35 shows the chemiluminescence obtained for the control and the $FeSO_4$ and Fe-EDTA catalyzed reactions. For the control reaction, in which no catalyst was present, there is no substantial increase in the chemiluminescence during the reaction. This indicates that few hydroxyl radicals were generated. This is expected as the reaction rate was very slow.

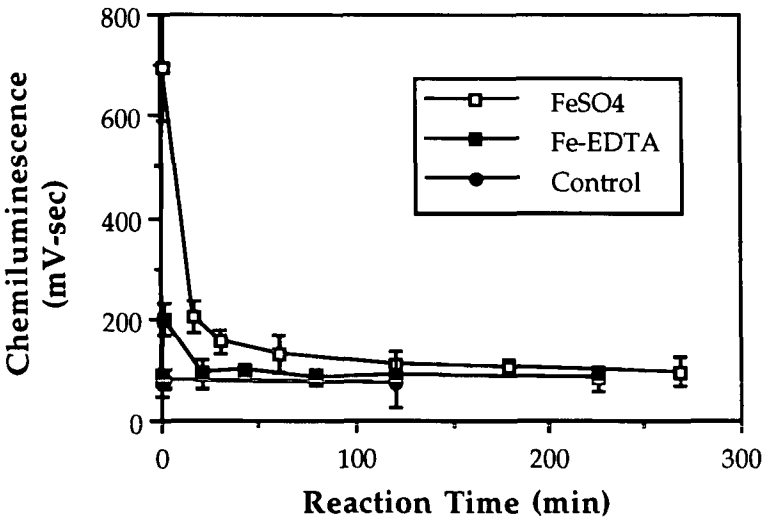

Figure 35. Chemiluminescence versus reaction time for the catalyzed oxidation of lignosulfonate.

For the $FeSO_4$ and Fe-EDTA catalyzed reactions, the chemiluminescence was great when the reaction was initiated (first sample taken < 2 minutes after initiation). As the reaction proceeds, the chemiluminescence rapidly decreased. The $FeSO_4$ reaction produced more chemiluminescence than the Fe-EDTA catalyzed reaction. After 60 minutes, the chemiluminescence from the $FeSO_4$ reaction drops to the level of Fe-EDTA and the control, which is essentially the baseline value. Although the chemiluminescence for these experiments are

relatively low, data between replicates indicate good agreement and reproducibility of the technique (Figures 36 and 37).

Figure 38 shows the chemiluminescence plotted against the amount of hydrogen peroxide which has reacted. With the control reaction (hydrogen peroxide but no catalyst) no variation in the chemiluminescence is observed. With the Fe-EDTA catalyzed reaction, a decrease in the chemiluminescence is observed as the amount of reacted hydrogen peroxide increases.

It would be expected that the concentration of hydroxyl radicals would be relatively constant during reactions. However, the initial increase in chemiluminescence indicates that most hydroxyl radicals are produced during the initial phase of the reaction. The steady-state concentration of hydroxyl radicals is extremely low. The chemiluminescence assay is not able to measure less than about 1 μM of hydroxyl radicals (see Calibration section).

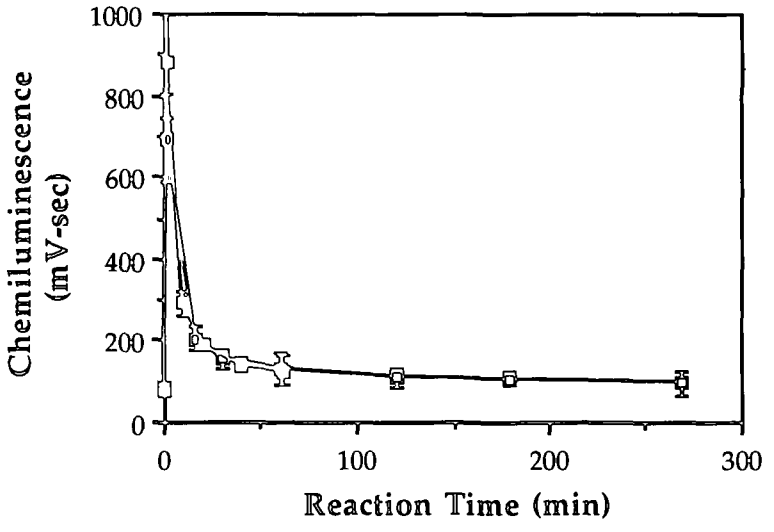

Figure 36. Chemiluminescence versus reaction time for the ferrous sulfate catalyzed hydrogen peroxide oxidation of lignosulfonate. Error bars represent 95% confidence intervals determined from three determinations.

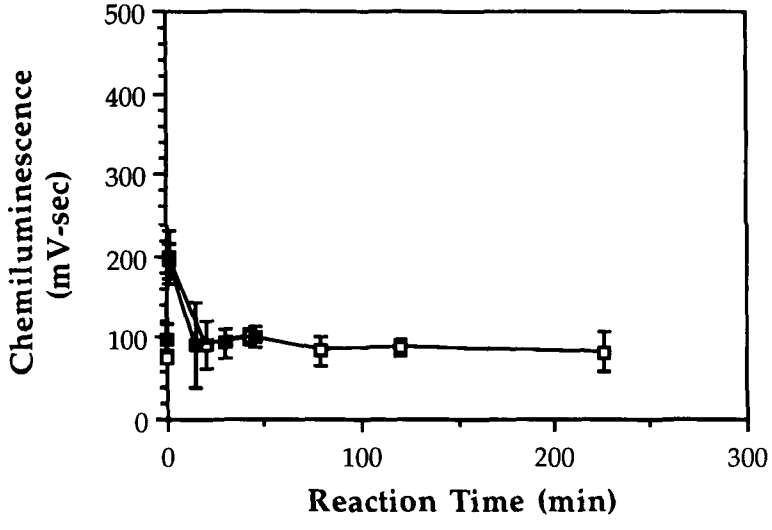

Figure 37. Chemiluminescence versus reaction time for the Fe-EDTA catalyzed hydrogen peroxide oxidation of lignosulfonate. Error bars represent 95% confidence intervals determined from three determinations.

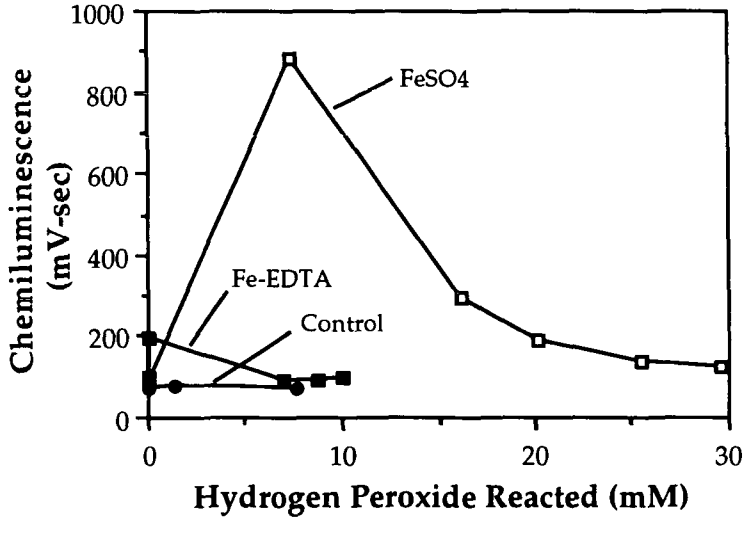

Figure 38. Chemiluminescence versus the amount of hydrogen peroxide reacted for the control, $FeSO_4$, and Fe-EDTA reactions.

In Figure 39 the chemiluminescence is plotted against the rate of hydrogen peroxide consumption for the $FeSO_4$ and Fe-EDTA catalyzed reactions. Two replicate reactions are shown

for each catalyst. For the $FeSO_4$ reactions, an excellent correlation is observed between the chemiluminescence, or hydroxyl radical concentration, and the rate at which hydrogen peroxide reacts.

This same trend is not observed with the Fe-EDTA catalyzed reaction. Figure 40 shows the data in Figure 39, but with a shortened time scale, more clearly presenting the data obtained at low reaction rates. It is possible that if the Fe-EDTA reactions reached a higher reaction rate then a correlation between chemiluminescence and reaction rate would be visible. However, even at a rate of 0.2 mM min^{-1}, the $FeSO_4$ catalyzed reaction exhibits a higher chemiluminescence than the Fe-EDTA reaction.

These results indicate that Fe-EDTA in the presence of hydrogen peroxide produces few radicals. The radicals which are produced are generated at a rate which is independent of the rate at which hydrogen peroxide reacts (Figure 40).

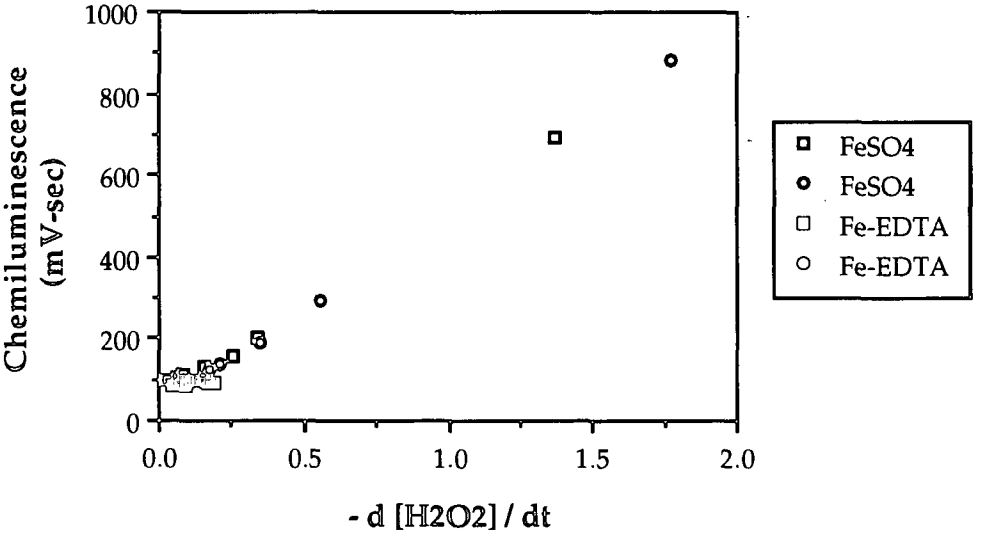

Figure 39. Chemiluminescence versus the rate of disappearance of hydrogen peroxide concentration for the $FeSO_4$ (empty symbols) and Fe-EDTA (filled symbols) catalyzed reaction.

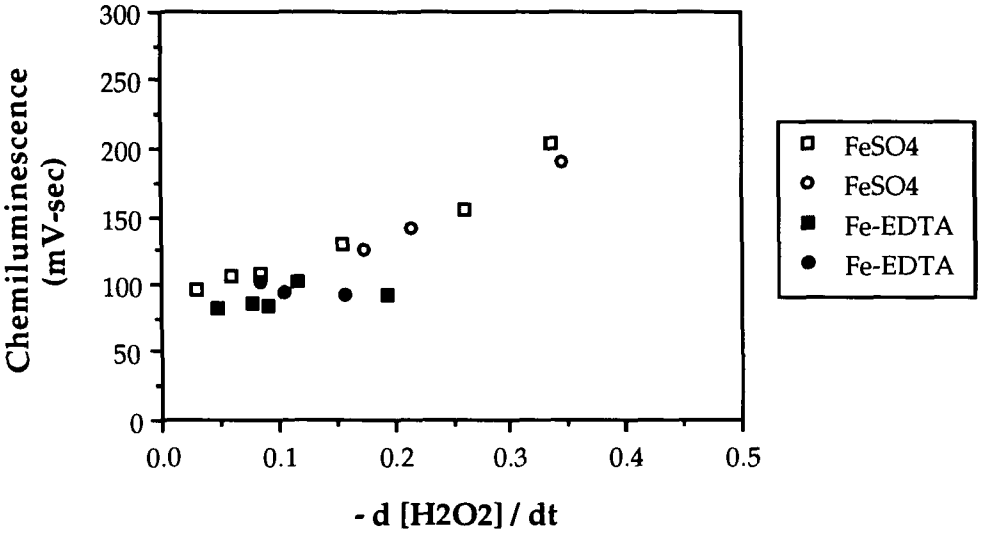

Figure 40. Identical to Figure 39, but with a shortened time scale.

As evidenced from the kinetic analysis presented above, the rate of hydrogen peroxide consumption determines the rate of bond breakage. Figure 41 shows the chemiluminescence from these reactions plotted against the rate of lignosulfonate bond breakage for the $FeSO_4$ and Fe-EDTA catalyzed reaction.

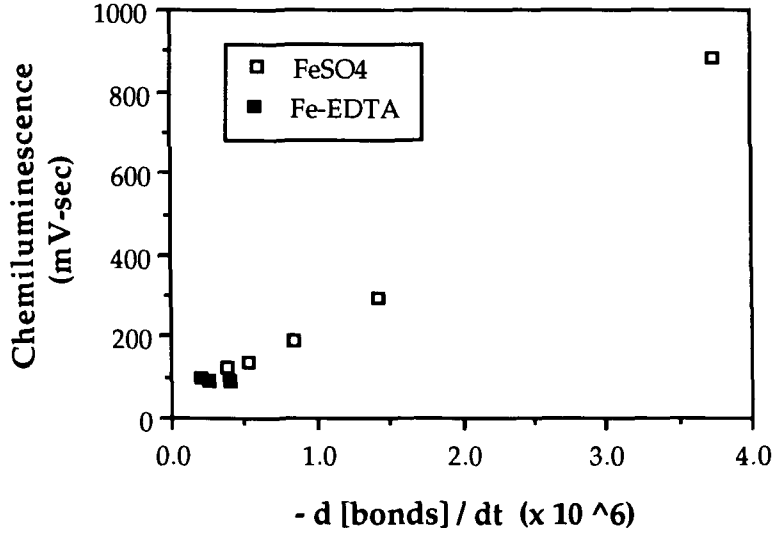

Figure 41. Chemiluminescence versus the rate of chain scission in lignosulfonate for the $FeSO_4$ and Fe-EDTA reaction.

For the $FeSO_4$ catalyzed reaction the chemiluminescence is directly proportional to the rate of bond cleavage. For the Fe-EDTA reaction, such a relationship does not exist. If an increased rate in bond breakage were obtained, a relationship may then be observed.

The data in Figure 41 indicate that hydroxyl radicals are necessary to achieve depolymerization of lignosulfonate. It would be expected that the rate of depolymerization would be reduced if hydroxyl radicals were removed from reactions. Phthalic hydrazide, the reagent for the chemiluminescence assay, was used to scavenge hydroxyl radicals in reactions. The rate at which hydrogen peroxide reacts was greatly increased by the addition of phthalic hydrazide (Figure 42).

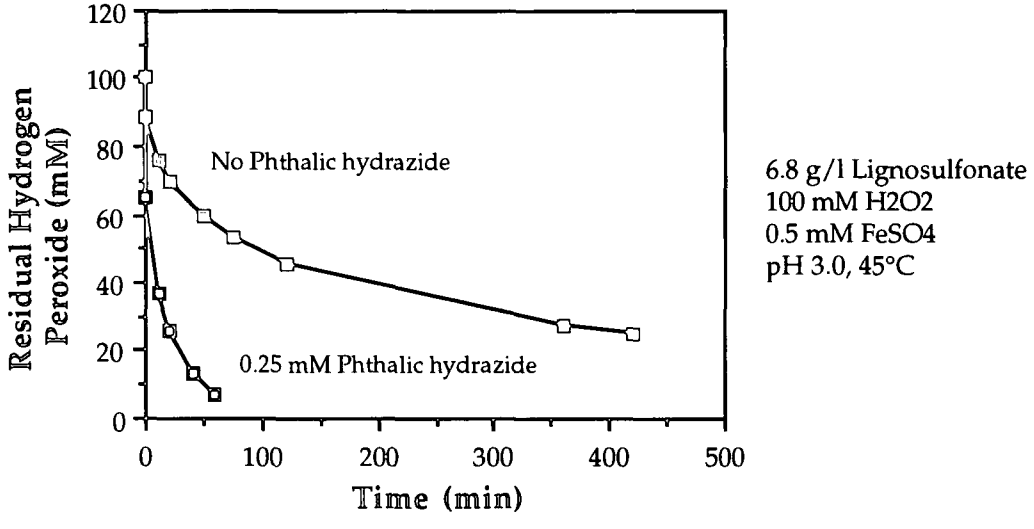

Figure 42. Residual hydrogen peroxide concentration versus reaction time for two similar reactions of lignosulfonate.

Figure 16 in the Chemiluminescence Assay section presents data from hydrogen peroxide and Fe-EDTA experiments with varying levels of phthalic hydrazide. For those experiments, as the concentration of phthalic hydrazide was increased, the rate at which hydrogen

peroxide reacted was decreased. This decrease was attributed to the slowing of reaction as hydroxyl radicals were scavenged.

When lignosulfonate is present in reaction solutions, the hydroxyl radicals generated should preferentially react with this substrate. Lignosulfonate, at 6.8 g/l, is nearly 200 times more concentrated than phthalic hydrazide at 0.25 mM or 0.04 g/l. The chemiluminescence for the reaction containing only phthalic hydrazide was very low (data not shown). This indicates that hydroxyl radicals were not reacting with the phthalic hydrazide.

Figure 43 shows the molecular weight data (determined by peak position) from these two reactions. The substantial increase in the rate hydrogen peroxide reacts does not result in a similar increase in the degradation of lignosulfonate.

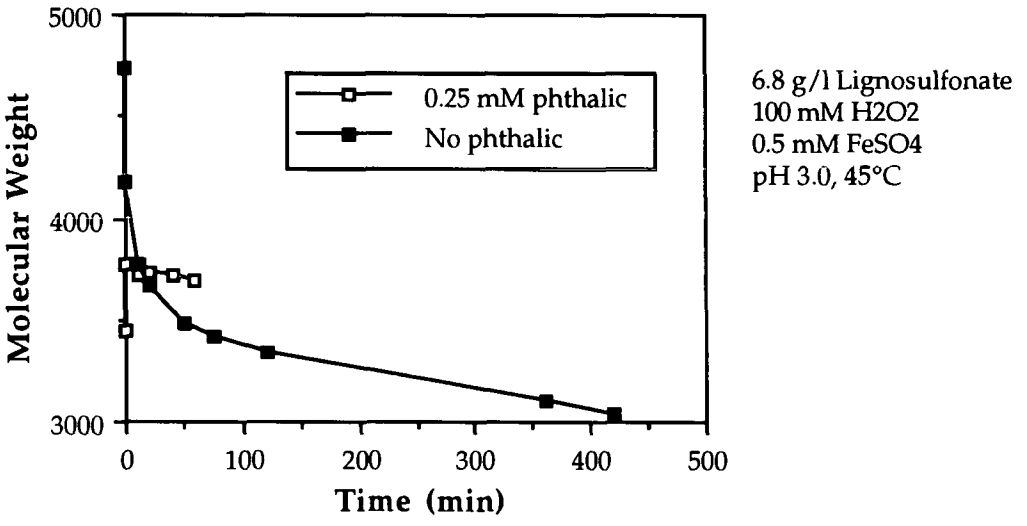

Figure 43. Molecular weight of lignosulfonate versus reaction time for two reactions, containing 0.0 and 0.5 mM phthalic hydrazide.

Significance of Results

All three biomimetic compounds were able to catalyze chain scission in lignosulfonate. Characterization of degradation rates indicated that these catalysts can be ranked in

the following order for their ability to catalyze lignosulfonate degradation: $FeSO_4$ > Fe-EDTA > Hemoglobin.

Results from these experiments indicate that hydroxyl radicals are necessary for the degradation of lignosulfonate. $FeSO_4$ in the presence of H_2O_2 produces hydroxyl radicals, and the greatest degradation of lignosulfonate is obtained with this catalyst. Fe-EDTA, which produces few hydroxyl radicals, does not achieve substantial degradation of lignosulfonate. Fe-EDTA greatly catalyzes peroxide decomposition over consumption by substrate as compared to $FeSO_4$ and hemoglobin.

Hydroxyl radicals were not measured in hemoglobin catalyzed reactions (see Appendix VII). However, the involvement of the hydroxyl radical in hemoglobin-catalyzed lignosulfonate degradation is likely. Little decomposition of hydrogen peroxide was detected in this reaction. This is similar to the $FeSO_4$ reaction, an $^{\circ}OH$-generating system. Hemoglobin in the presence of excess H_2O_2 is reported to degrade and produce free iron.[87] This free iron is believed to produce the hydroxyl radicals observed in hemoglobin plus H_2O_2 systems. The stability of hemoglobin was not measured during these experiments.

The ability of the catalyst and H_2O_2 to react near the lignosulfonate must also be considered. $FeSO_4$ dissociates in solution and is very small, enabling close association with the lignosulfonate. Hence, most hydroxyl radicals formed in this system react with the substrate. Fe-EDTA is slightly larger, and fewer hydroxyl radicals are produced in the Fe-EDTA + H_2O_2 system. HO_2° radicals may be more prevalent, and these radicals can react with Fe(III) to produce O_2.

Hemoglobin is substantially larger than both $FeSO_4$ and Fe-EDTA. The protein mass of the hemoglobin must closely associate with the lignosulfonate, else the hydroxyl radicals generated by the hemoglobin plus H_2O_2 system would be lost in side reactions with H_2O_2, other radicals, or with the protein in hemoglobin itself.

CATALYZED OXIDATION OF HYDROXYETHYL CELLULOSE

Catalytic oxidation of hydroxyethyl cellulose (HEC) was performed using the same three biomimetic compounds as for the lignosulfonate reactions. Concentrations of hydrogen peroxide and catalysts (Table 9) were selected to achieve measurable degradation of HEC within a sufficient reaction time, preferably 100 - 500 minutes. The concentration of iron was selected to maintain the Fe : H_2O_2 ratio used in the lignosulfonate reactions.

Table 9. Reaction conditions for the catalytic oxidation of hydroxyethyl cellulose (HEC) by hydrogen peroxide.

Hydroxyethyl Cellulose	3.0 g/l
H_2O_2	20 and 40 mM
Catalyst	
$FeSO_4$ and Fe-EDTA	0.2 mM
Hemoglobin (as Fe)	0.025 mM
Temperature	45°C
pH	3.0

For these experiments the intrinsic viscosity of reaction samples was measured using a capillary viscometer. Viscosity-average molecular weights were calculated using the Mark-Houwink equation, as described in the Materials and Methods section. All data from these experiments are tabulated in Appendix V.

Only a small amount of hydrogen peroxide reacted during these experiments (< 20%). In order to determine the dependence of the rate of degradation on hydrogen peroxide, two different initial concentrations of hydrogen peroxide were selected for evaluation.

As only a small amount of hydrogen peroxide reacted, little oxygen was evolved from the decomposition of peroxide. Accurate determination of the amounts of peroxide consumed and decomposed were not available. Even at the higher initial concentration of H_2O_2 (40 mM),

only a slight decrease in residual hydrogen peroxide concentration was observed. Consequently, a discussion of the decomposition versus consumption of hydrogen peroxide will be omitted.

HEC Degradation

All three biomimetic compounds catalyzed degradation of HEC over that of the control at 40 mM H_2O_2 (Figure 44). Degradation of HEC by all biomimetic compounds is also obtained at the lower peroxide concentration of 20 mM (Figure 45). The $FeSO_4$ catalyzed reaction resulted in the greatest degradation of HEC at both concentrations of hydrogen peroxide. Fe-EDTA provides a sufficient catalytic environment to also degrade the HEC polymer. Hemoglobin, even at its relatively low molar iron concentration, also catalyzes the degradation of the HEC polymer.

The attack of sugars and polysaccharides by radical-generating systems has been extensively studied.[110,111,112] Results from these efforts on the radical attack of glucose indicate that six different primary glucosyl radicals are formed in equal yields.[113] For polysaccharides, these radicals then decompose, resulting in cleavage of glycosidic bonds.

The hydroxyl radical will abstract hydrogens which are bound to carbons.[105] This will predominate over addition of the hydroxyl radical to the sugar itself or the hydroxyethyl side chains of HEC. The initial abstraction of a hydrogen will create a radical structure, which eventually leads to chain cleavage. Therefore, the system generating the most hydroxyl radicals will demonstrate the greatest rate of chain cleavage. These topics are discussed in the next sections.

Kinetics of HEC Depolymerization

A plot of the number of chain scissions (Equation 13) versus reaction time yields straight lines for all reactions (Figure 46 and 47). This indicates that the depolymerization of HEC occurs at a constant rate throughout the reaction.

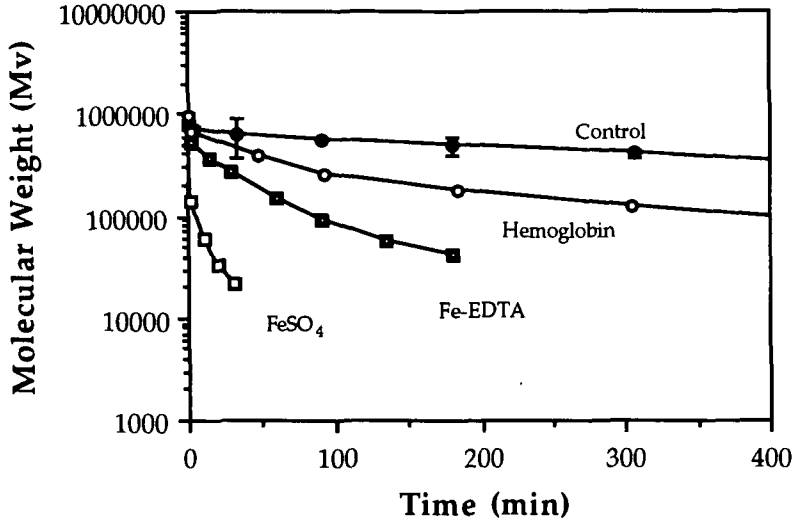

Figure 44. Viscosity-average molecular weight of HEC versus reaction time for the control (no catalyst), $FeSO_4$, Fe-EDTA, and hemoglobin at 40 mM H_2O_2.

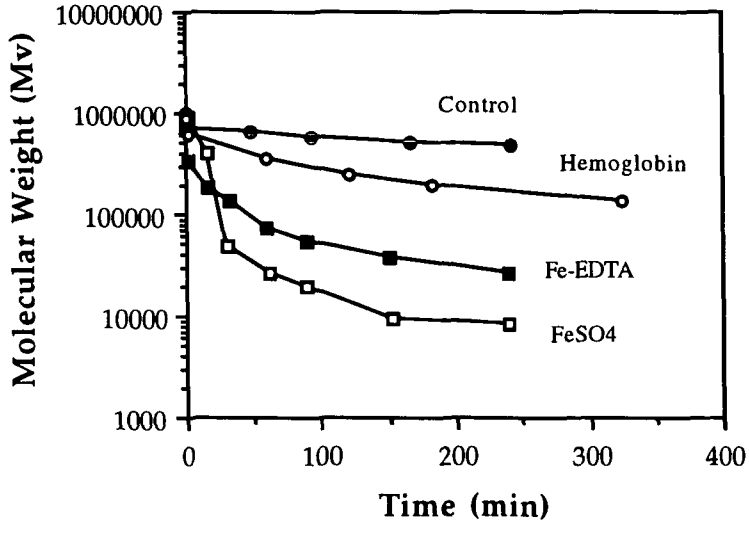

Figure 45. Viscosity-average molecular weight of HEC versus reaction time for the control (no catalyst), $FeSO_4$, Fe-EDTA, and hemoglobin at 20 mM H_2O_2.

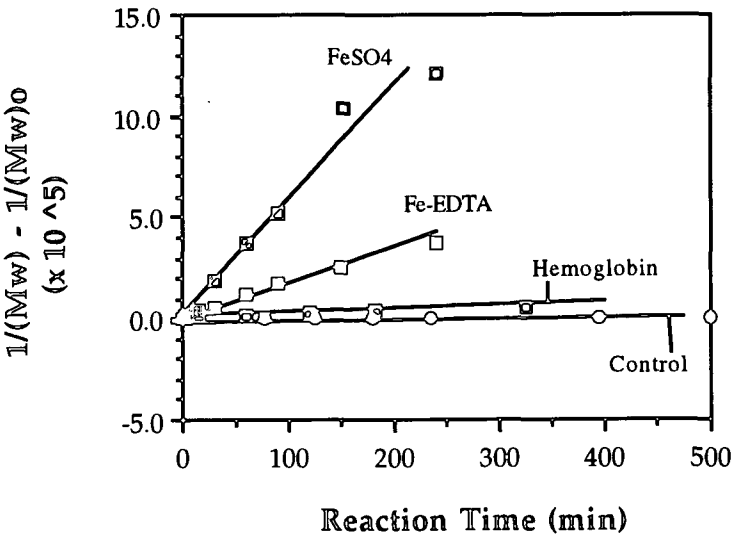

Figure 46. Number of chain scissions in HEC versus reaction time for each catalyst and a control (no catalyst) at 20 mM H_2O_2.

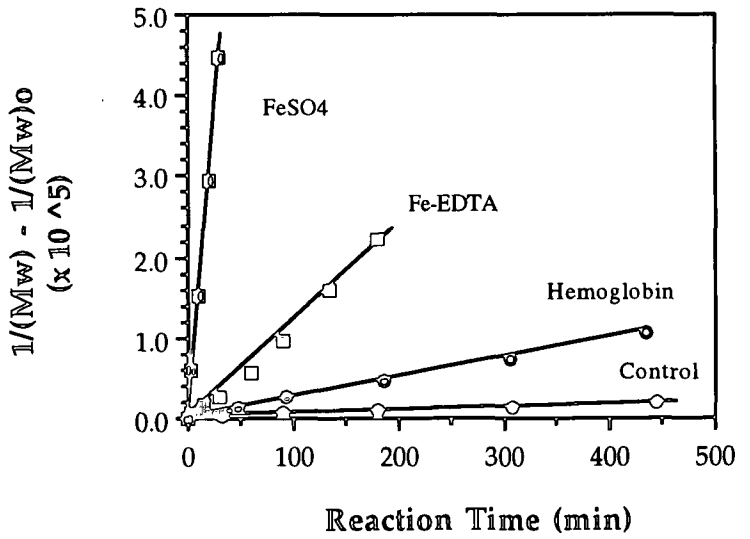

Figure 47. Number of chain scissions in HEC versus reaction time for each catalyst and a control (no catalyst) at 40 mM H_2O_2.

The generalized rate equation given for lignosulfonate degradation (Equation 11) can also be applied to the data from these experiments. As mentioned previously, the hydrogen peroxide concentration remains relatively constant during these reactions. Using the data from the 20 and 40 mM experiments, the dependence on hydrogen peroxide was determined.

For the catalyzed hydrogen peroxide depolymerization of HEC, $FeSO_4$ exhibits the greatest dependence on hydrogen peroxide (Table 10). The control, Fe-EDTA and hemoglobin reactions show only a slight dependence on hydrogen peroxide.

Table 10. Rate laws for the catalyzed hydrogen peroxide depolymerization of HEC. Reaction conditions as given in Table 9.

CATALYST	Reaction Order, b	Rate Constant, k_1 (x 10^{-9}) [a]
Control	0.21	1.54
$FeSO_4$	2.1	0.60
Fe-EDTA	0.87	4.92
Hemoglobin	0.32	6.92

[a] units (order): $mM^{-0.21}\ min^{-1}$ (0.21), $mM^{-2.1}\ min^{-1}$ (2.1), $mM^{-0.87}\ min^{-1}$ (0.87), $mM^{-0.32}\ min^{-1}$ (0.32).

Generation of Hydroxyl Radicals

Hydoxyl radicals generated during HEC degradation reactions were measured using the chemiluminescence assay. As described in a previous section, phthalic hydrazide, the reagent for this assay, has been observed to affect reaction rates when present in reaction solutions. Identical HEC degradation reactions, performed in the presence and absence of phthalic hydrazide, indicated that phthalic hydrazide did not significantly affect reaction rates in these experiments.

Therefore, the original method of the chemiluminescence assay, in which phthalic hydrazide was added to reaction solutions, was used.

When hemoglobin was present in samples, results obtained from the chemiluminescence assay, using either the original or external methods, were ambiguous. The external method, where phthalic hydrazide was not added to reaction solutions, was used for reactions containing hemoglobin. These data, although their utility is questionable, are included in Appendix VII.

Chemiluminescence values obtained using the original method of the chemiluminescence assay, with phthalic hydrazide present in reaction solutions, are shown in Figures 48 and 49 for the $FeSO_4$ and Fe-EDTA catalyzed reactions. These figures differ from those obtained during lignosulfonate degradation reactions (Figure 35) as the data in Figures 48 and 49 are cumulative. The given charge of phthalic hydrazide initally present in the reaction solution is continually hydroxylated throughout the experiment. Therefore, each data point represents the chemiluminescence produced from all phthalic hydrazide hydroxylated up to that point. This is proportional to the total amount of hydroxyl radicals produced during the reaction up to the point of sampling.

The chemiluminescence produced during HEC degradation as catalyzed by $FeSO_4$ (Figure 48) was greater at 40 mM H_2O_2 than at 20 mM. During the 40 mM reaction, the rate at which phthalic hydrazide is hydroxylated (the slope of the line at a given time) slowly decreases during the reaction. This decrease results from a decreased rate of hydroxylation as all phthalic hydrazide becomes hydroxylated. In the 20 mM reaction, an increase in the chemiluminescence is observed initially, although it is not quite linear. However, after a maximum value at approximately 125 minutes is achieved, the rate becomes negative. A negative slope indicates that the phthalic hydrazide was consumed in secondary reactions.

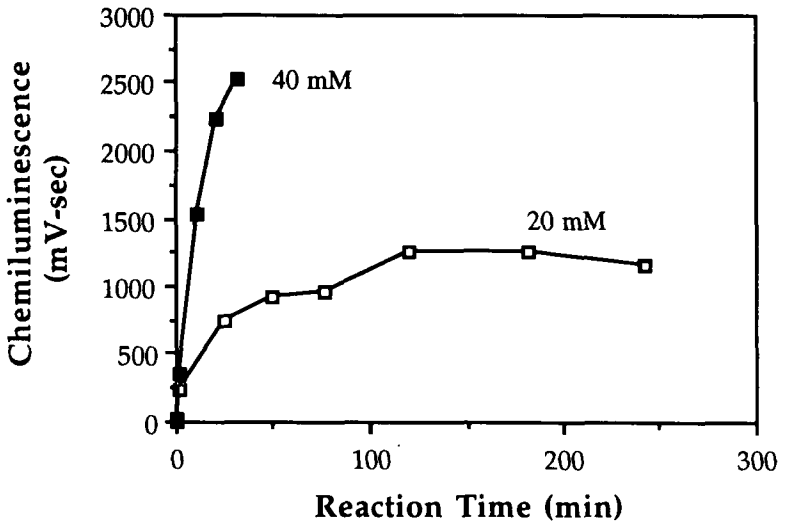

Figure 48. Chemiluminescence versus reaction time for the $FeSO_4$ catalyzed oxidations of HEC at 20 and 40 mM H_2O_2.

For HEC degradations catalyzed by Fe-EDTA (Figure 49), the chemiluminescence produced at 40 mM is also greater than that produced at 20 mM. The chemiluminescence increased linearly throughout the reaction for both experiments. This linear increase indicates that phthlic hydrazide was hydroxylated at a constant rate throughout the reaction. This rate is equal to the slopes in Figure 49, and is greater for the 40 mM reaction.

Results from Figures 48 and 49 indicate that hydroxyl radicals are produced at a varying rate in the $FeSO_4$ catalyzed reactions, and at a relatively constant rate in the Fe-EDTA catalyzed reactions. Figures 50 and 51 compare the chemiluminescence data from these experiments at 40 and 20 mM H_2O_2, respectively. At both 20 and 40 mM H_2O_2, the $FeSO_4$ system produces the greater amount of chemiluminescence or hydroxyl radicals. This difference in hydroxyl radical generation may be correlated to the rate at which H_2O_2 reacts. However, in these experiments the H_2O_2 concentration changed very little, making accurate determinations of peroxide reactivity impossible.

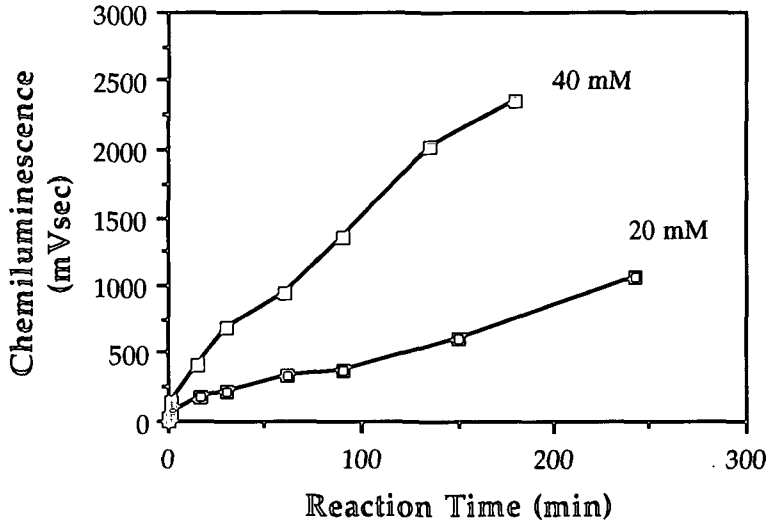

Figure 49. Chemiluminescence versus reaction time for the Fe-EDTA catalyzed oxidations of HEC at 20 and 40 mM H_2O_2.

The dependence of chain scission in HEC on hydroxyl radical formation is obtained by comparing rates of °OH formation to rates of chain scission. The rate of chain scission in HEC was constant throughout all reactions. This is apparent from the straight lines observed in Figures 46 and 47. The rate at which hydroxyl radicals were produced in the $FeSO_4$ reactions (tangents to the curve in Figure 48) gradually decreased from an initially high rate. In the Fe-EDTA reaction, the rate at which hydroxyl radicals were produced was relatively constant (Figure 49).

These observations indicate that in the Fe-EDTA system a constant rate of hydroxyl radical production yields a constant rate of chain scission. In the $FeSO_4$ system the rate of hydroxyl radical production is not constant, although the rate of chain scission is constant. The slight variation in the rate of hydroxyl radical production in the $FeSO_4$ system may be due to experimental error.

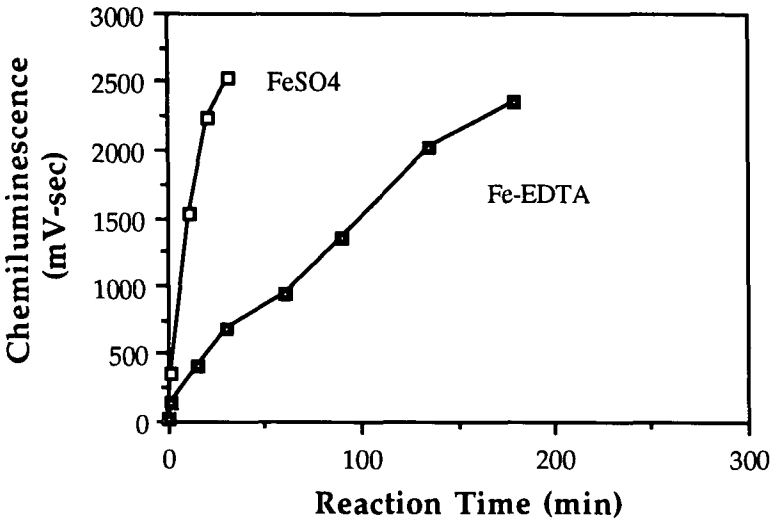

Figure 50. Chemiluminescence versus reaction time for the $FeSO_4$ and Fe-EDTA catalyzed oxidations of HEC at 40 mM H_2O_2.

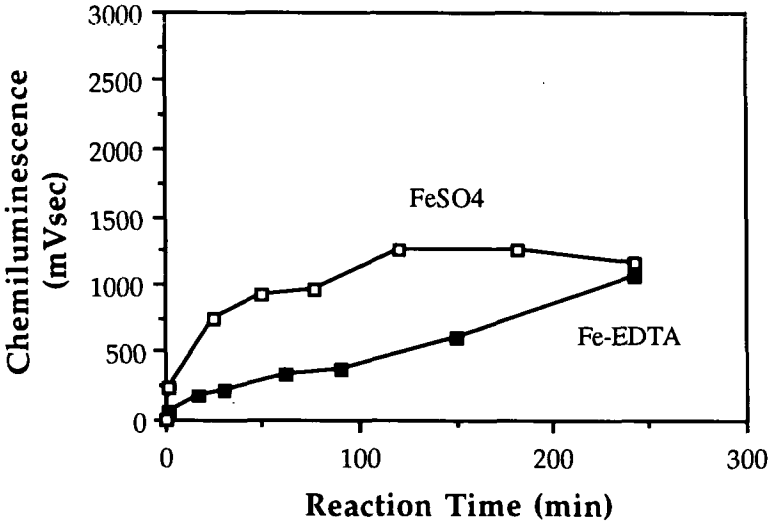

Figure 51. Chemiluminescence versus reaction time for the $FeSO_4$ and Fe-EDTA catalyzed oxidations of HEC at 20 mM H_2O_2.

Significance of Results

All three biomimetic compounds were able to catalyze degradation of HEC. These results indicate that these biomimetic compounds are capable of damaging the carbohydrates found in pulp. Even at relatively low peroxide concentrations (20 mM), significant damage to HEC was observed. The dependence of the rate of chain scission on hydrogen peroxide is very different for $FeSO_4$ (2.1) as compared to Fe-EDTA (0.87), and hemoglobin (0.32).

Hydroxyl radicals were detected in both the $FeSO_4$ and Fe-EDTA experiments. As the concentration of hydrogen peroxide was increased from 20 to 40 mM, an increase in the amount of hydroxyl radicals produced was observed for both catalytic systems. Although the rate of hydrogen peroxide reactivity could not be measured in these experiments, the increase in hydroxyl radicals with increased hydrogen peroxide concentration suggests that the hydroxyl radical concentration is a function of the hydrogen peroxide concentration.

The rate at which hydroxyl radicals were produced (tangents to lines in Figures 48 and 49) were relatively constant throughout the reaction, althought the data for the $FeSO_4 + H_2O_2$ experiments are poor. The rate of chain scission was also constant for all reactions. From these results it can be concluded that hydroxyl radicals are necessary for chain scission in HEC.

It can be assumed that hydroxyl radicals were also produced in the reactions containing hemoglobin. Hydroxyl radicals are known to be produced in reaction solutions containing hemoglobin and hydrogen peroxide.[87] The concentration of hydroxyl radicals could not be measured using the chemiluminescence assay for hemoglobin-containing reactions.

SELECTIVITY IN THE SINGLE SUBSTRATE SYSTEM

Depolymerization of Substrates

Selectivity is most appropriately evaluated by comparing rate constants from empirically determined rate laws. For the work presented here, a simple comparison of rate

constants can not be made as the rate laws for each catalyst in the lignosulfonate and HEC system are not identical.

Selectivity, S, can be evaluated by comparing the rate of chain scission of each polymer:

$$S = \frac{\text{rate of chain scission in lignosulfonate}}{\text{rate of chain scission in HEC}}$$

For the control reaction, the selectivity is decreased by increasing the hydrogen peroxide concentration (Table 11). Alternatively, for all catalyzed reactions, the selectivity is increased by increasing the hydrogen peroxide concentration.

Table 11. Selectivity based on the rate of chain scission of lignosulfonate and HEC at 20 and 40 mM H_2O_2.

CATALYST	SELECTIVITY* 20 mM H_2O_2	40 mM H_2O_2
Control	5.7	1.0
$FeSO_4$	0.75	1.4
Fe-EDTA	0.71	1.6
Hemoglobin	0.48	7.4

* S > 1 Lignosulfonate degradation predominates.
S < 1 HEC degradation predominates.

At high hydrogen peroxide concentrations (40 mM), the rate of bond breakage in lignosulfonate for all reactions exhibits a significant dependence on hydrogen peroxide (see Table 7). The rate of chain scission in HEC is not highly dependent on hydrogen peroxide (see Table 10). Consequently, from this information it would be expected that at higher concentrations of hydrogen peroxide, an increased selectivity would be observed. Selectivity values in Table 11 at 40 mM H_2O_2 reflect this.

Selectivity values also reflect inherent differences in these catalytic systems. Size, ability to generate hydroxyl radicals, and extent of side reactions are different for each of these systems. Although hemoglobin is a very large molecule, compared to $FeSO_4$ and Fe-EDTA, it is very selective. A great increase in selecitivity is observed with hemoglobin at the higher peroxide concentration. This indicates that there exists an optimum H_2O_2 : Fe ratio for this system, and warrants further study.

In these very complex systems, it is difficult to fully characterize reaction behavior. It was beyond the scope of this work to develop a detailed mechanistic explanation for these reactions. The rate of substrate degradation has only been expressed in terms of the substrate and hydrogen peroxide. Despite these shortcomings, the selectivity values in Table 11 are meaningful. In catalyzed systems, greater selectivity was achieved at higher concentrations of hydrogen peroxide.

Generation of Hydroxyl Radicals

Two different methods were used to measure hydroxyl radicals produced during the lignosulfonate and HEC reactions. The external method of the chemiluninesce assay was used for the lignosulfonate degradation reactions and all reactions containing hemoglobin. The external method measures the amount of hydroxyl radicals produced during one minute at a given point in the reaction. When the external method of the chemiluninescence assay was used for the HEC degradation reactions, no chemiluminescence was observed. This was due to the low rate at which hydroxyl radicals were produced in this system. For the HEC degradation reactions, the original method of the chemiluminescence assay yields measureable values, while not interfering with reactions rates.

In reactions with lignosulfonate, the generation of hydroxyl radicals was greatest at reaction initiation, but declined quickly as the reaction proceeded. This was observed for both $FeSO_4$ and Fe-EDTA catalyzed reactions. This behavoir correlated directly with the rate of

lignosulfonate degradation. In reactions with HEC, hydroxyl radicals were produced at relatively constant rates for the $FeSO_4$ and Fe-EDTA systems. Rates of HEC degradation were also constant for these reactions.

These results indicate that hydroxyl radicals are directly involved in the degradation of both lignosulfonate and HEC. $FeSO_4 + H_2O_2$ produced more hydroxyl radicals than Fe-EDTA $+ H_2O_2$ in both substrate systems, and more substrate degradation was observed in the $FeSO_4$ system over that of Fe-EDTA. Unfortunately, no conclusions can be drawn regarding hydroxyl radical production in hemoglobin reactions, as the data from these experiments are ambiguous.

Oxidation of organic compounds by Fenton's reagent [Fe(II) and H_2O_2] has been widely studied. Hydroxyl radicals will react either by adding to rings or aliphatic chains, or abstracting carbon-bound hydrogen atoms. Rates of •OH addition to aromatic compounds are typically greater than those of hydrogen abstraction.[104] Consequently, greater reactivity would be expected in the lignosulfonate system. However, hydroxyl radicals react slightly faster with aromatic compounds than with Fe(II) or H_2O_2.[50] Consequently, hydroxyl radicals must be generated near the desired substrate.

COMBINED SUBSTRATE EXPERIMENTS

Preceding sections described experiments designed to determine the selectivity of three biomimetic catalysts for the hydrogen peroxide oxidation of lignosulfonate over hydroxyethyl cellulose (HEC). The lignin and carbohydrate model compounds were individually exposed to each of the chosen catalysts in the presence of hydrogen peroxide. Selectivities determined from these experiments gave absolute values, as other organic substrates were not present.

This section describes experiments in which the selectivity of each of the three biomimetic catalysts has been evaluated when the two model compounds were combined in reaction solutions. This approach provides a more realistic environment in which to evaluate selectivity.

A carbohydrate to lignin ratio of 6 : 1 was chosen (Table 12). In unbleached pulp (kappa number = 30), a ratio of approximately 22 : 1 (carbohydrate to lignin) is typical. This large ratio was impossible to achieve due to analytical constraints. As the viscosity of HEC solutions were large, concentrations greater than 3.0 g/l result in solutions too viscous to stir. If the lignosulfonate concentration is dropped too low, it can not be detected by the UV-detector used for chromatography. Hence, the ratio of 6 : 1 was found to be satisfactory.

Table 12. Reaction conditions for combined substrate experiments.

Lignosulfonate	0.5 g/l
Hydroxyethyl Cellulose	3.0 g/l
H_2O_2	20 mM
Catalyst	
$FeSO_4$ and Fe-EDTA	0.2 mM
Hemoglobin (as Fe)	0.025 mM
Temperature	45°C
pH	3.0

In these experiments, selectivity can be measured directly by following the degradation of each model compound during the reaction. However, in all reactions, including that with hydrogen peroxide alone, analysis of reaction samples by size-exclusion chromatography indicated that a large molecular weight product was formed. Although this complicates the determination of selectivity, the appearance of this product, and the rate of formation thereof, provide evidence for condensation reactions occurring between lignin and carbohydrate structures even under mild reaction conditions (low pH and temperature).

Molecular Weight Data

Reaction samples from these combined substrate experiments were prepared for analysis by both size-exclusion chromatography and viscometry. Calibration of these techniques are discussed in the Materials and Methods section.

High Performance Size-Exclusion Chromatography (HPSEC)

Several HPSEC profiles from reaction samples from the $FeSO_4$ catalyzed reaction are shown in Figure 52. The unreacted lignosulfonate peak (prior to reaction initiation) is clearly visible at an elution time of approximately 13 minutes. Once the reaction has begun and the first sample taken (t = 2 minutes), this peak is no longer visible. Instead a large peak is observed, eluting at approximately 7 minutes, which is of much greater molecular weight.

This large molecular weight product is a result of the lignosulfonate and HEC polymers condensing onto one another. The molecular weight of this peak (see Figure 56) approaches 800,000. This is very near the molecular weight of HEC (undegraded), which is approximately 1,000,000. In addition, such a peak was never observed to occur in reactions which contained only lignosulfonate, even under extremely reactive conditions.

As the reaction proceeds, the large molecular weight product was degraded. This is evidenced by the rightward shifting of the peak to later elution times. By the end of the reaction

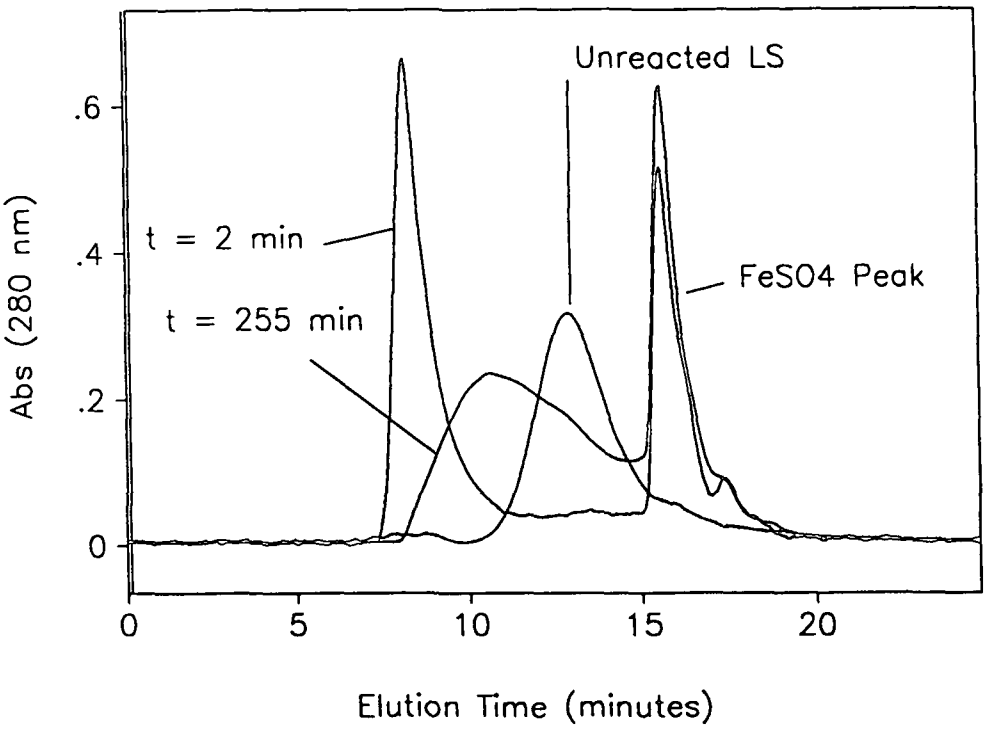

Figure 52. HPSEC profiles of several samples taken during the $FeSO_4$ catalyzed reaction. Reaction conditions: 3.0 g/l HEC, 0.5 g/l Lignosulfonate, 20 mM H_2O_2, 0.2 mM $FeSO_4$, pH 3.0, and 45°C.

(255 minutes), the molecular weight of the condensation product was nearly equal to that of the original unreacted lignosulfonate.

Figure 53 shows several HPSEC profiles of reaction samples from the Fe-EDTA catalyzed reaction. The condensation product forms immediately, as in the $FeSO_4$ catalyzed reaction (Figure 52). Degradation of the condensation product is clearly visible.

Figure 54 shows several chromatographic profiles from the hemoglobin catalyzed reaction. The large molecular weight product was formed, but not immediately as in the $FeSO_4$ or Fe-EDTA reactions. For the hemoglobin reaction, approximately 50% (or 0.075 g out of 0.15 g total) of the lignosulfonate condenses onto the HEC polymer. The condensation product again undergoes degradation in this reaction. In addition, the molecular weight of the uncondensed lignosulfonate decreases during the reaction (Figure 57).

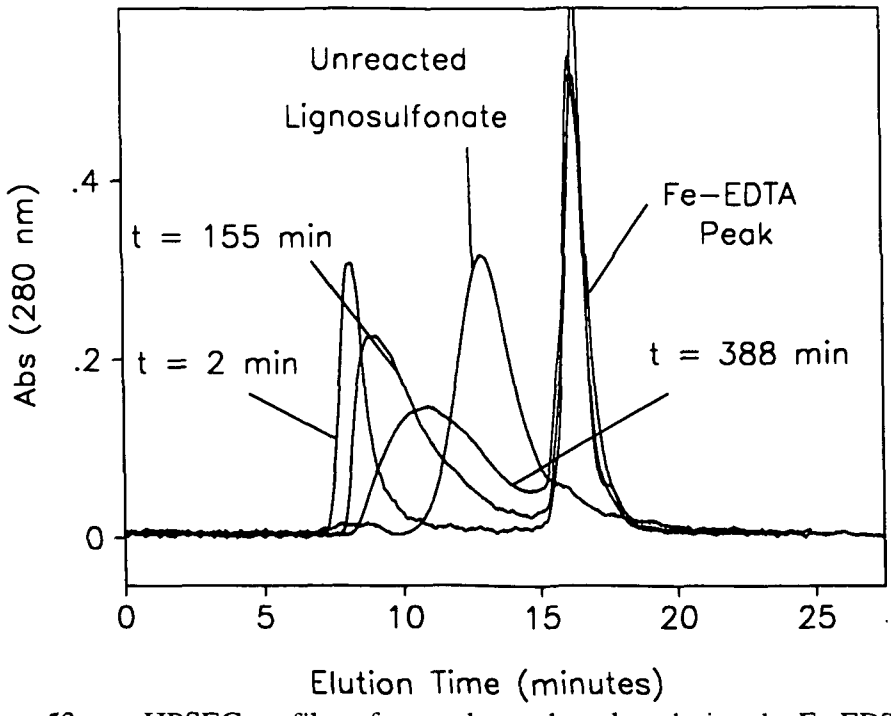

Figure 53. HPSEC profiles of several samples taken during the Fe-EDTA catalyzed reaction. Reaction conditions: 3.0 g/l HEC, 0.5 g/l Lignosulfonate, 20 mM H_2O_2, 0.2 mM Fe-EDTA, pH 3.0, and 45°C.

Figure 55 shows several HPSEC profiles of reaction samples from the control reaction (hydrogen peroxide alone). Even in the absence of catalysts, the condensation product forms. It is visible in the first sample, taken at t = 2 minutes. During the reaction, the condensation product was degraded. Not all of the lignosulfonate condenses onto the HEC polymer. The uncondensed lignosulfonate was slightly degraded during the reaction (Figure 57).

Molecular weights determined for the condensation product are shown in Figure 56 for all reactions. These values were determined from HPSEC calibration curves. However, the molecular weight distribution of this polymer exceeded the linear calibration range of the size-exclusion column. It was difficult to obtain accurate values beyond this linear region; therefore, these are only approximate molecular weights.

The decrease in the molecular weight of the condensation product is similar for the $FeSO_4$ and Fe-EDTA catalyzed reactions. The product forms immediately and was degraded throughout the reaction. In the control reaction the condensation product forms slowly, with maximum molecular weight obtained at approximately 50 minutes. The condensation product was

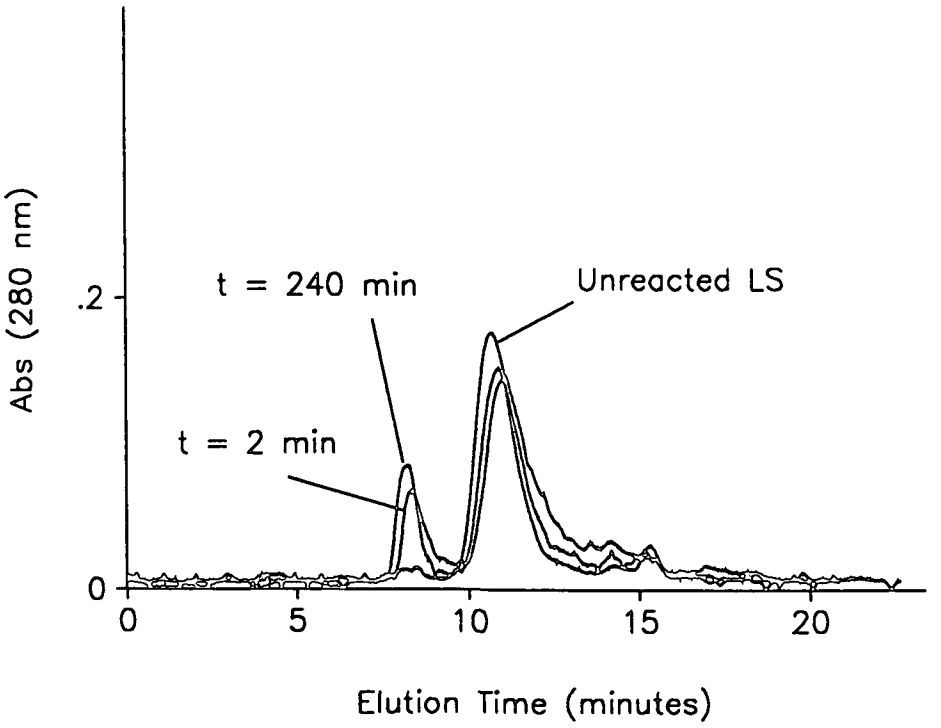

Figure 54. HPSEC profiles of several samples taken during the hemoglobin catalyzed reaction. Reaction conditions: 3.0 g/l HEC, 0.5 g/l Lignosulfonate, 20 mM H_2O_2, 0.4 g/l Hemoglobin, pH 3.0, and 45°C.

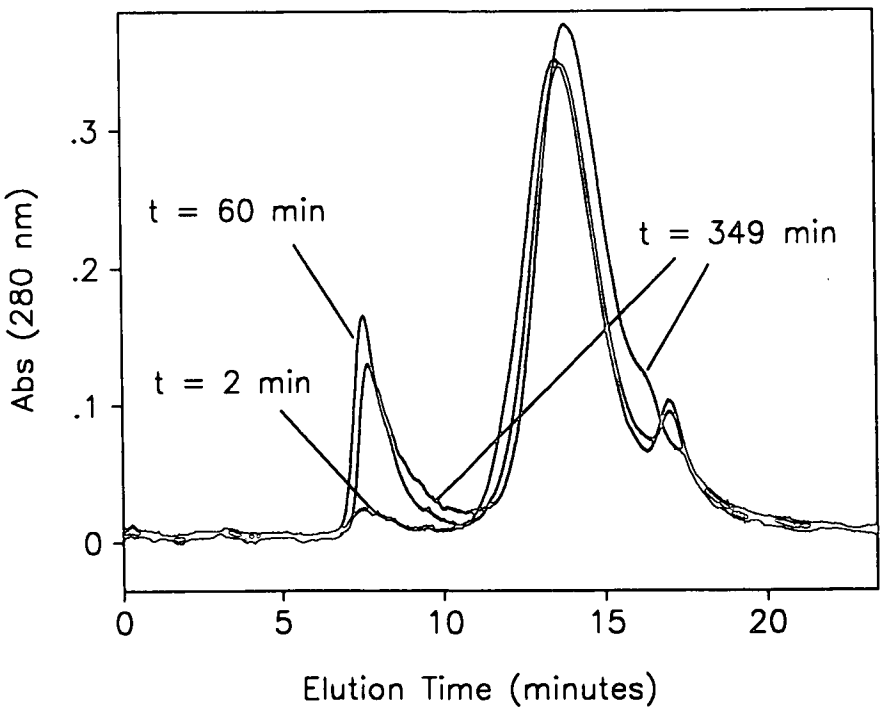

Figure 55. HPSEC profiles of several samples taken during the control reaction. Reaction conditions: 3.0 g/l HEC, 0.5 g/l Lignosulfonate, 20 mM H_2O_2, pH 3.0, and 45°C.

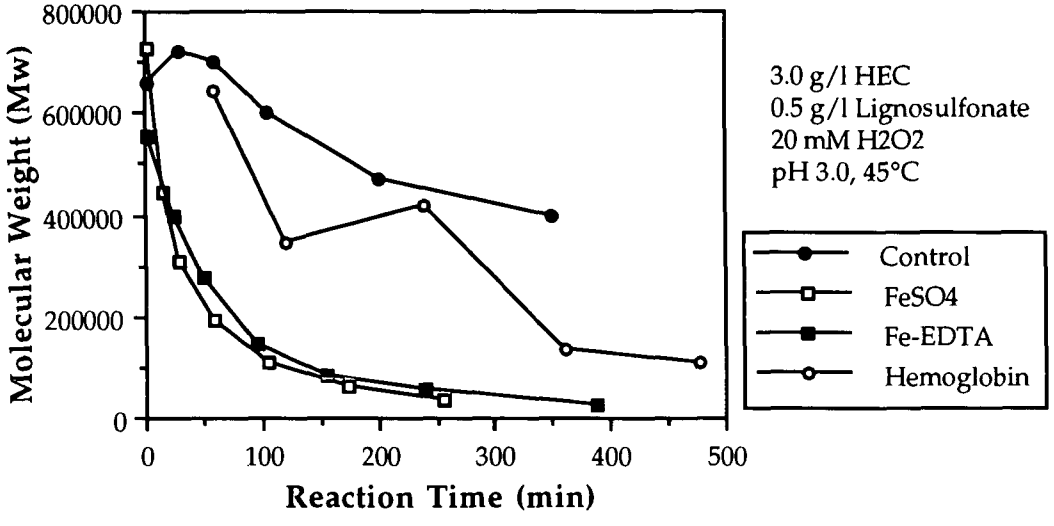

Figure 56. Weight-average molecular weight of the condensation product as determined from HPSEC for the control and three catalyzed reactions.

then slowly degraded. The formation of the condensation product was also slow in the hemoglobin catalyzed reaction, but subsequent degradation was still observed.

Molecular weight decreases in Figure 56 for the condensation product are large, ranging from 300,00 to 700,000. As lignosulfonate has a molecular weight of only 4000, these reductions obviously reflect chain scissions occurring within the HEC polymer. It is probable that some bonds in lignosulfonate are also cleaved, but it is impossible to distinguish whether this weight loss reflects lignosulfonate degradation in addition to that of HEC.

Figure 57 shows the molecular weights for the uncondensed lignosulfonate in the control and hemoglobin reactions. The addition of hemoglobin to solutions containing lignosulfonate causes a decrease in the molecular weight of the lignosulfonate. This is seen in the drop in molecular weight visible in Figure 57 for the hemoglobin run. This was also observed in reactions with lignosulfonate alone (see Lignosulfonate Degradation section). The molecular weight of HEC was not affected by the addition of hemoglobin.

The molecular weight of the lignosulfonate in the hemoglobin catalyzed reaction continues to drop, but then appears to slowly increase at latter reaction times. For the control reaction, the molecular weight of the uncondensed lignosulfonate slowly drops during the reaction.

It is difficult to evaluate selectivity in the combined substrate system. The formation of the condensation product precludes evaluation of lignosulfonate degradation as compared to HEC degradation. For the hemoglobin and control reactions, not all lignosulfonate condensed onto the HEC polymer. The molecular weight of this uncondensed lignosulfonate decreased during reactions (Figure 57). These results indicate that although mostly HEC linkages were cleaved during reactions, lignosulfonate degradation also occurred. It is likely that the lignosulfonate portion of the condensation product was also degraded during reactions in which it formed.

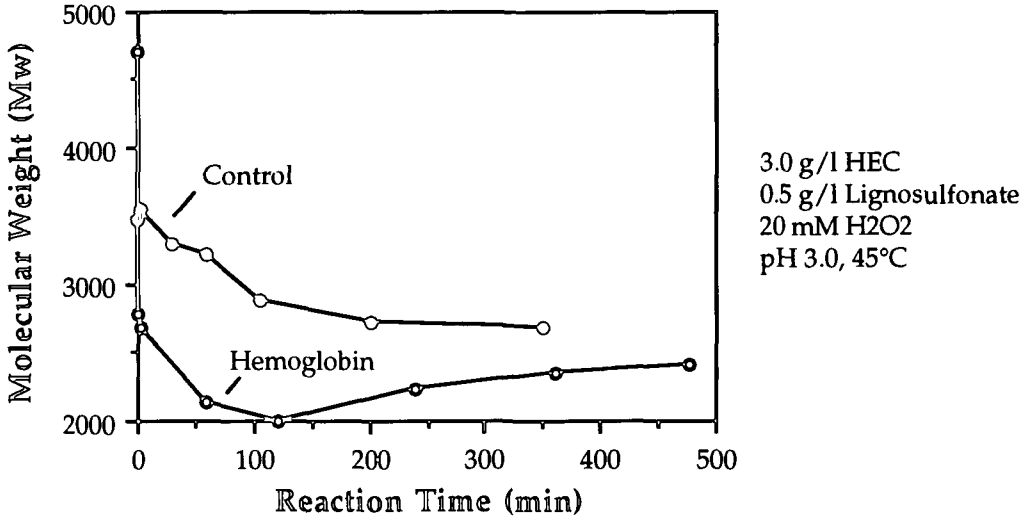

Figure 57. Weight-average molecular weight versus reaction time for uncondensed lignosulfonate in the control and hemoglobin reactions.

Viscometry

The intrinsic viscosity of reaction samples was measured during these experiments. The calibration curve used to determine these values is based on the Mark-Houwink approach used for HEC solutions. It is most probable that the Mark-Houwink parameters used in this relationship are not valid. However, the approximate molecular weight values obtained provide some useful information.

The molecular weight data obtained from intrinsic viscosity measurements are shown in Figure 58. The most degradation occurred in the presence of $FeSO_4$, followed by Fe-EDTA, hemoglobin, and the control (hydrogen peroxide only).

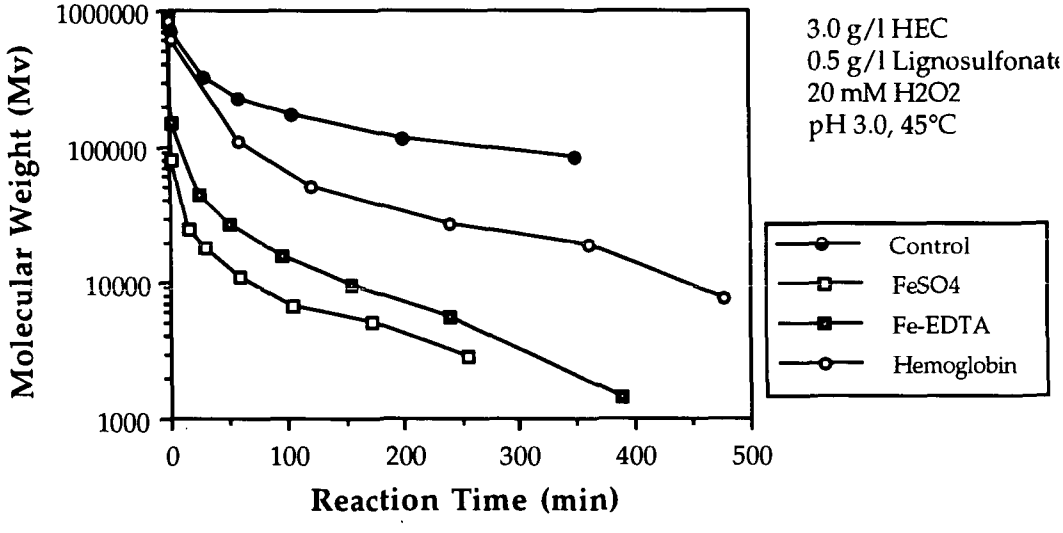

Figure 58. Molecular weight of reaction samples determined by viscometry.

Figure 59 shows a comparison between the molecular weights determined by HPSEC and viscometry for the hemoglobin-catalyzed experiments. Although the viscosity-average molecular weight is, theoretically, closer to the weight-average molecular weight,[98] this is not what is observed in Figure 59. It must be kept in mind that HPSEC and viscometry were not calibrated using representative standards. This could explain the discrepancy between these results and theory.

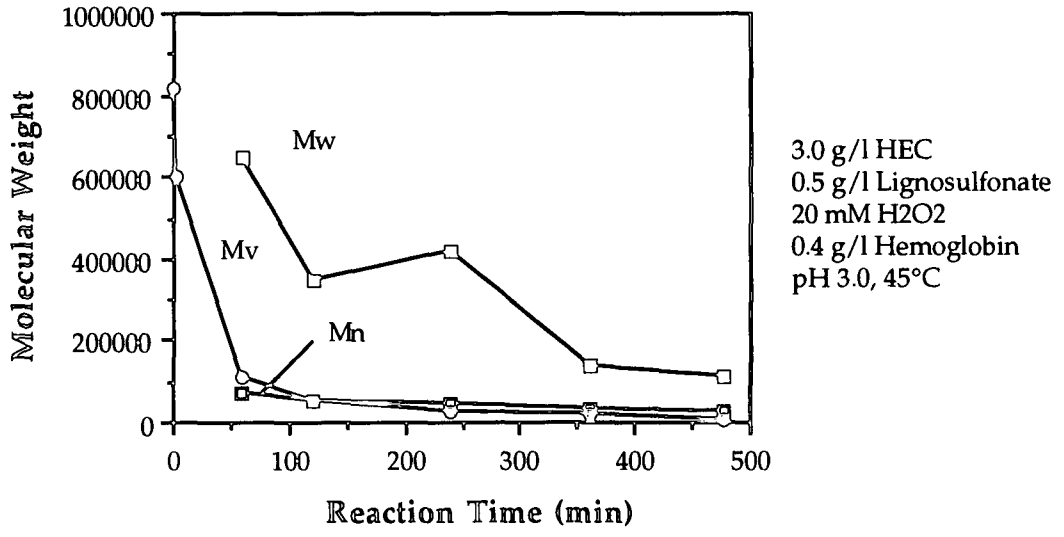

Figure 59. Viscosity- , number- , and weight- average molecular weights determined for the condensation product formed in the hemoglobin reaction.

Hydrogen Peroxide Data

The residual hydrogen peroxide concentration during the four reactions in the combined substrate system are shown in Figure 60. For the $FeSO_4$ and Fe-EDTA catalyzed reactions, the rate at which hydrogen peroxide reacts was similar. The control and hemoglobin reactions occur more slowly.

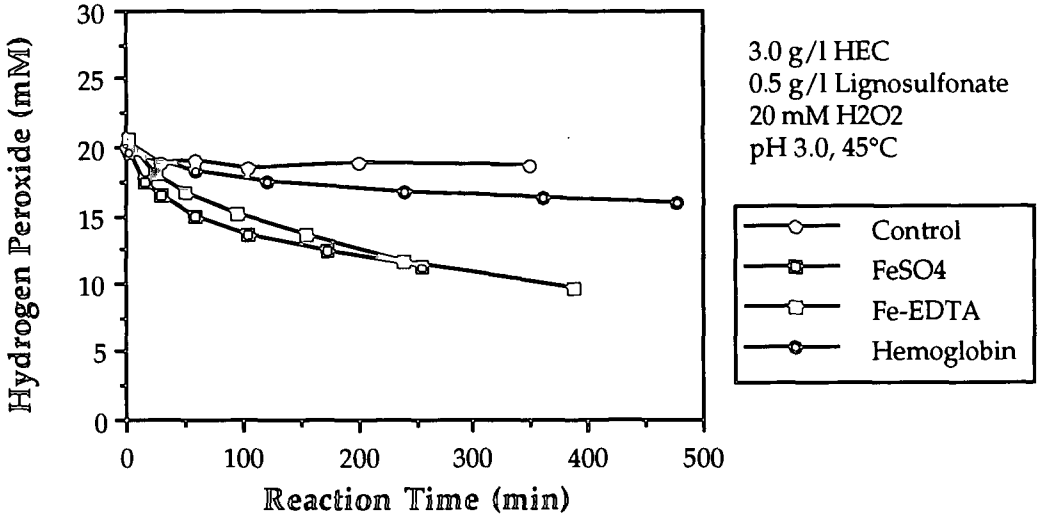

Figure 60. Residual hydrogen peroxide concentration versus reaction time for the control, $FeSO_4$, Fe-EDTA, and hemoglobin reactions.

For all reactions less than 50% of the original hydrogen peroxide charge was consumed during these reactions. Even though little peroxide reacted (~ 10 mM), degradation of the condensation product was clearly accomplished in the $FeSO_4$ and Fe-EDTA catalyzed reactions (Figures 52 and 53).

Generation of Hydroxyl Radicals

Only a slight difference in the residual hydrogen peroxide concentration for the $FeSO_4$ and Fe-EDTA catalyzed reactions was observed when phthalic hydrazide was present (Figures 61 and 62). As the phthalic hydrazide did not affect reaction rates, the original method of the chemiluminescence assay was used.

The chemiluminescence from the Fe-EDTA reaction produced substantially more hydroxyl radicals than the $FeSO_4$ reaction (Figure 63). Both reactions show a nearly equal increase in the initial (from 0 to 50 minutes) rate of phthalic hydrazide hydroxylation. The chemiluminescence in the $FeSO_4$ reaction then levels off, while hydroxylation continues in the Fe-EDTA reaction.

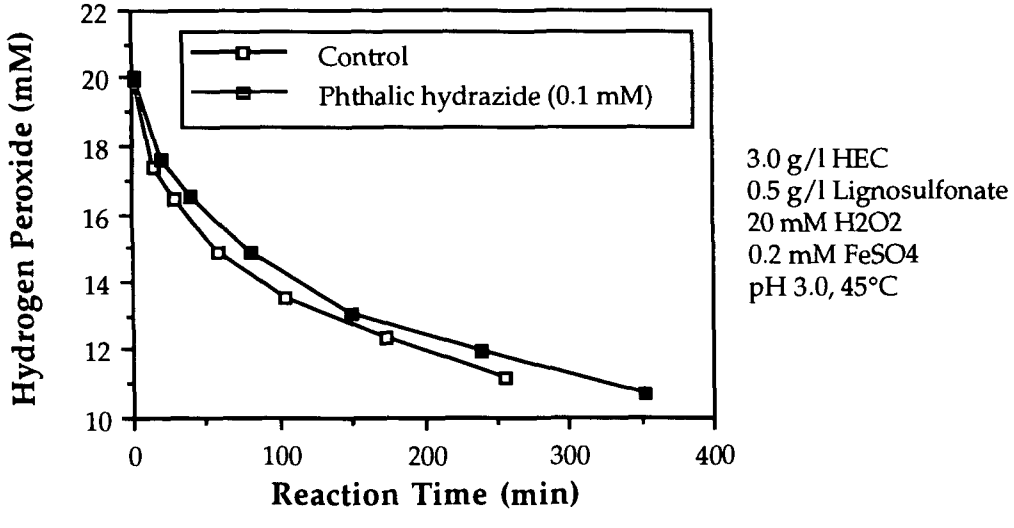

Figure 61. Residual hydrogen peroxide versus reaction time for two similar reactions in the presence and absence of phthalic hydrazide.

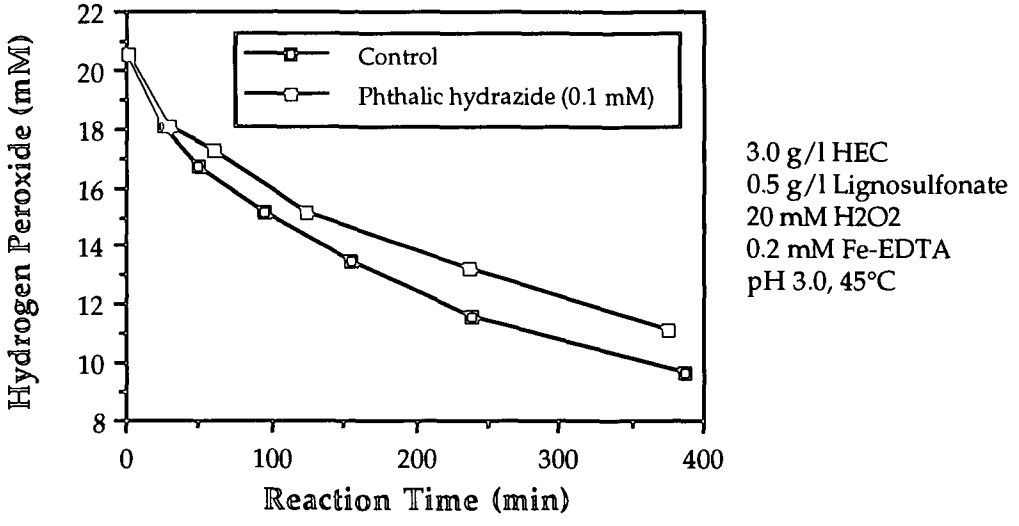

Figure 62. Residual hydrogen peroxide concentration versus reaction time for two similar reactions in the presence and absence of phthalic hydrazide.

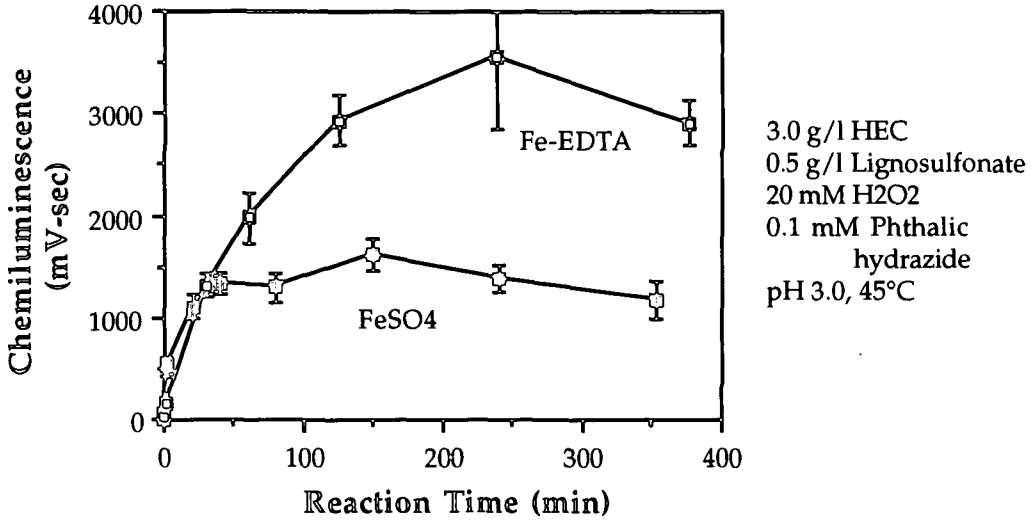

Figure 63. Chemiluminescence versus reaction time for $FeSO_4$ and Fe-EDTA catalyzed reactions, using the original method of the chemiluminescence assay.

These results differ from those obtained when substrates were individually exposed to these catalysts. In those experiments the $FeSO_4$ catalyzed reaction produced more hydroxyl radicals than the Fe-EDTA reaction for both the lignosulfonate and HEC reactions. It is possible that in the $FeSO_4$ experiment, $^{\circ}OH$ reacted with substrates more readily than in the Fe-EDTA

system. Alternatively, the concentration of phthalic hydrazide may have been less than 0.1 mM as required.

Acid Hydrolysis of the Condensation Product

Acid hydrolysis of the condensation product will cleave the glycosidic linkages within the HEC polymer. After a treatment of appropriate duration, all of the HEC attached to the lignosulfonate can be removed. The resulting sample can be re-analyzed by size-exclusion chromatography to determine the molecular weight of the lignosulfonate.

For this method to provide accurate results, lignosulfonate must not degrade during the hydrolysis treatment. Acid hydrolysis of lignosulfonate, alone or in the presence of HEC, produced no significant changes in the molecular weight or molecular weight distribution of lignosulfonate (Figure 64). These results indicate that lignosulfonate was stable to the acid hydrolysis conditions employed.

HPSEC profiles of the condensation product before and after acid hydrolysis are shown in Figure 65 for the $FeSO_4$ catalyzed reaction. The original lignosulfonate peak is also shown for comparison. The molecular weight distribution of the acid-hydrolyzed sample has shifted toward the right and broadened. This peak extends past the original lignosulfonate peak, indicating that some lignosulfonate has been degraded during the reaction.

Acid hydrolysis of the condensation product from reaction samples indicates that the lignosulfonate portion of the condensation product was degraded during this reaction. However, it is impossible to distinguish whether all HEC has been removed from the lignosulfonate.

The isolation and full characterization of the condensation product would require extensive analytical work, which is beyond the scope of this thesis. The acid hydrolysis experiments performed provide evidence for actual covalent bonding of the two substrates.

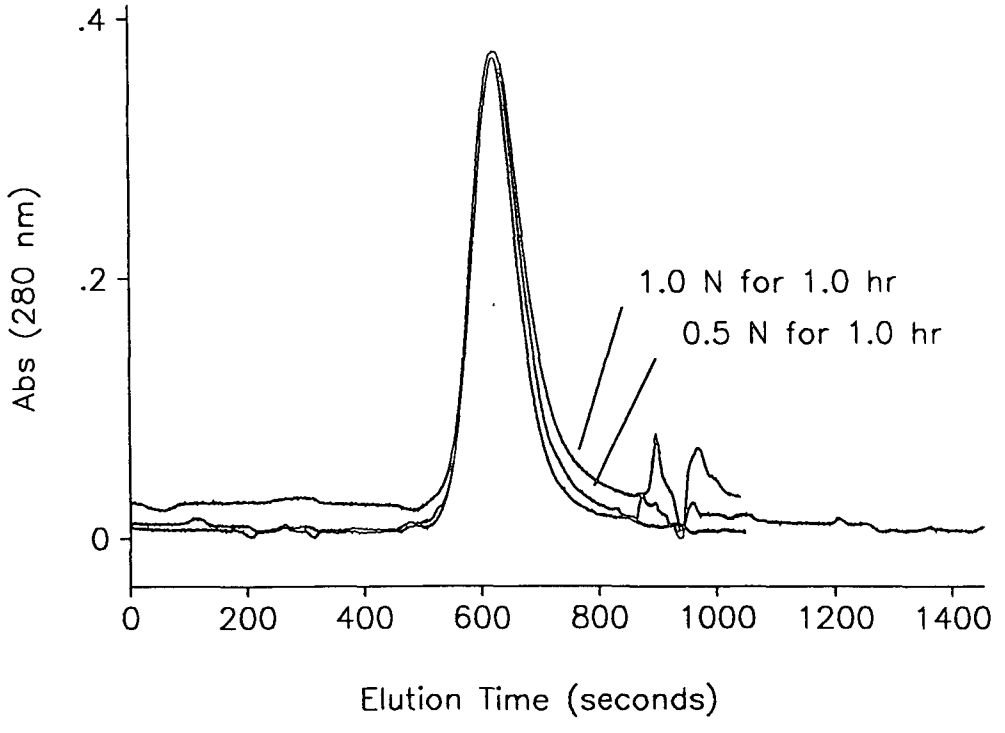

Figure 64. Lignosulfonate before and after acid hydrolysis.

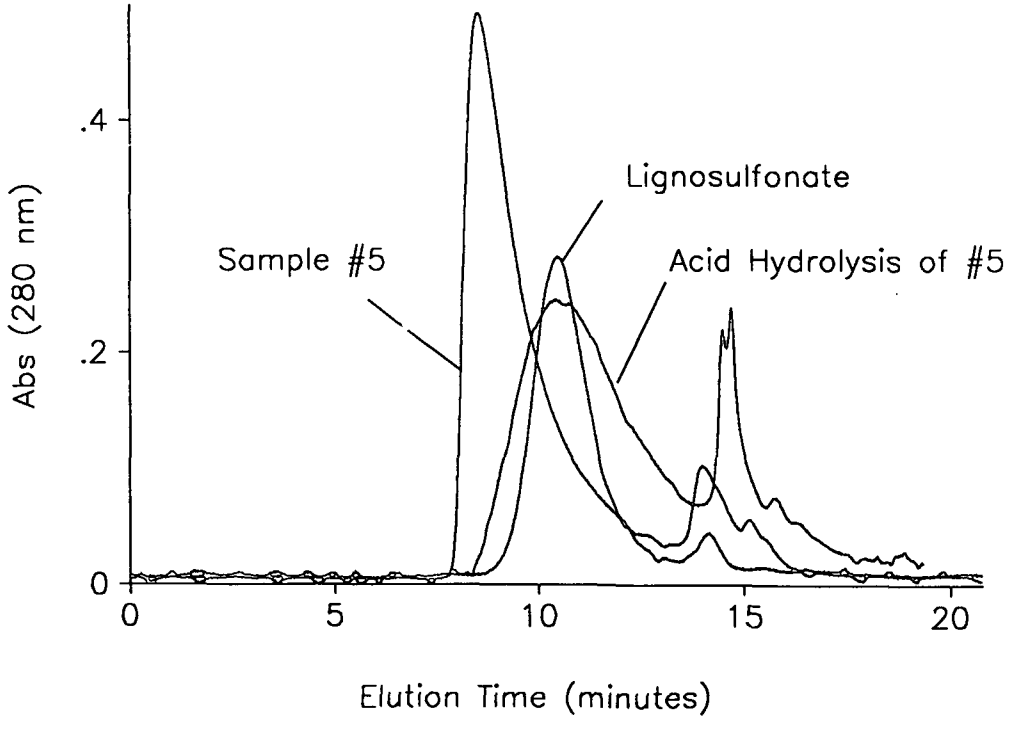

Figure 65. Sample #5 (t = 30 minutes) from the $FeSO_4$ catalyzed reaction before and after acid hydrolysis.

Condensation Product: Formation and Composition

In the above experiments, a condensation product was observed to form during reactions containing lignosulfonate and HEC in the presence of hydrogen peroxide alone or with catalysts. The condensation product did not form in reactions which did not contain hydrogen peroxide. The formation of this product is believed to be a result of radical-induced coupling of the two polymer substrates. To provide additional evidence for this hypothesis, concentrations of substrates were changed. If the condensation product results from radical-induced coupling, reducing the concentration of one of the components would reduce the amount of condensation product formed.

In previous experiments the ratio of HEC to lignosulfonate was chosen to be 6 : 1 to approximate the ratio of lignin to cellulose found in pulp. This ratio was altered to determine the effect of substrate concentration on formation of the condensation product. In one case the concentration of lignosulfonate was increased to achieve a ratio of 1 : 1. In another case, the concentration of HEC was lowered to achieve a ratio of 0.4 : 1.0. These experiments were only performed with $FeSO_4$ as catalyst.

Figure 66 shows sample HPSEC chromatograms when a 1 : 1 ratio of lignosulfonate to HEC was used. As seen in previous experiments with $FeSO_4$ and hydrogen peroxide, the condensation product forms immediately. In this case only a small amount of lignosulfonate condenses onto the HEC. The free lignosulfonate was not degraded during this experiment, while the condensation product was degraded. As only a small amount of the lignosulfonate condensed, the condensation product is mostly HEC. As the uncondensed lignosulfonate was not degraded during this reaction, the selectivity in this system was poor.

Figure 67 shows sample HPSEC chromatograms from a reaction in which the HEC to lignosulfonate ratio was 0.4 : 1.0. The condensation product forms, but its molecular weight was relatively small. It was quickly degraded, resulting in the chromatographic profile showing

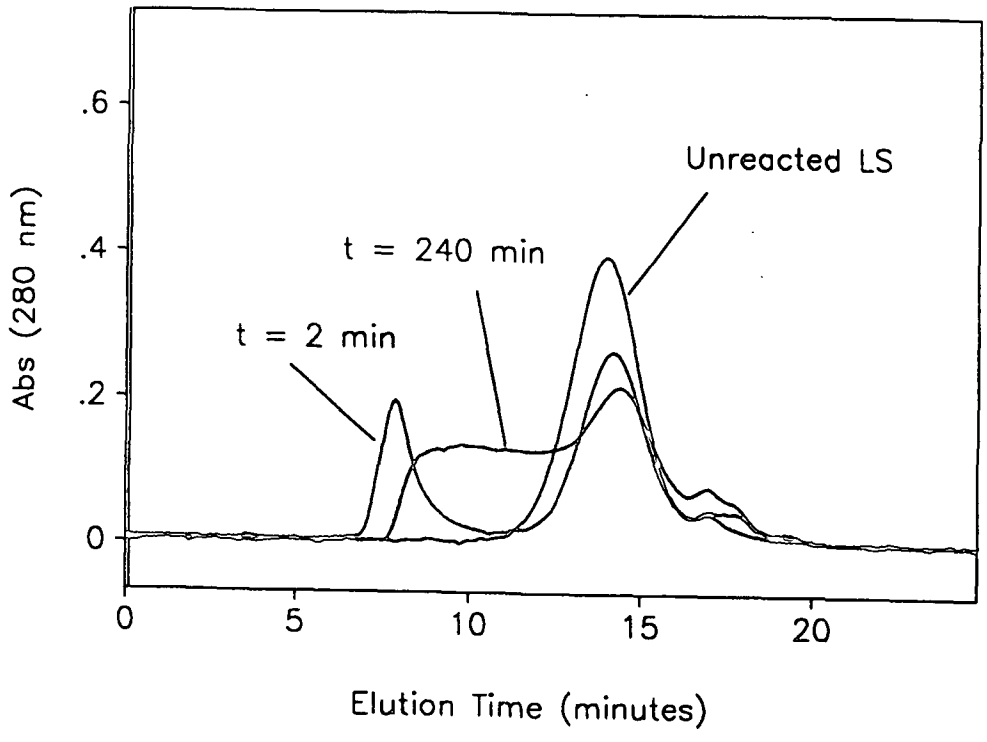

Figure 66. HPSEC profiles of several samples taken during the $FeSO_4$ catalyzed reaction with a substrate ratio of 1 : 1. Reaction conditions: 3.0 g/l HEC, 3.0 g/l Lignosulfonate, 20 mM H_2O_2, 0.2 mM $FeSO_4$, pH 3.0, and 45°C.

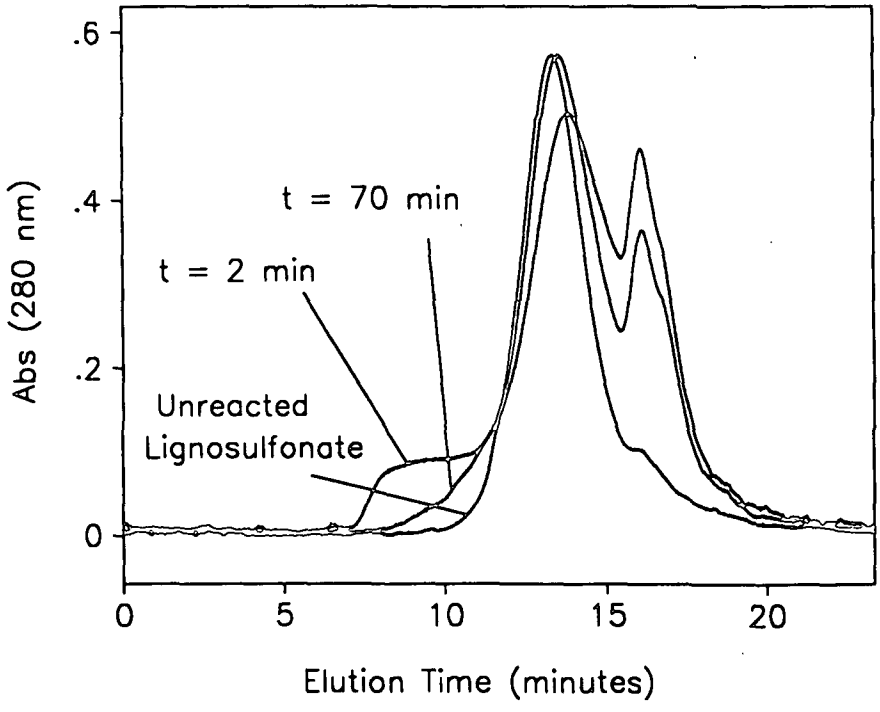

Figure 67. HPSEC profiles of several samples taken during the $FeSO_4$ catalyzed reaction with a substrate ratio of 0.4 : 1. Reaction conditions: 0.2 g/l HEC, 0.5 g/l Lignosulfonate, 20 mM H_2O_2, 0.2 mM $FeSO_4$, pH 3.0, and 45°C.

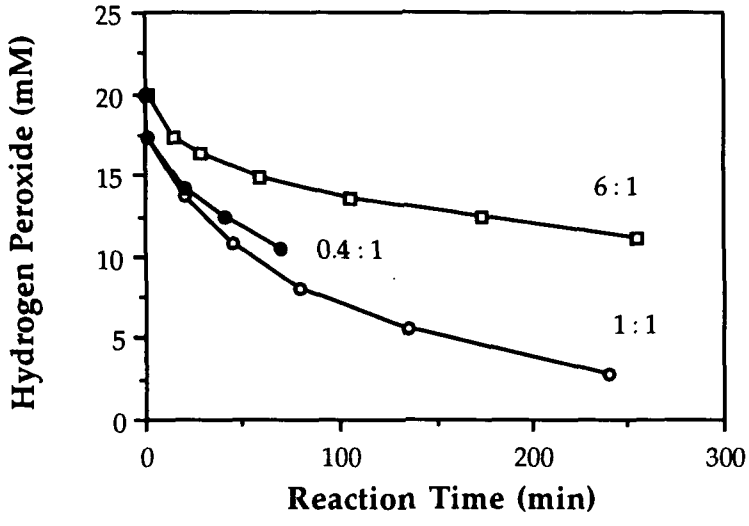

Figure 68. Residual hydrogen peroxide concentration versus reaction time for varying ratios of HEC to lignosulfonate concentration.

the original lignosulfonate. The molecular weight of the uncondensed lignosulfonate was also seen to decrease slightly.

There was a substantial increase in the rate at which hydrogen peroxide reacts (Figure 68) when the concentration of lignosulfonate was increased from 0.5 g/l (6 : 1) to 3.0 g/l (1 : 1). When this ratio was lowered further to 0.4 : 1, there was only a slight increase in the consumption of hydrogen peroxide observed for the time period evaluated (0 to 70 minutes).

In addition, when more lignosulfonate was present in solution (a 1 : 1 ratio), the amount of hydrogen peroxide decomposed quickly increased and then leveled off (Figure 69). However, when the concentration of lignosulfonate was lower (a 6 : 1 ratio), the amount of hydrogen peroxide decomposed during the reaction was significantly decreased.

This decrease in the amount of hydrogen peroxide decomposed was not a true decrease. During this experiment, oxygen was initially evolved. After approximately 50 minutes (for the 6 : 1 ratio), the volume of collected gas began to decrease. This decrease resulted from the

consumption of oxygen. As the oxygen in solution was consumed in reaction, additional oxygen dissolved in the solution, causing a decrease in the peroxide decomposed.

The consumption of oxygen indicates a mechanism other than peroxide oxidation predominates. Oxygen consumption begins when the condensation product is substantially degraded and when all lignosulfonate condenses onto the HEC (6 : 1 ratio). This implies that oxygen, as opposed to peroxide or hydroxyl radicals, was being consumed in the degradation of the condensation product.

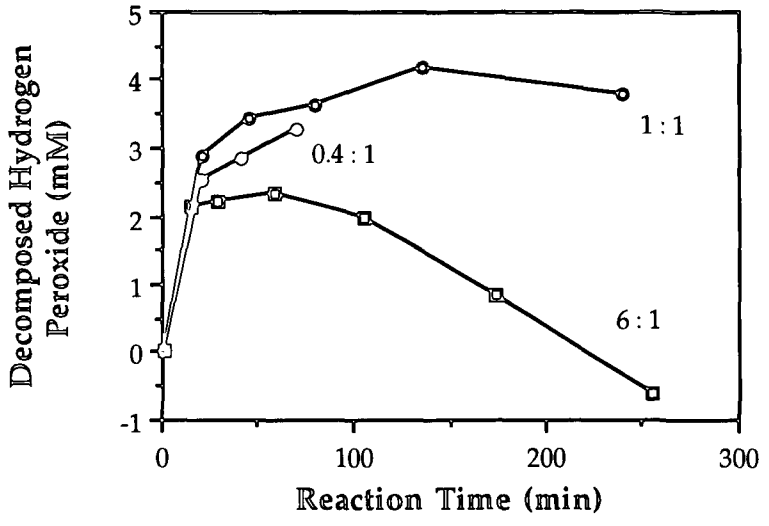

Figure 69. Hydrogen peroxide decomposed to oxygen versus reaction time for varying ratios of HEC to lignosulfonate concentration.

Figure 70 shows the percentage of the H_2O_2 reacted which has been decomposed versus the amount of H_2O_2 reacted. For the 6 : 1 ratio, the amount of H_2O_2 decomposed was initially high, but was quickly reduced, indicating that most of the H_2O_2 was being consumed by reactions. For the 1 : 1 and 0.4 : 1 ratios, the data are similar; after an initially fast increase (from reaction initiation) the percentage of hydrogen peroxide decomposed to oxygen decreased slowly.

As the concentration of lignosulfonate was increased, the rate at which hydrogen peroxide reacts increases (Figure 71). An increase in the rate of reaction could be attributed to an increased concentration of trace metals contained in the lignosulfonate preparation.

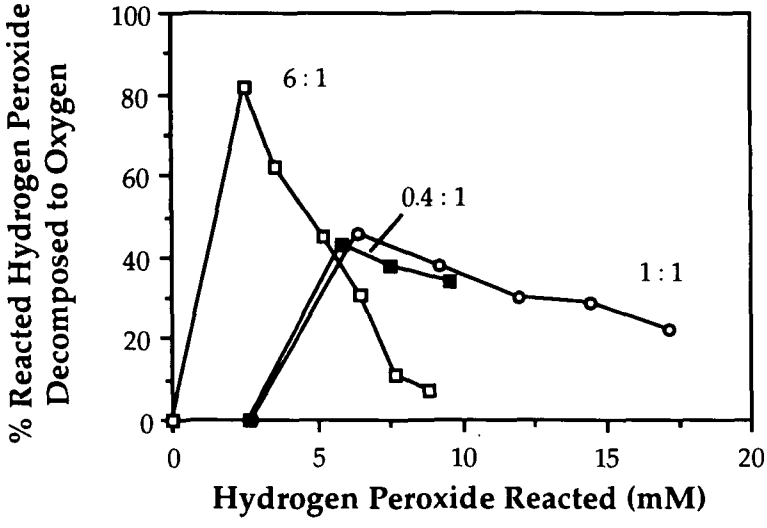

Figure 70. Percentage of reacted hydrogen peroxide which has been decomposed to oxygen versus the amount of hydrogen peroxide reacted for three ratios of HEC to lignosulfonate.

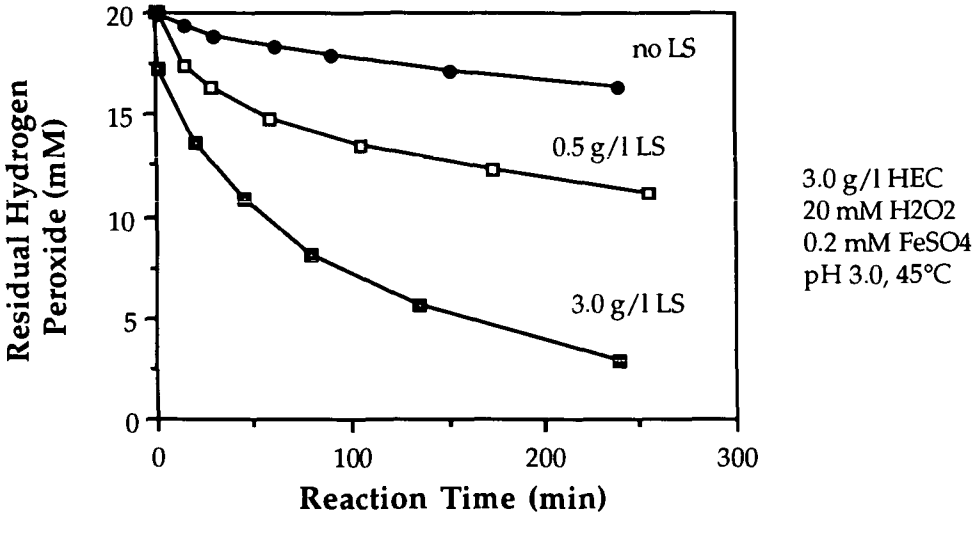

Figure 71. Residual hydrogen peroxide concentration versus reaction time for HEC in the presence of varying levels of lignosulfonate.

Generation of Hydroxyl Radicals

The external method of the chemiluminescence assay was used to measure hydroxyl radicals in these experiments. Figure 72 shows the chemiluminescence from the 6 : 1 and 1 : 1 reactions. As noted above (Figure 71), the rate at which hydrogen peroxide reacts was increased

by increasing the concentration of lignosulfonate. Figure 72 shows that at the higher lignosulfonate concentration, and therefore at higher reactivity, there are fewer hydroxyl radicals detected, as evidenced by the lower chemiluminescence.

There was a substantial difference between chemiluminescence obtained with 0.2 g/l HEC (0.4 : 1 ratio) as compared to 3.0 g/l HEC (1 : 1 ratio) in the presence of 0.5 g/l lignosulfonate (Figure 73). As the concentration of HEC increases, the concentration of hydroxyl radicals was significantly reduced.

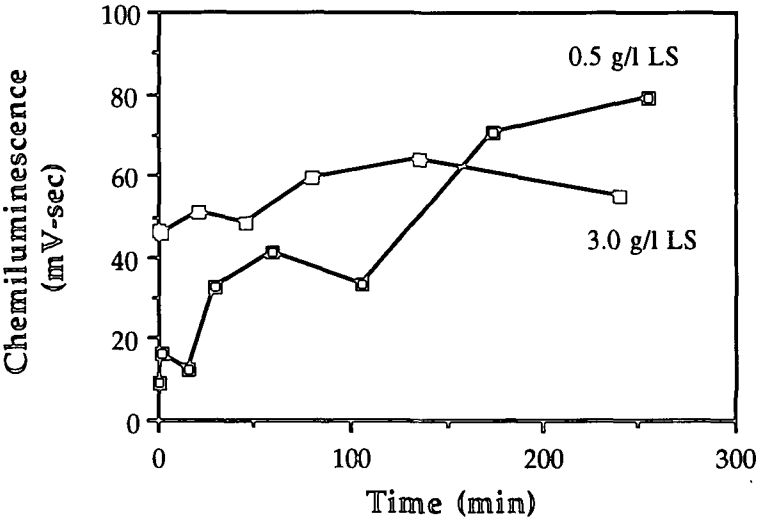

Figure 72 Chemiluminescence versus reaction time for the $FeSO_4$ catalyzed reaction containing 3.0 g/l HEC and 0.5 and 3.0 g/l lignosulfonate.

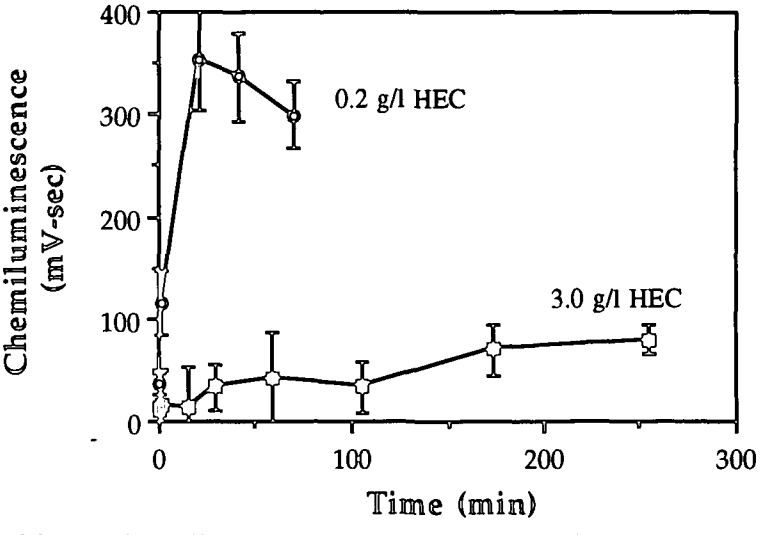

Figure 73. Chemiluminescence versus reaction time for the $FeSO_4$ catalyzed reaction containing 0.5 g/l lignosulfonate and either 0.2 or 3.0 g/l HEC.

Significance of Results

Selectivity of bleaching agents has typically been evaluated by examining lignin versus carbohydrate degradation. Results from these combined substrate experiments suggest that the condensation of wood components may be an important factor limiting bleaching effectiveness at low pH values.

The formation of the condensation product in combined substrate experiments presents a different and more complex reaction scenario. The following general equations (unbalanced) can be used to describe events occurring in these experiments:

$$H_2O_2 + \text{catalyst} \xrightarrow{k_1} HO\bullet \qquad [14]$$

$$OH\bullet + \text{Lignin} + \text{Carbohydrate} \xrightarrow{k_2} \text{Condensation Product (CP)} \qquad [15]$$

$$CP + H_2O_2/OH\bullet \xrightarrow{k_3} \text{CP Degradation Products} \qquad [16]$$

$$\text{Lignin} + H_2O_2/OH\bullet \xrightarrow{k_4} \text{Lignin Degradation Products} \qquad [17]$$

$$\text{Carbohydrate} + H_2O_2/OH\bullet \xrightarrow{k_5} \text{Carbohydrate Degradation Products} \qquad [18]$$

Selectivity as defined in the traditional sense for pulp bleaching is k_4/k_5. However, in all experiments with this combined system, some or all of the lignosulfonate was consumed by reaction [15]. A new selectivity can therefore be defined as k_4/k_3. This new selectivity may be useful in the determination of bleaching effectiveness. Another parameter of interest is the rate of the condensation reaction. A reaction system which possessed a lower k_2 would possibly favor easier lignin removal with less carbohydrate damage in pulp bleaching.

With the given analytical system and design of experiments, it was difficult to determine values for these rate constants. Only qualitative assessments can be made at this point. These catalysts can be ranked according to their ability to form the condensation product: $FeSO_4$ > Fe-EDTA > Hemoglobin > Control.

The existence and formation of lignin-carbohydrate complexes (LCC's) has been an area of active research. The formation of the condensation product in this study provides strong evidence for the formation of such complexes during acidic bleaching processes.

Results from studies on the formation of LCC's provide some indication on the likely structure of the condensation product. Reactions have been performed with different types of sugars in the presence of several lignin model compounds under different reaction conditions. Ohara and coworkers[114] reacted apocynol with methyl-α-D-glucoside in a 1 : 5 molar ratio in several cooking liquors. Ether linkages between the α-carbon and the glucoside, at the C_6 position, were isolated.

Perhaps of even greater relevance is a study performed by Katayama and coworkers[115] in which they studied the formation of LCC's generated during enzymatic lignification. Coniferyl alcohol was reacted with D-glucose in the presence of peroxidase and hydrogen peroxide under relatively mild conditions (30 minutes at room temperature). The compounds isolated after this procedure contained α-ether linkages to the C_6 position of the sugar.

Results presented in this thesis provide convincing evidence for the formation of condensation products between lignin and carbohydrate compounds under relatively mild conditions. The formation of this product was a result of a radical-induced polymerization of the two substrates. Hydroxyl radicals in other bleaching systems, such as ozone and alkaline hydrogen peroxide have been documented. The formation of the condensation product under ozone bleaching conditions should be investigated.

Alkaline Conditions

To determine if the condensation product is likely to form under conventional alkaline hydrogen peroxide bleaching conditions, an experiment similar to those previously described was performed except at a pH of 11.0. At this alkaline pH, no condensation product

was observed to form. The viscosity of reaction solutions decreased quickly (observation only), while no degradation of lignosulfonate was observed.

The alkaline reaction proceeds much more quickly than the acid peroxide reaction (Figure 74). Even though the alkaline reaction proceeds at a much quicker rate, no condensation product was formed. From these results it can be concluded that the formation of the condensation product is an acid catalyzed reaction.

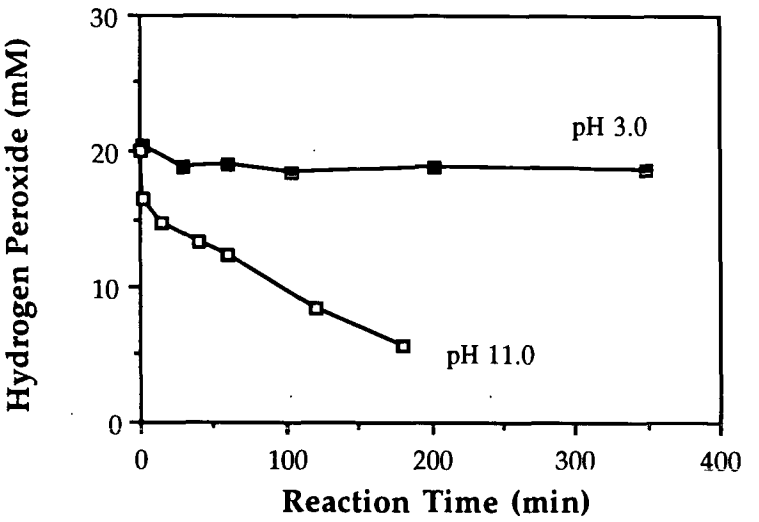

Figure 74. Residual hydrogen peroxide versus reaction time for similar reactions at initial pH of 3.0 and 11.0.

CONCLUSIONS

The focus of this work was to explore the use of biomimetic compounds as catalysts for hydrogen peroxide delignification of wood pulp. To accomplish this goal, the selectivity of three iron-based biomimetic compounds for lignin degradation over that of carbohydrate was evaluated.

SELECTIVITY

Lignosulfonate and HEC, the polymeric model compounds chosen for this study, were individually exposed to each of three biomimetic catalysts (FeSO4, Fe-EDTA and hemoglobin) in the presence of hydrogen peroxide. Degradation of these polymeric substrates was characterized and compared. Hemoglobin was found to be the most selective for lignosulfonate degradation relative to that of carbohydrate.

When lignosulfonate and HEC were combined in reaction solution, a large molecular weight condensation product was observed to form. This product formed in all reactions which contained hydrogen peroxide and catalysts, as well as the control reaction (hydrogen peroxide alone). The condensation production did not form in the absence of hydrogen peroxide. The formation of this condensation product is significant as it provide evidence for counterproductive reactions occurring in acidic bleaching environments.

HYDROXYL RADICALS

Hydroxyl radicals were measured in reactions using a chemiluminescence assay. The original method as described by the authors suffered from several shortcomings, which were overcome by modifying the existing method. Hydroxyl radicals were detected in both the $FeSO_4$ and Fe-EDTA catalyzed oxidation reactions, in the presence of lignosulfonate or HEC (or when combined). Hydroxyl radicals were not measured in reactions containing hemoglobin as catalyst, due to a limitation of the assay.

Evidence obtained herein supports involvement of the hydroxyl radical in the degradation of lignosulfonate as well as HEC during catalyzed hydrogen peroxide oxidation. During lignosulfonate degradation reactions, results obtained indicated that hydroxyl radicals were necessary for chain scission of the polymer to occur. These radicals, also observed during the degradation of HEC, cause chain scission of the carbohydrate. Careful selection of a catalyst in a commercial pulp bleaching system will possibly enable hydroxyl radicals to be directed toward lignin, achieving greater delignification without substantial degradation of the carbohydrate.

Biomimetic compounds for pulp bleaching must be designed to be selective for lignin degradation. The chosen catalyst must closely associate with lignin so as to produce hydroxyl radicals near this desired substrate. These issues must be considered in further evaluation of biomimetic compounds for pulp bleaching applications. Hydroxyl radicals are necessary for the degradation of lignosulfonate, and, by extension, are also required for the degradation of kraft residual lignins by biomimetic systems.

RECOMMENDATIONS FOR FUTURE WORK

BIOMIMETIC CATALYSTS

The direct involvement of lignin peroxidase in the enzymatic degradation of lignin has been questioned. Evidence has been obtained which indicates that polymerization of lignins occurs when exposed to enzymatic treatments. The generation of hydroxyl radicals during the enzymatic degradation of lignin is also still debated.

Biomimetic compounds have been successfully used to help elucidate the mechanisms for enzymatic degradation of lignin. Results from this thesis show that certain catalysts do exhibit some selectivity.

To further elucidate the role of the hydroxyl radical in bleaching systems with iron-based catalysts, iron chelated with DTPA could be used. Iron chelated by DTPA does not participate in the Fe(II)-Fe(III) redox cycle. Experiments using Fe-DTPA would limit the radical-reduction of Fe, allowing radicals to react specifically with the substrate and reactant (hydrogen peroxide). Other metal-based catalysts should also be investigated.

In a pulp system, heterogeneous reaction conditions prevail. Achieving close association between the lignin in the pulp fibers and a water-soluble catalyst seems unlikely. The hydroxyl radical is known to react with substrates at nearly diffusion-controlled rates. Hydroxyl radicals generated in pulp systems would react most readily with the closest substrates, be it pulp, hydrogen peroxide, or other extraneous material. Hence, this system would result in excessive damage of carbohydrate (the more abundant substrate in pulp) and loss of oxidizing power through miscellaneous side reactions.

THE COMBINED SUBSTRATE SYSTEM

Results from the combined substrate experiments have provided unique evidence for the production of a lignin-carbohydrate complex to form under relatively mild conditions. Experiments using this unique system could be designed to further evaluate under what conditions this product is formed. Whether the condensation product forms under conditions used in ozone bleaching would perhaps provide an explanation for the limited selectivity of ozone. The optimization of reaction conditions which minimize the formation of this condensation product would provide evidence for a better bleaching agent.

THE CHEMILUMINESCENCE ASSAY

The chemiluminescence assay is a useful way to measure the production of hydroxyl radicals in reaction solutions. Limited utility of this assay was found in this work, but this was due to instrumentation problems. Changing the system which was used to measure light produced from these chemiluminescent reactions, or direct measurement of the hydroxylated product, would be modifications to improve the assay.

An old photometer was used to measure chemiluminescence from samples. The maximum volume suggested for use in this instrument is 100 - 150 µl. Using such a small sample volume limits the amount of light produced during the assay. This greatly reduces the sensitivity of the assay as well. By using a different photometer with a larger sample volume, the amount of light produced from a given sample will be greatly increased. This will increase the sensitivity of the assay.

Reitberger and Gierer, who developed this assay, have published modifications to their procedure which involves using High Performance Liquid Chromatography (HPLC) to measure the hydroxylated phthalic hydrazide produced during reactions.

ACKNOWLEDGMENTS

I am extremely grateful for the guidance and support provided over the years by my advisor, Dr. Ron Dinus, and his wife Linda. I am also grateful for the insightful discussions with my thesis advisory committee members, Drs. Tom McDonough and Karl-Erik Eriksson. I thank the member companies of the Institute of Paper Science and Technology for the financial support to complete my thesis. I thank IPST for providing the stipend and fellowship necessary to make working and living in Atlanta feasible.

The help and support provided by the Institute faculty and staff are gratefully acknowledged. Without the help of these people, I would not have made it this far. I also thank all of the Institute students I have known over the years. These friendships will be treasured. I thank the Forest Biology technicians: Shannon, Cammie, Bobbie and Yolanda (and Sonja), for all their help and encouragement. Special thanks go to René, Lois, Mike, and Vinny for inspiring technical and philosophical discussions, and being there for me through the hard parts. I'd like to thank everyone by name, but just refer to the IPST telephone directory!

I thank my parents and siblings for their continued support and enthusiasm as I endeavored to capture yet one more degree. I especially thank my father for his continued support. I thank my Atlanta friends, Nancy and Gladys, for hanging in with me until the end. But, most of all, I thank my soon-to-be husband, Chris Verrill. Despite the miles and long phone calls, he was always there for me. My wish to any of you who read this, is that you have someone in your life who loves you very much, and whom you love, and that you enjoy your life to the fullest.

LITERATURE CITED

1). Trotter, P. C. Biotechnology in the pulp and paper industry. Part I: Tree improvement, pulping and bleaching, and dissolving pulp applications. Tappi J. 73(4):198-204(1990).

2). Kirk, T. K. Biotechnology in pulp and paper manufacture: 1989 International Conference Overview. Proceedings of 1989 International Symposium on Wood and Pulping Chemistry, Vol. I. pp. 339-343 (1989).

3). Eriksson, K.-E. Biotechnology in the pulp and paper industry. Academy Lecture presented on May 18, 1989 at the Fourth International Conference on Biotechnology in the Pulp and Paper Industry, Raleigh, NC. (1989).

4). Yang, J.; Eriksson, K.-E. L. Use of hemicellulytic enzymes as one stage in bleaching of kraft pulp. Holzforschung 46(6):481-488(1992).

5). Yang, J. L.; Sacon, B.; Lowe, E., Eriksson, K.-E. L. Bleaching of eucalyptus kraft pulp with the EnZone process. Tappi J. 76(7):91-96(1993).

6). Yang, J. L.; Cates, D. H.; Law, S. E.; Eriksson, K.-E. L. Bleaching of softwood kraft pulps with the EnZone process. Tappi J. 77(3):243-250(1994).

7). Eriksson, K.-E. L. Biotechnology will play key role in future non-chlorine bleaching. Pulp Paper Canada. 66(2):149-150(1992).

8). Eriksson, K.-E.; Blanchette, R. A.; Ander, P., Enzymatic Degradation of Wood and Wood Components, Springer-Verlag, New York, 1990.

9). Higuchi, T., ed., Biosynthesis and Biodegradation of Wood Components, Academic Press, Inc., New York, 1985.

10). Pettersson, B.: Yang, J.-L.; Eriksson, K.-E. Biotechnical approaches to pulp bleaching. Nordic Pulp and Paper Res. J. 3:198-202(1988).

11). Paszczynski, A.; Crawford, R. L.; Blanchette, R. A. Delignification of wood chips and pulps by using natural and synthetic porphyrins: Models of fungal decay. App. Env. Microbio. 54(1):62-68(1988).

12). Skerker, P. S.; Farrell, R. L.; Dolphin, D.; Cui, F.; Wijesekera, T. Biomimetic bleaching of kraft pulp. In: Biotechnology in Pulp and Paper Manufacture, Kirk, T. K.; Chang, H.-M., eds., Butterworth-Heinemann, Boston, 1990, pp. 203-210.

13). Crawford, R. L., Paszczynski, A. Delignification and bleaching of pulps using H_2O_2 and iron organic chelant complexes under acidic conditions as a biomimetic approach. Fourth International Conference on Biotechnology in the Pulp and Paper Industry, p. 50 May 1989.

14). Crawford, R. L. Lignin Biodegradation and Transformation, John Wiley & Sons, New York, 1981.

15). Tien, M.; Kirk, T. K. Lignin-degrading enzyme from the hymenomycete Phanerochaete chrysosporium burds. Science. 221:661-663(1983).

16). Glenn, J. K.; Morgan, M. A.; Mayfield, M. B.; Kuwahara, M. Gold, M. H. An extracellular H_2O_2-requiring enzyme preparation involved in lignin biodegradation by the white rot basidiomycete Phanerochaete chrysosporium. Biochem. Biophy. Res. Comm. 114(3):1077-1083(1983).

17). Farrell, R. L.; Murtagh, K. E.; Tien, M.; Mozuch, M. D.; Kirk, T. K. Physical and enzymatic properties of lignin peroxidase isoenzymes from Phanerochaete chrysosporium. Enzyme Micro. Technol. 11:322-328(1989).

18). Stryer, L. Biochemistry. 3rd ed., W. H. Freeman and Co., New York, 1988, p. 45.

19). Paszczynski, A.; Huynh, V. - B.; Crawford, R. L. Comparison of ligninase-I and peroxidase-M2 from the white-rot fungus Phanerochaete chrysosporium. Arch. Biochem. Biophys. 244(2):750-765(1986).

20). Troller, J.: Smith, J. D. G.; Leisola, M. S. A.; Kallen, J.; Winterhalter, K. H.; Fiechter, A. Crystallization of a lignin peroxidase from the white-rot fungus Phanerochaete chrysosporium. Bio/Technology. 6(5):571-573(1988).

21). Renganathan, V.; Gold, M. H. Spectral characterization of the oxidized states of lignin peroxidase, an extracellular heme enzyme from the white-rot basidiomyceter Phanerochaete chrysosporium. Biochemistry. 25:1626-1631(1986).

22). Glenn, J. K.; Akileswaran, L.; Gold, M. H. Mn(II) oxidation if the principal function of the extracellular Mn-peroxidase from Phanerochaete chrysosporium. Arch. Biochem. Biophys. 251(2):688-696(1986).

23). Glenn, J. K.; Gold, M. H. Purification and characterization of an extracellular Mn(II)-dependent peroxidase from the lignin-degrading Basidiomycete, Phanerochaete chrysosporium. Arch. Biochem. Biophys. 242(2):329-341(1985).

24). Paszczynski, A.; Huynh, V. - B.; Crawford, R. L. Enzymatic activities of an extracellular, manganese-dependent peroxidase from Phanerochaete chrysosporium. FEMS Microbiol. Letters. 29:37-41(1985).

25). Gold, M. H.; Akileswaran, L. Wariishi, H. Mino, Y. Loehr, T. M. Spectroal characterization of Mn-peroxidase, an extracellular heme enzyme from Phanerochaete chrysosporium. In: Odier, E. ed., Lignin Enzymic and Microbial Degradation. Symp Intern INRA, Paris, 113-118 (1987).

26). Dean, J. F. D.; Eriksson, K.-E. L. Laccase and the deposition of lignin in vascular plants. Holzforschung 48:21-24(1994).

27). Kawai, S.; Umezawa, T.; Shimada, M.; Higuchi, T. Aromatic ring cleavage of 4,6-di(tert-butyl)guaiacol, phenolic lignin model compound, by laccase of Coriolus versicolor. FEBS Letters 236:309-311(1988).

28). Samejima, M.; Eriksson, K.-E. L. A comparison of the catalytic properties of cellobiose:quinone oxidoreductase and cellobiose oxidase from Phanerochaete chrysosporium. Eur. J. Biochem. 207:103-107(1992).

29). Samejima, M.; Eriksson, K.-E. L. Redox interactions between lignin peroxidase, cellobiose:quinone oxidoreductase, and cellobiose oxidase. Proc. Fifth Int. Cong. Biotechnology in the Pulp and Paper Industry, Kyoto, Japan, pp. 327-332(1992).

30). Brock, T. D.; Smith, D. W.; Madigan, M. T. Biology of Microorganisms, Fourth Ed., Prentic-Hall, Inc., Englewood Cliffs, NJ (1984).

31). Wojtas-Wasilewska, M.; Luterek, J.; Leonowicz, A.; Dawidowicz, A. Dearomatization of lignin derivatives by fungal protocatechuate 3,4-dioxygenase immobilized on porosity glass. Biotech. Bioengg. 32:507-511(1988)

32). Leonowicz, A.; Szklarz, G.; Wojtas-Wasilewska, M. The effect of fungal laccase on fractionated lignosulphonates (Peritan Na). Photochemistry 24(3):393-396(1985).

33). Wojtas-Wasilewska, M.; Luterek, J. The effect of fungal protocatechuate 3,4-dioxygenase on sodium lignosulphonate fractions. Photochemistry 26(10):2671-2674(1987).

34). Higuchi, T. Lignin biochemistry: Biosynthesis and biodegradation. Wood Sci. Technol. 24(1):23-63(1990).

35). Kirk, T. K.; Tien, M.; Kersten, P. J.; Mozuch, M. D.; Kalyanaraman, B., Ligninase of Phanerochaete chrysosporium: mechanisms of its degradation of the non-phenolic arylglycerol ß-aryl ether substructure of lignin. Biochem. J. 236:279-287(1986).

36). Miki, K.; Renganathan, V.; Gold, M. H. Mechanism of ß-aryl ether dimeric lignin model compound oxidation by lignin peroxidase of Phanerochaete chrysosporium. Biochemistry 25(17):4790-4796(1986).

37). Miki, K.; Kondo, R.; Renganathan, V.; Mayfield, M. B.; Gold, M. H. Mechanism of aromatic ring cleavage of ß-biphenylether dimer catalyzed by lignin peroxidase of Phanerochaete chrysosporium. Biochemistry 27(13):4787-4794(1988).

38). Lewis, N. B.; Yamamoto, E. Lignin: occurrence, biogenesis and biodegradation. Annu. Rev. Plant Physiol. Plant Mol. Biol. 41:455-496(1990).

39). Sarkanen, S. Enzymatic lignin degradation: An extracurricular view. In: Enzymes in Biomass Conversion, ACS Symposium Series 460, Leatham, G. F. and Himmel, M. E. eds., ACS Washington, DC (1991).

40). Tonon, R.; Odier, E. Influences of veratryl alcohol and hydrogen peroxide on ligninase activity and ligninase production by Phanerochaete chrysosporium. Appl. Envir. Microbio. 54(2):466-472(1988).

41). Faison, B. D.; Kirk, T. K.; Farrell, R. L. Role of veratryl alcohol in regulating ligninase activity in Phanerochaete chrysosporium. Appl. Envir. Microbio. 52(2):251-254(1986).

42). Faison, B. D.; Kirk, T. K. Factors involved in the regulation of a ligninase activity in Phanerochaete chrysosporium. Appl. Envir. Microbio. 49(2):299-304(1985).

43). Harvey, P. J.; Schoemaker, H. E.; Palmer, J. M. Veratryl alcohol as a mediator and the role of radical cations in lignin biodegradation by Phanerochaete chrysosporium. FEBS Letters 195(1,2):242-246(1986).

44). Gold, M. H. Kutsuki, H.; Morgan, M. A. Oxidative degradation of lignin by photochemical and chemical radical generating system. Photochem. Photobiol. 28:647-651(1983).

45). Forney, L. J.; Reddy, C. A.; Tien, M.; Aust, S. D. The involvement of hydroxyl radical derived from hydrogen peroxide in lignin degradation by the white-rot fungus Phanerochaete chrysosporium. J. Biol. Chem. 257(19):11455-11462(1982).

46). Kutsuki , H.; Gold, M. H. Generation of hydroxyl radical and its involvement in lignin degradation by Phanerochaete chrysosporium. Biochem. Biophys. Res. Comm. 109(2):320-327(1982).

47). Bes, B.; Ranjeva, R. Boudet, A. M. Evidence for the involvement of activated oxygen in fungal degradation of lignocellulose. Biochimie 65:283-289(1983).

48). Kirk, T. K.; Mozuch, M. D.; Tien, M. Free hydroxyl radical is not involved in an important reaction of lignin-degradation by Phanerochaete chrysosporium Burds. Biochem. J. 226:455-460(1985).

49). Barr, D. P.; Shah, M. M.; Grover, T. A.; Aust, S. D. Production of hydroxyl radical by lignin peroxide from Phanerochaete chrysosporium. Arch. Biochem. Biophys. 298(2):480-485(1992).

50). Barb, W. G.; Baxendale, J. H.; George, P.; Hargrave, K. R. Reactions of ferrous and ferric ions with hydrogen peroxide. Part II -- The ferric ion reaction. Trans. Faraday Soc. 47:591-616(1951).

51). Halliwell, B.; Grootveld, M. An aromatic hydroxylation assay for hydroxyl radicals utilizing high-performance liquid chromatography (HPLC). Use to investigate the effect of EDTA on the Fenton reaction. Free Rad. Res. Comms. 1:243-250(1986).

52). Reitberger, T.; Gierer, J. Chemiluminescences as a means to study the role of hydroxyl radicals in oxidative processes. Holzforschung 42(6):351-356(1988).

53). Backa, S.; Gierer, J.; Reitberger; Nilsson, T. Hydroxyl radical activity associated with the growth of white-rot fungi. Holzforschung. 47(3):181-187(1993).

54). Backa, S.; Gierer, J.; Reitberger, T.; Nilsson, T. Hydroxyl radical activity in brown-rot fungi studied by a new chemiluminescence method. Holzforschung. 46(1):61-67(1992).

55). Eriksson, T.; Gierer, J. Fifth Int'l Symp. Wood and Pulping Chem. Proceedings, 59-63 (1989).

56). Kirk, T. K. The action of ligninase on lignin model compounds and lignin. Proceedings of the 1986 TAPPI Research and Development Conference, pp. 73-78 (1986).

57). Farrell, R. U.S. patent 4,687,745 (1987).

58). Olsen, W. L.; Slocomb, J. P. Gallagher, H. P.; Burris, A. K. European patent EP0345715 (1989).

59). Arbeloa, M; de Leseleuc, J.; Goma, G.; Pommier, J.-C. An evaluation of the potential of lignin peroxidase to improve pulp. Tappi Journal. 75(3):215-221(1992).

60). Farrell, R. L. Kraft pulp bleaching with ligninolytic enzymes. 1986 3rd Int'l Conference on Biotechnology in the Pulp and Paper Industry, pp. 61-63(1986).

61). Farrell, R. L. Biocatalysts hold promise of better pulp quality. Tappi J. 67(10):31-33(1984).

62). Fish, R. H.; Fong, R. H.; Price, R. T.; Vincent, J. B.; Christou, G. Hydroxylation of C2, C3 and cyclo-C6 hydrocarbons by manganese porphyrin and nonporphyrin catalysts. In: Biocatalysis and Biomimetics. Burrington, J. D.; Clark, D. S., eds., ACS Symposium Series 392, ACS Washington DC (1989).

63). Sheldon, R. A.; Kochi, J. K. Metal-Catalyzed Oxidations of Organic Compounds, Academic Press, New York, 1981.

64). Shimada, M.; Habe, T.; Umezawa, T. Higuchi, T.; Okamoto, T. The C-C bond cleavage of a lignin model compound, 1,2,-diarylpropane-1,3-diol, with a heme-enzyme model catalyst tetraphenylprophyrinatoiron(III)chloride in the presence of tert-butylhydro-peroxide. Biochem. Biophys. Res. Comm. 122(3):1247-1252(1984).

65). Habe, T.; Shimada, M.; Higuchi, T. Biomimetic approach to lignin degradation I. H_2O_2-dependent C-C bond cleavage of the lignin model compounds with a natural iron porphyrin and imidazole complex. Mokuzzai Gakkaishi 31(1):54-55(1985).

66). Shimada, M.; Habe, T.; Higuchi, T.; Okamoto, T.; Panijpan, B. Biomimetic approach to lignin degradation II. The mechanism of oxidative C-C bond cleavage reactions of lignin model compounds with natural iron (III) porphyrin chloride as a heme-enzyme model system. Holzforschung. 41(5):277-285(1987).

67). Huynh, V. - B. Biomimetic oxidation of lignin model compounds by simple inorganic complexes. Biochem. Biophys. Res. Comm. 139(3):1104-1110(1986).

68). Cui, F.; Dolphin, D.; Wijesekera, T.; Farrell, R. L.; Skerker, P. Biomimetic Studies of Lignin Degradation and Bleaching

69). Singh, R. P., ed. The Bleaching of Pulp, 2nd ed. TAPPI Press, Atlanta, GA (1979).

70). Crawford, R. L. personal communication, March 1990.

71). Shimada, M.; Nakagawa, M; Hattori, T.; Higuchi, T. A new biomimetic lignin degradation system developed with Mn/Co catalysts and its application to the chlorine-free bleaching of kraft pulps. Mokuzzai Gakkaishi, 35(9):859-860(1989).

72). Casey, J. P. Pulp and Paper Chemistry and Chemical Technology, 3rd ed. Vol I, John Wiley & Sons, New York (1980).

73). Walling, C. Fenton's reagent revisited. Accts. Chem. Res. 8:125-131(1975).

74). Burton, J. T.; Campbell, L. L. Hydrogen peroxide decomposition by metal catalysts: Bad actors in a bleaching stage. Intl. Symp. Wood and Pulping Chemistry, pp. 255-259 (1985).

75). Smith, P. K.; McDonough, T. J. Transition metal ion catalysis of the reaction of a residual lignin-related compound with alkaline hydrogen peroxide. Svensk Papperstidning. 88(12):R106-R112(1985).

76). Hobbs, G. C. Abbot, J. Peroxide bleaching reactions under alkaline and acidic conditions. J. Wood Chem. Tech. 11(2):225-246(1991).

77). Smith, P. K. Transition metal ion catalyzed oxiddation of a residual lignin-related compound by alkaline hydrogen peroxide. Doctoral Dissertation. The Institute of Paper Chemistry, Appleton, Wis. (1984).

78). Landucci, L. L. Metal-catalyzed phenoxy radical generation during lignin oxidation. Trans. Tech. Sect. CPPA 4(1):TR25-TR29(1978).

79). Lachenal, D.; soria, L; de choudens, C.; Monzie, P. Optimization of bleaching sequences using peroxide as first stage. 1982 International Pulp Bleaching Conference, May 24-27, pp. 145-151 (1982).

80). Suss, H. U.; Helmling, O. Acidic hydrogen peroxide/oxygen treatment of kraft pulp prior to oxygen delignification. 1987 International Oxygen Delignification Conference, pp 179-182 (1987).

81). Gierer, J. Chemistry of delignification. Part 2: Reactions of lignin during bleaching. Wood Sci. Technol. 20:1-33(1986).

82). Dence, C. W. The reactions of hydrogen peroxide with lignin-Current status. In: Gratzl, J. S.; Nakano, J.; Singh, R. P. eds., Chemistry of Delignification with Oxygen, Ozone, and Peroxides, pp. 199-205, Tokyo, Japan, Uni Publishers Co., Ltd. 1980.

83). Hobbs, G. C.; Abbot, J. Peroxide bleaching reactions under alkaline and acidic conditions. Wood Chem. Tech. 11(2):225-246(1991).

84). Schumb, W. C.; Satterfield, C. N.; Wentworth, R. L. Hydrogen Peroxide, Reinhold Publishing Corp., New York 1955.

85). Sepp, R. G.; Faust, B. C.; Holgne, J. Hydroxyl radical formation in aqueous reactions (pH 3-8) of Iron (II) with hydrogen peroxide: The photo-fenton reaction. Environ. Sci. Tech. 363(2):313-319(1992).

86). Singh, S.; Hider, R. C. Colorimetric detection of the hydroxyl radical: Comparison of the hydroxyl-radical-generating ability of various iron complexes. Anal. Biochem. 171:47-54(1988).

87). Puppo, A.; Halliwell, B. Formation of hydroxyl radicals from hydrogen peroxide in the presence of iron: Is Haemoglobin a biological Fenton reagent? Biochem. J. 249:185-190(1988).

88). Ek, M.; Gierer, J.; Jansbo, K. Study of the selectivity of bleaching with oxygen-containing species. Holzforschung 43:391-396(1989).

89). Aitken, M. D.; Irvine, R. L. Stability testing of ligninase and Mn-peroxidase from Phanerochaete chrysosporium. Biotech. Bioeng. 34(12):1251-1260(1989).

90). Sarkenen, K. V.: Ludwig, C. H., eds., Lignins: Occurrence, Formation, Structure, and Reactions. Wiley-Interscience, New York (1971).

91). Weast, R. C., ed., CRC Handbook of Chemistry and Physics, 63rd ed., CRC Press Inc., Boca Raton, Florida, 1983, pg D-140.

92). TAPPI Test Method T 650 om-89. Solids content of black liquor.

93). Lewis, N. G.; Yean, W. Q. High performance size-exclusion chromatography of lignosulphontes. J. Chrom. 331:419-424(1985).

94). Forss, K.; Kokkonen, R.; Sågfors, P.-E. Determination of the molar mass distribution of lignins by gel-permeation chromatography. In: Lignin: Properties and Materials, Glasser, W. G. and Sarkenen, S., eds., ACS Symposium Series 397, ACS Washington DC, 1989, pp. 124-134.

95). Froment, P.; Pla, F. Determinations of average molecular weights and molecular weight distributions of lignin. In: Lignin: Properties and Materials, Glasser, W. G. and Sarkenen, S., eds., ACS Symposium Series 397, ACS Washington DC, 1989, pp. 135-143.

96). Friese, M. A. Equilibrium adsorption of polyallylamine from aqueous media. Doctoral Dissertation. The Institute of Paper Science and Technology, Atlanta, Georgia (1993).

97). Yan, W. W.; Kirkland, J. J.; Bly, D. D. Modern Size-Exclusion Chromatography, John Wiley & Sons, New York, 1979.

98). Rudin, A. The Elements of Polymer Science and Engineering, Academic Press, NY (1982).

99). Brown, W.; Henley, D.; Ohman, J. Studies on cellulose derivatives Part II. The influence of solvent and temperature on the configuration and hydrodynamic behavior of hydroxyethyl cellulose in dilute solution. Makro. Chem. 64:49-67(1963).

100). Hubbard, G., Georgia Institute of Technology, personal communication, August 1991.

101). TAPPI Test Method T 236 cm-85. Kappa number of pulp.

102). TAPPI Test Method T 230 om-89. Viscosity of pulp (capillary viscometer method).

103). Steiner, M. G.; Babbs, C. F. Quantitation of the hydroxyl radical by reaction with dimethyl sulfoxide. Arch. Biochem. Biophysics. 278(2):478-481(1990).

104). Tatsumi, K.; Murayama, K.; Terashima, N. Reaction of lignin with hydroxyl radicals. 1987 International Oxygen Delignification Conference, pp. 99-104.

105). Ander, P.; Stalmasek, M.; Petterson, B. Reactivity of lignin-related phenols with hemoglobin and $NaClO_3$. Appl. Microbiol. Biotechol.

106). Huheey, J. E. Inorganic Chemistry: Principles of Structure and Reactivity, 2nd Ed., Harper and Row, Publishers, 1978.

107). DeCroes, G. C.; Tamblyn, J. W. Stabilization of cellulose esters. Polymer Degradation Mechanisms, National Bureau of Standards Circular 525, 1953:187.

108). Elias, H.-G. Macromolecules 2: Synthesis and Materials, Plenum Press, New York (1977).

109). Walker, C. C. Progress Report XV, March 1994.

110). Gilbert, B. C.; King, D. M.; Thomas, C. B. The oxidation of some polysaccharides by the hydroxyl radical: An E.S.R. investigation. Carbo. Res. 125:217-235(1984).

111). Moody, G. J. The action of hydrogen peroxide on carbohydrates and related compounds. Adv. Carbo. Chem. 19:149-179(1964).

112). von Sonntag, C. Free-radical reactions of carbohydrates as studied by radiation techniques. Adv. Carbo. Chem. Biochem. 37:7-77(1980).

113). Schuchmann, M. N.; von Sonntag, C. J. Chem. Soc. Perkin Trans. 2:1958-1963(1978).

114). Ohara, S.; Hosoya, S. Nakano, J. Studies on the formation of lignin-carbohydrate complex during alkaline pulping processes. 26(6):408-413(1980).

115). Katayama, Y.; Morohoshi, N. Haraguchi, T. Formation of lignin-carbohydrate complex in enzymatic dehydrogenation of coniferyl alcohol II. Isolation of lignin-carbohydrate complex with guaiacylglycerol-ß-coniferyl ether or other dimeric compound as lignin moiety. Mokuzai Gakkaishi 26(6):414-420(1980).

APPENDICES

APPENDIX I

DATA FROM CHEMILUMINESCENCE CALIBRATION AND SENSITIVITY EXPERIMENTS

This appendix contains data from the calibration and sensitivity experiments performed during the development of the chemiluminescence assay.

Table 13. Data from the UV-irradiation of 50 mM H_2O_2 containing 0.5 mM phthalic hydrazide (six replicates for each sample).

Time (min)	Chem. (mv-sec)	Std.[a]	95% Conf. Limits
0	20.68	7.18	7.54
0.2	102.51	9.47	9.94
10.25	2769.89	372.62	390.95
20.0	3232.78	487.96	511.96
30.0	5953.48	674.04	707.20
40.0	5369.76	389.90	409.09
50.2	8309.15	467.82	490.84
60.0	10209.98	1142.01	1198.19
80.0	10248.99	1148.73	1205.24
100.0	9913.25	859.44	901.72
120.0	9477.31	838.67	879.94
180.0	8290.72	792.17	831.15
240.0	7832.73	931.51	977.34

[a] Standard deviation based on six determinations of a sample.

Table 14. Reaction data for the 100 mM H_2O_2, 0.1 mM Fe-EDTA, 0.5 mM phthalic hydrazide, pH 3.0, 45°C. HR-21, Nbk. 4080, Pg. 159.

	Hydrogen Peroxide (mM)					
Time (min)	Residual	Decomposed	Consumed	pH	Chemi. (mV-sec)	Std.[a]
0	—	—	—	3.10	19.29	16.55
1	102.38	0.00	0.00	3.05	68.11	10.85
40	102.13	0.00	0.00	3.04	440.89	71.44
80	102.38	0.00	0.00	3.03	765.14	134.34
120	102.44	0.00	0.00	3.08	1557.35	352.54
160	102.50	—	—	3.06	1824.18	70.68
204	—	—	—	3.05	2437.96	894.82
238	—	—	—	3.06	1609.59	260.05
302	—	—	—	3.07	1996.03	175.14
360	—	—	—	3.07	1317.14	81.72

[a] Standard deviation based on three samples.

Table 15. Reaction data for the 100 mM H_2O_2, 0.25 mM Fe-EDTA, 0.5 mM phthalic hydrazide, pH 3.0, 45°C. HR-23, Nbk. 4080, Pg. 166.

	Hydrogen Peroxide (mM)					
Time (min)	Residual	Decomposed	Consumed	pH	Chemi. (mV-sec)	Std.[a]
0	101.00	0.00	0.00	3.09	16.60	8.03
1	101.00	0.00	0.00	3.11	190.26	15.14
30	100.75	1.92	-1.67	3.11	612.35	92.62
60	100.63	2.12	-1.75	3.10	1122.75	46.20
90	---	2.30	---	3.10	1788.88	274.35
120	100.00	2.51	-1.50	3.10	1271.99	109.96
165	99.25	2.93	-1.18	3.10	1151.42	185.98
211	98.56	3.47	-1.03	3.14	619.08	84.75
256	97.56	4.12	-0.69	3.15	693.07	43.03
300	96.50	4.90	-0.40	3.19	542.99	49.38
368	94.75	5.88	0.37	3.19	478.54	69.86

[a] Standard deviation based on three samples.

Table 16. Reaction data for the 100 mM H_2O_2, 0.5 mM Fe-EDTA, 0.5 mM phthalic hydrazide, pH 3.0, 45°C. HR-17, Nbk. 4080, Pg. 148.

	Hydrogen Peroxide (mM)					
Time (min)	Residual	Decomposed	Consumed	pH	Chemi. (mV-sec)	Std.[a]
1	99.63	0.00	0.00	3.16	172.82	96.56
30	99.13	1.92	-1.42	3.15	542.08	58.18
60	98.50	2.21	-1.08	3.13	1487.93	385.86
94	98.00	2.62	-0.99	3.14	1265.28	52.46
120	96.50	3.23	-0.10	3.14	1159.10	189.37
150	94.50	4.20	0.93	3.17	892.75	36.76
183	92.13	5.81	1.69	3.27	572.17	174.19
211	89.13	9.56	0.94	3.29	431.11	21.22
240	85.00	11.98	2.65	3.22	231.13	48.57
271	80.00	15.27	4.35	3.21	117.23	36.71
330	68.38	23.78	7.47	3.14	73.77	3.04

[a] Standard deviation based on three samples.

Table 17. Reaction data for the 100 mM H_2O_2, 10.0 mM Fe-EDTA, 0.5 mM phthalic hydrazide, pH 3.0, 45°C. HR-16, Nbk. 4080, Pg. 146.

	Hydrogen Peroxide (mM)					
Time (min)	Residual	Decomposed	Consumed	pH	Chemi. (mV-sec)	Std.[a]
0	100.00	0.00	0.0	2.91	414.97	86.86
1	96.63	0.00	3.38	2.87	934.45	112.18
15	64.88	7.15	27.97	2.86	110.30	10.58
22	6.75	—	—	2.88	148.20	34.46
25	4.50	—	—	2.93	—	—
28	—	—	—	2.96	—	—
35	—	—	—	2.98	166.90	3.67
40	—	—	—	—	178.35	19.39

[a] Standard deviation based on three samples.

Table 18. Reaction data for the 100 mM H_2O_2, 0.5 mM Fe-EDTA, 0.25 mM phthalic hydrazide, pH 3.0, 45°C. HR-19, Nbk. 4080, Pg. 152.

	Hydrogen Peroxide (mM)					
Time (min)	Residual	Decomposed	Consumed	pH	Chemi. (mV-sec)	Std.[a]
0	100.00	0.00	0.00	3.18	239.60	8.62
1	99.63	0.00	0.00	3.18	438.38	60.17
29	99.63	1.92	-1.92	3.18	2060.83	341.68
62	97.13	2.21	0.29	3.22	862.26	85.17
91	91.38	2.62	5.63	3.19	258.36	31.62
154	69.00	3.23	27.40	3.20	26.84	3.65
210	58.00	4.20	37.42	3.20	40.50	14.93
270	50.63	5.82	43.18	3.20	36.37	11.32
330	45.63	9.58	44.42	3.22	47.25	10.11

[a] Standard deviation based on three samples.

Table 19. Reaction data for the 100 mM H_2O_2, 0.25 mM Fe-EDTA, pH 3.0, 45°C. HR-30, Nbk. 4143, Pg. 3.

	Hydrogen Peroxide (mM)					
Time (min)	Residual	Decomposed	Consumed	pH	Chemi. (mV-sec)	Std.[a]
0	—	—	—	3.09	12.67	5.71
1	102.75	0.00	0.00	3.12	18.62	7.66
30	97.38	2.15	3.23	3.10	75.43	21.91
60	86.75	6.07	9.93	3.10	64.58	9.82
80	82.13	9.09	11.53	3.10	43.42	11.85
100	78.88	11.36	12.51	3.10	16.75	4.61
130	74.88	14.61	13.26	3.12	24.99	10.38
180	71.88	17.75	13.13	3.14	13.92	7.42
270	66.88	20.82	15.06	3.14	10.90	7.70

[a] Standard deviation based on three samples.

Table 20. Reaction data for the 100 mM H_2O_2, 0.1 mM Fe-EDTA, pH 3.0, 45°C. HR-28, Nbk. 4080, Pg. 188.

	Hydrogen Peroxide (mM)					
Time (min)	Residual	Decomposed	Consumed	pH	Chemi. (mV-sec)	Std.[a]
0	—	—	—	3.11	5.16	3.72
1	104.88	0.00	0.00	3.08	18.42	3.12
30	102.25	2.97	-0.34	3.11	29.19	7.61
60	99.13	4.53	1.22	3.11	39.92	8.69
90	95.75	6.73	2.40	3.12	36.61	10.72
120	93.00	8.56	3.31	3.16	25.59	8.86
180	90.00	11.22	3.65	3.19	25.94	12.92
240	88.13	13.25	3.50	3.19	21.15	4.73
330	85.75	15.48	3.65	3.13	10.33	7.56
420	83.63	17.30	3.95	3.15	7.08	3.61

[a] Standard deviation based on three samples.

Table 21. Reaction data for the 100 mM H_2O_2, 10.0 mM Fe-EDTA, pH 3.0, 45°C. HR-29, Nbk. 4080, Pg. 190.

	Hydrogen Peroxide (mM)					
Time (min)	Residual	Decomposed	Consumed	pH	Chemi. (mV-sec)	Std.[a]
0	100.00	0.00	4.88	3.10	6.20	3.72
1.0	47.63	0.00	57.25	3.02	408.06	42.97
3.0	14.38	8.92	81.58	3.00	60.63	16.03
4.5	—	16.80	—	—	51.74	29.86
6.0	3.50	24.68	76.69	2.99	8.59	3.30
8.25	—	—	—	—	10.78	5.97
12	—	—	—	—	11.27	8.99

[a] Standard deviation based on three sample determinations.

Table 22. Reaction data for the 100 mM H_2O_2, 0.5 mM Fe-EDTA, pH 3.0, 45°C. HR-27, Nbk. 4080, Pg. 184.

	Hydrogen Peroxide (mM)				Chemiluminescence (mV-sec)			
Time (min)	Res.	Dec.	Cons.	pH	1 min. Hold	Std.[a]	5 min. Hold	Std.[a]
0	—	—	—	3.05	3.90	2.91	7.91	4.16
1	101.75	0.00	0.00	3.07	25.63	12.73	49.71	4.96
15	98.85	2.90	1.97	3.08	102.18	19.28	132.65	21.53
30	94.04	7.71	7.54	3.06	116.16	34.06	150.86	12.98
46	85.72	16.03	10.03	3.05	99.09	10.38	130.69	22.49
60	81.04	20.71	11.91	3.08	68.19	8.99	62.79	9.05
80	76.26	25.49	13.64	3.06	42.14	9.31	66.69	14.40
100	72.70	29.05	13.32	3.06	11.56	5.66	42.53	7.91
120	69.38	32.37	13.13	3.07	11.10	4.15	28.02	9.89
150	65.56	36.19	12.93	3.08	20.87	8.95	42.21	13.48
180	52.17	39.58	15.05	3.06	29.86	13.89	52.45	5.59
240	57.27	44.48	11.65	3.06	6.17	3.54	35.88	6.34

[a] Standard deviation based on three separate determinations.

APPENDIX II

REACTIVITY OF LIGNOSULFONATE PREPARATIONS

Several batches of lignosulfonate were prepared to obtain enough substrate for all reactions. The same procedures were used each time, as outlined in the Materials and Methods section. Figure 75 shows HPSEC chromatographic profiles obtained from several different preparations of lignosulfonate. There is no difference in the molecular weight distributions of these two preparations. This verifies that a uniform product was obtained each time.

To further insure reproducible lignosulfonate preparations were obtained, the reactivity of several lignosulfonate preparations were compared. Figure 76 shows the residual hydrogen peroxide data obtained from similar reactions in which different lignosulfonate preparations were used. The slight discrepancies in the consumed and decomposed hydrogen peroxide data are due to the variability in the oxygen collection system. From Figure 76 it is evident that the reactivities of the two lignosulfonate preparations are identical.

Comparisons of HPSEC chromatograms (see Figure 75) show that a uniform product was obtained from this procedure. For LS Prep IX, fewer low molecular weight chains are included in this preparation, as seen by the narrower distribution of the HPSEC profile in Figure 75. This was obtained by increased washing of the sample to remove these lower molecular weight fragments. LS Prep X (not shown), used for all experiments presented in this report, was thoroughly washed to remove these low molecular weight fragments.

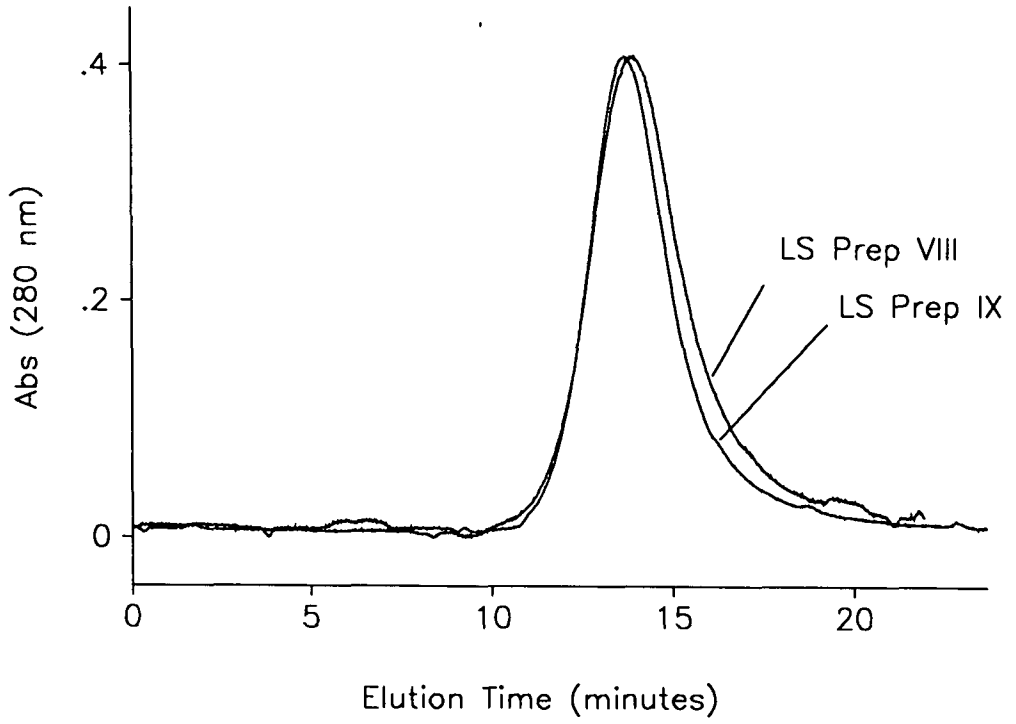

Figure 75. HPSEC chromatographic profile of two different lignosulfonate preparations.

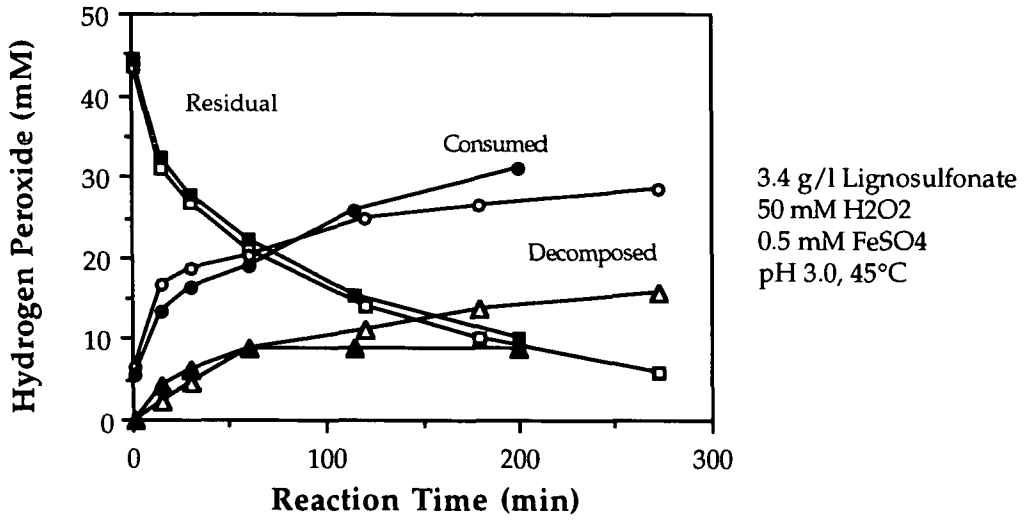

Figure 76. Residual, consumed and decomposed hydrogen peroxide versus reaction times for two identical experiments, except for the lignosulfonate preparation used. Filled symbols: LS Prep VIII. Empty symbols: LS Prep IX.

Effect of SEC Column

Size-exclusion chromatography was initially performed using a column (Bio-Sil SEC 250) with a molecular weight range of 10,000 - 300,000. During lignosulfonate degradation reactions, the lower portion of the lignosulfonate molecular weight distribution curve fell below the lower limit of the linear calibration range. The poor resolution of molecular weights in this region lead to inaccurate determinations of weight- and number- average molecular weights.

A new column (Bio-Sil SEC 125) with a 5,000 - 100,000 molecular weight range was purchased. The linear calibration range of this column extended well below the lowest point of the lignosulfonate molecular weight distribution, even for degraded lignosulfonate samples.

In Figure 77 the weight-average molecular weights of lignosulfonate, as determined from the old column (SEC 250) and the new column (SEC 125), are plotted against reaction time for the $FeSO_4$ catalyzed reaction of hydrogen peroxide. As expected for these identical reactions, the shapes of the curves are similar.

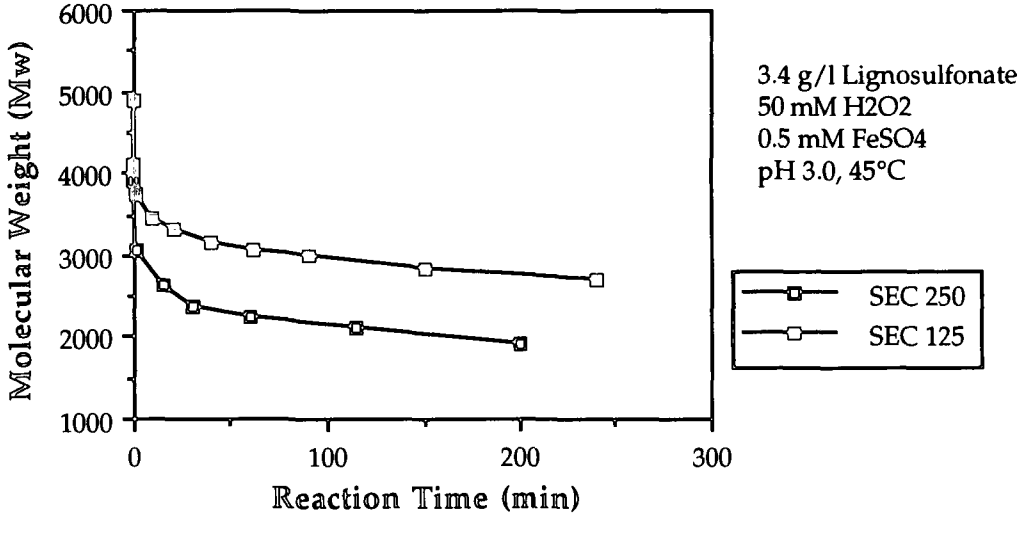

Figure 77. Weight-average molecular weights of lignosulfonate versus reaction time for the $FeSO_4$ catalyzed reaction of hydrogen peroxide using two different size-exclusion columns to determine molecular weights. Old column: SEC 250. New column: SEC 125.

APPENDIX III

DATA FROM LIGNOSULFONATE EXPERIMENTS

This appendix contains all data from experiments with lignosulfonate. Tables 23 - 40 are numerical values for data obtained. High Performance Size-Exclusion Chromatograph (HPSEC) profiles from these experiments are shown in Figures 78 - 86. This appendix includes data from control experiments with no hydrogen peroxide (lignosulfonate alone, and plus catalysts).

Table 23. Data for the control reaction (no catalyst). Reaction conditions: 3.4 g/l lignosulfonate, 50 mM H_2O_2, pH 3.0, 45°C. LH-30, Nbk. 4201, Pg. 134.

	Hydrogen Peroxide (mM)					
Time (min)	Residual	Decomposed	Consumed	pH	Chemi. (mV-sec)	Std.
0	50.0	—	—	3.05	71.4	9.10
1	50.0	0.0	1.4	3.08	81.0	7.45
60	46.1	5.2	2.4	2.90	73.7	19.50
120	44.0	5.7	4.0	2.80	—	—
240	42.7	5.9	5.2	2.74	—	—
480	39.2	6.0	8.5	2.66	—	—
1535	33.7	6.0	14.0	2.57	—	—
2918	28.3	6.6	18.9	2.50	—	—
3273	28.0	8.7	17.1	2.50	—	—

Table 24. Lignosulfonate molecular weights for LH-30.

	Lignosulfonate Molecular Weight				
Time (min)	Mw	Std.	Mn	Std.	Mw/Mn
0	4018	5.6	2760	—	1.46
1	3968	10.6	2704	—	1.47
60	3649	19.1	2472	—	1.48
120	3544	7.1	2391	—	1.48
240	3477	21.2	2342	—	1.49
480	3369	2.1	2262	—	1.49
1535	3023	4.2	2022	—	1.50
2918	2766	0.7	1853	—	1.49
3273	2705	5.7	1810	—	1.49

Table 25. Data for the $FeSO_4$ catalyzed reaction. Reaction conditions: 3.4 g/l lignosulfonate, 50 mM H_2O_2, 0.5 mM $FeSO_4$, pH 3.0, 45°C. LH-28, Nbk. 4201, Pg. 126.

	Hydrogen Peroxide (mM)					
Time (min)	Residual	Decomposed	Consumed	pH	Chemi. (mV-sec)	Std.
0	50.0	---	---	3.22	82.3	7.2
1	42.6	0.0	7.4	3.12	882.8	55.1
10	33.9	2.0	14.1	2.91	292.1	11.7
20	29.9	4.1	16.0	2.82	189.4	2.6
40	24.5	6.7	18.8	2.74	140.4	6.0
62	20.4	7.9	21.7	2.68	125.1	14.3
90	16.5	7.9	25.6	2.61	---	---
150	11.3	8.0	30.6	2.55	---	---
240	6.5	10.8	32.7	2.49	---	---

Table 26. Lignosulfonate molecular weights for LH-28.

	Lignosulfonate Molecular Weight				
Time (min)	Mw	Std.	Mn	Std.	Mw/Mn
0	4114	---	2740	---	1.50
1	3756	8.5	2494	---	1.50
10	3443	25.5	2262	---	1.52
20	3306	1.4	2162	---	1.53
40	3170	3.5	2056	---	1.54
62	3070	2.1	1986	---	1.54
90	2987	19.8	1938	---	1.54
150	2842	15.6	1856	---	1.53
240	2698	6.4	1745	---	1.55

Table 27. Data for the Fe-EDTA catalyzed reaction. Reaction conditions: 3.4 g/l lignosulfonate, 50 mM H_2O_2, 0.5 mM Fe-EDTA, pH 3.0, 45°C. LH-29, Nbk. 4201, Pg. 130.

Time (min)	Hydrogen Peroxide (mM) Residual	Decomposed	Consumed	pH	Chemi. (mV-sec)	Std.
0	52.0	—	—	3.12	99.5	6.9
1	51.6	—	—	3.11	195.4	8.6
15	44.6	3.4	3.6	3.06	92.0	21.2
30	42.8	5.0	3.8	3.01	93.5	6.9
45	41.7	6.6	3.4	2.97	101.3	4.6
75	39.3	8.4	4.0	2.91	—	—
120	36.0	9.2	6.4	2.89	—	—
248	29.9	9.8	11.9	2.71	—	—
378	23.9	11.6	16.1	2.64	—	—

Table 28. Lignosulfonate molecular weights for LH-29.

Time (min)	Lignosulfonate Molecular Weight Mw	Std.	Mn	Std.	Mw/Mn
0	4213	21.2	2521	—	1.67
1	4132	23.3	2578	—	1.60
15	3997	21.2	2500	—	1.60
30	3924	2.1	2453	—	1.60
45	3860	14.1	2406	—	1.61
75	3787	9.9	2313	—	1.64
120	3688	16.3	2251	—	1.64
248	3444	8.5	2087	—	1.65
378	3265	12.7	1971	—	1.66

Table 29. Data for the hemoglobin catalyzed reaction. Reaction conditions: 3.4 g/l lignosulfonate, 50 mM H_2O_2, 1.0 g/l hemoglobin, pH 3.0, 45°C. LH-27, Nbk. 4201, Pg. 122.

	Hydrogen Peroxide (mM)					
Time (min)	Residual	Decomposed	Consumed	pH	Chemi. (mV-sec)	Std.
0	—	—	—	—	70.2	5.3
0	52.0	—	—	3.06	567.9	38.4
1	52.2	—	—	3.08	618.9	186.5
30	43.8	3.4	5.0	2.94	105.8	13.7
60	42.2	4.4	5.6	2.89	79.0	5.8
180	37.4	4.4	10.5	2.77	85.8	2.4
361	34.8	4.5	12.9	2.70	70.3	10.9
602	31.6	4.5	16.1	2.62	—	—
912	29.2	4.5	18.5	2.60	—	—
1873	23.0	4.5	24.7	2.55	—	—
3114	20.3	4.7	27.2	2.75	—	—

Table 30. Lignosulfonate molecular weights for LH-27.

	Lignosulfonate Molecular Weight				
Time (min)	Mw	Std.	Mn	Std.	Mw/Mn
0	3940	5.0	2656	—	1.48
0	3341	33.9	2391	—	1.40
1	3300	3.5	2384	—	1.39
30	3157	9.9	2274	—	1.39
60	3073	9.9	2171	—	1.41
180	2991	—	2024	—	1.44
361	2761	—	1825	—	1.46
602	2622	—	1730	—	1.52
912	2460	—	1609	—	1.53
3114	2130	—	1390	—	1.53

Table 31. Data for the Fe-EDTA catalyzed reaction. Reaction conditions: 3.4 g/l lignosulfonate, 50 mM H_2O_2, 0.06 mM Fe-EDTA, pH 3.0, 45°C. LH-32, Nbk. 4201, Pg. 154.

	Hydrogen Peroxide (mM)					
Time (min)	Residual	Decomposed	Consumed	pH	Chemi. (mV-sec)	Std.
0	—	—	—	3.24	95.8	20.8
1	52.12	0.00	0.00	3.26	78.4	3.0
30	45.68	4.11	2.33	3.15	67.5	29.7
30	45.29	5.29	1.54	3.08	62.6	5.2
120	43.94	6.49	1.69	2.99	76.2	10.3
210	42.16	7.10	2.86	2.90	72.2	18.3
391	39.39	9.07	3.66	2.78	—	—
1437	30.13	9.24	12.75	2.62	—	—
2915	21.78	10.03	20.31	2.62	—	—

Table 32. Lignosulfonate molecular weights for LH-32.

	Lignosulfonate Molecular Weight				
Time (min)	Mw	Std.	Mn	Std.	Mw/Mn
0	3995	14.8	2714	—	1.47
1	3924	10.6	2654	—	1.48
30	3749	7.1	2534	—	1.48
30	3675	18.4	2476	—	1.49
120	3561	9.2	2396	—	1.49
210	3470	6.4	2340	—	1.49
391	3324	29.7	2224	—	1.50
1437	2834	4.2	1895	—	1.50
2915	2596	3.5	1732	—	1.50

Table 33. Data for the lignosulfonate control reaction. Reaction conditions: 3.4 g/l lignosulfonate, pH 3.0, 45°C. LH-20, Nbk. 4201, Pg. 50.

	Hydrogen Peroxide (mM)					
Time (min)	Residual	Decomposed	Consumed	pH	Chemi. (mV-sec)	Std.
1	---	---	---	3.04	---	---
60	---	---	---	2.89	---	---
123	---	---	---	2.86	---	---
177	---	---	---	2.85	---	---
287	---	---	---	2.84	---	---
360	---	---	---	2.83	---	---

Table 34. Lignosulfonate molecular weights for LH-20.

	Lignosulfonate Molecular Weight				
Time (min)	Mw	Std.	Mn	Std.	Mw/Mn
1	3968	30.4	2306	9.2	1.73
60	4074	202.2	2298	4.9	1.78
123	4062	262.3	2315	4.2	1.76
177	3902	5.7	2299	12.7	1.70
287	3895	15.6	2309	2.8	1.68
360	3872	3.5	2284	0.7	1.70

Table 35. Data for the $FeSO_4$ control reaction. Reaction conditions: 3.4 g/l lignosulfonate, 0.5 mM $FeSO_4$, pH 3.0, 45°C. LH-18, Nbk. 4201, Pg. 40.

Time (min)	Hydrogen Peroxide (mM) Residual	Decomposed	Consumed	pH	Chemi. (mV-sec)	Std.
0	---	---	---	3.4	34.98	1.69
2.5	---	---	---	3.10	33.60	5.58
59	---	---	---	3.01	33.67	4.36
122	---	---	---	2.98	33.79	1.02
216	---	---	---	2.97	---	---
301	---	---	---	2.96	34.97	16.65

Table 36. Lignosulfonate molecular weights for LH-18.

Time (min)	Lignosulfonate Molecular Weight Mw	Std.	Mn	Std.	Mw/Mn
0	3908	22.6	2361	15.6	1.66
2.5	3802	21.9	2291	5.7	1.66
59	3780	14.8	2274	26.2	1.66
122	3822	9.9	2314	27.6	1.66
216	3778	31.8	2269	52.3	1.66
301	3785	1.4	2262	3.5	1.68

Table 37. Data for the Fe-EDTA control reaction (no peroxide). Reaction conditions: 3.4 g/l lignosulfonate, 0.5 mM Fe-EDTA, pH 3.0, 45°C. LH-19, Nbk. 4201, Pg. 42.

Time (min)	Hydrogen Peroxide (mM) Residual	Decomposed	Consumed	pH	Chemi. (mV-sec)	Std.
0	---	---	---	3.40	32.27	6.42
3	---	---	---	3.11	34.99	4.00
59	---	---	---	3.03	35.39	1.64
115	---	---	---	2.99	35.73	7.23
228	---	---	---	2.99	37.04	15.27
325	---	---	---	2.98	30.56	0.83

Table 38. Lignosulfonate molecular weights for LH-19.

Time (min)	Lignosulfonate Molecular Weight Mw	Std.	Mn	Std.	Mw/Mn
0	3963	18.4	2394	26.2	1.66
3	3800	38.2	2127	19.8	1.79
59	3770	9.2	2122	6.4	1.78
115	3714	2.1	2094	5.7	1.78
228	3727	39.6	2118	13.4	1.76
325	3706	28.9	2108	2.1	1.76

Table 39. Data for the hemoglobin control reaction (no peroxide). Reaction conditions: 3.4 g/l lignosulfonate, 1.0 g/l hemoglobin, pH 3.0, 45°C. LH-31, Nbk. 4201, Pg. 138.

	Hydrogen Peroxide (mM)					
Time (min)	Residual	Decomposed	Consumed	pH	Chemi. (mV-sec)	Std.
0	—	—	—	3.06	—	—
1	—	—	—	3.01	—	—
66	—	—	—	2.91	—	—
120	—	—	—	2.90	—	—
239	—	—	—	2.87	—	—
480	—	—	—	2.83	—	—
2913	—	—	—	2.81	—	—

Table 40. Lignosulfonate molecular weights for LH-31.

	Lignosulfonate Molecular Weight				
Time (min)	Mw	Std.	Mn	Std.	Mw/Mn
0	4064	—	2044	—	1.99
1	3396	—	1811	—	1.88
66	3340	—	1756	—	1.90
120	3342	—	1766	—	1.90
239	3304	—	1780	—	1.86
480	3429	—	1774	—	1.94
2913	3360	—	1772	—	1.90

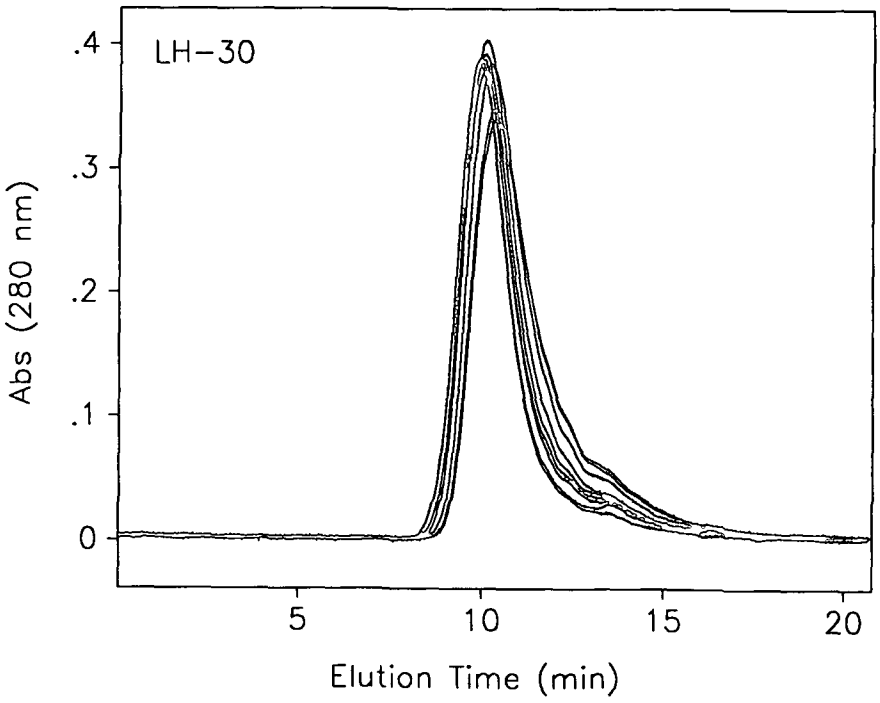

Figure 78. HPSEC profiles of reaction samples taken from the control reaction. LH-30. Reaction conditions: 3.4 g/l lignosulfonate, 50 mM H_2O_2, pH 3.0 and 45°C. Sample times as indicated in Table 24.

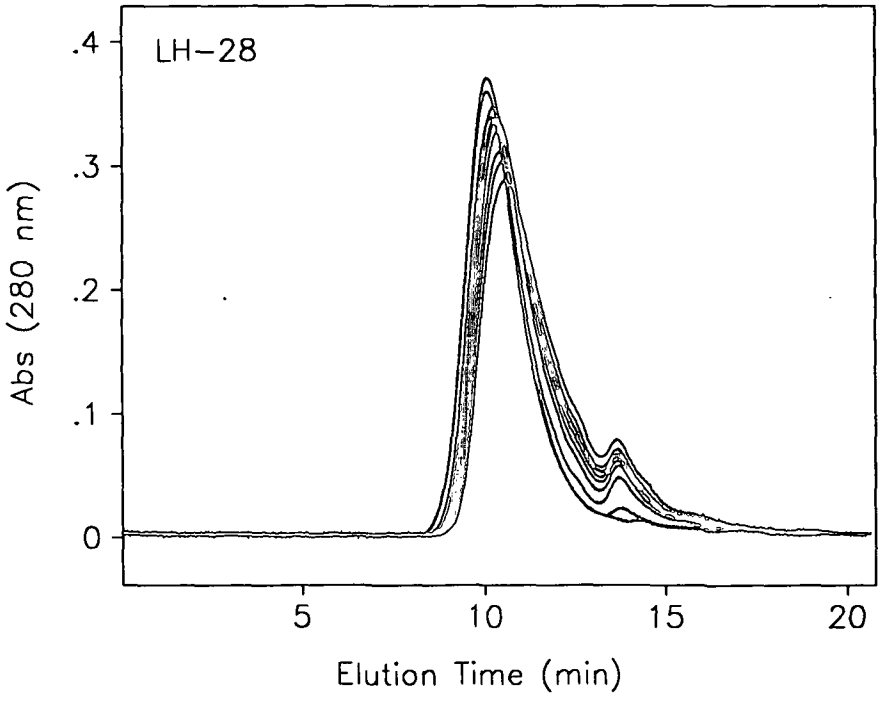

Figure 79. HPSEC profiles of reaction samples taken from the $FeSO_4$ catalyzed reaction. LH-28. Reaction conditions: 3.4 g/l lignosulfonate, 50 mM H_2O_2, 0.5 mM $FeSO_4$, pH 3.0 and 45°C. Sample times as indicated in Table 26.

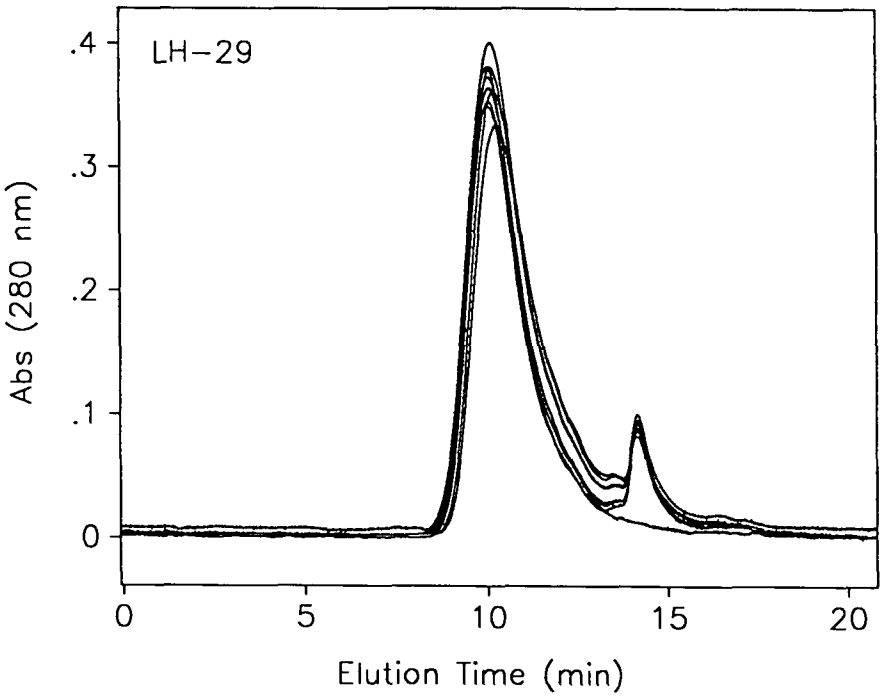

Figure 80. HPSEC profiles of reaction samples taken from the Fe-EDTA catalyzed reaction. LH-29. Reaction conditions: 3.4 g/l lignosulfonate, 50 mM H_2O_2, 0.5 mM Fe-EDTA, pH 3.0 and 45°C. Sample times as indicated in Table 28.

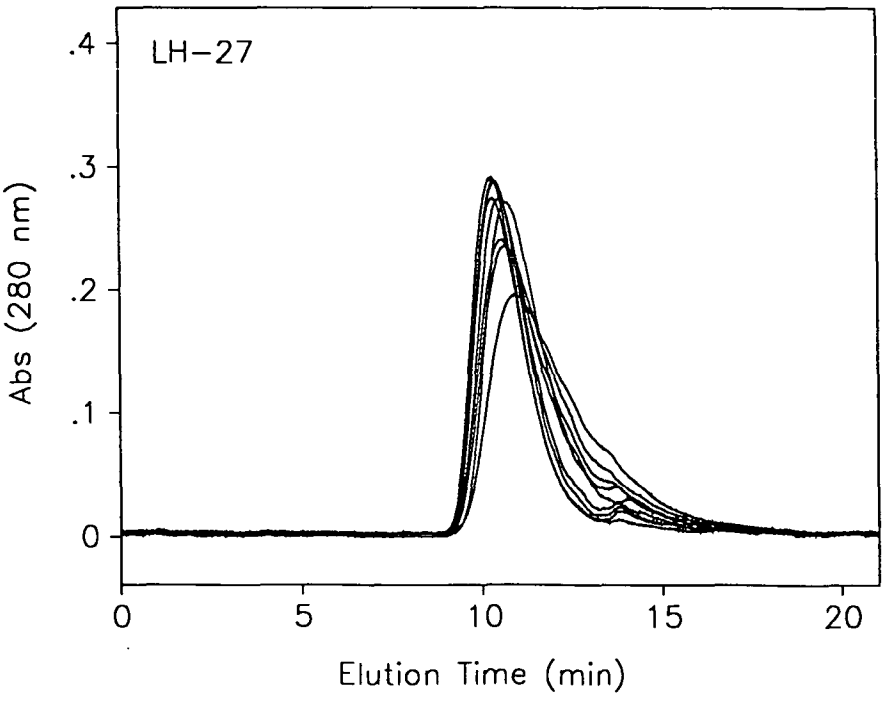

Figure 81. HPSEC profiles of reaction samples taken from the hemoglobin catalyzed reaction. LH-27. Reaction conditions: 3.4 g/l lignosulfonate, 50 mM H_2O_2, 1.0 g/l hemoglobin, pH 3.0 and 45°C. Sample times as indicated in Table 30.

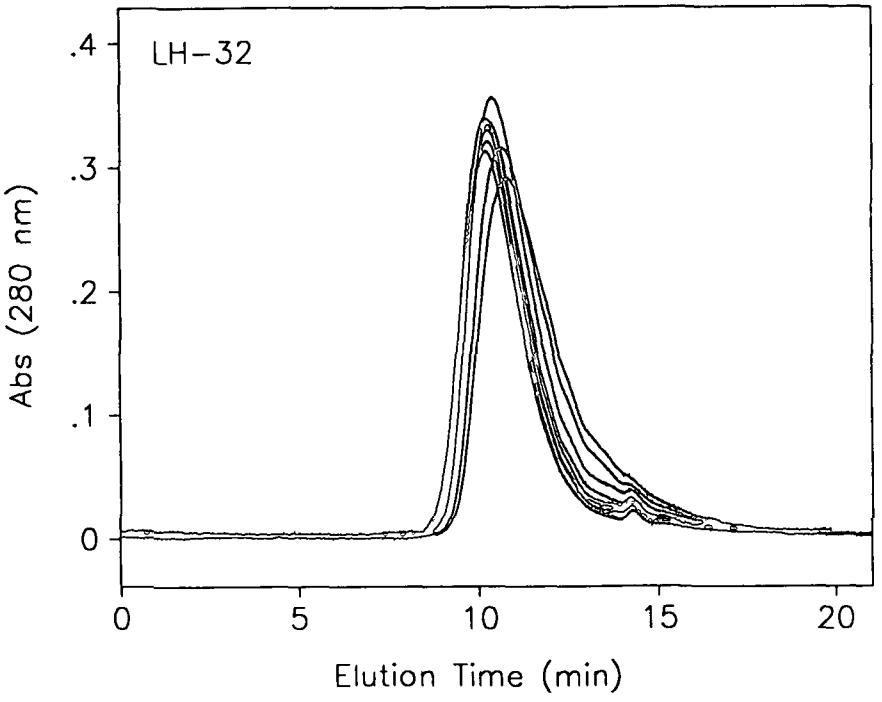

Figure 82. HPSEC profiles of reaction samples taken from the Fe-EDTA reaction at reduced Fe-EDTA concentration. LH-32. Reaction conditions: 3.4 g/l lignosulfonate, 50 mM H_2O_2, 0.06 mM Fe-EDTA, pH 3.0 and 45°C. Sample times as indicated in Table 32.

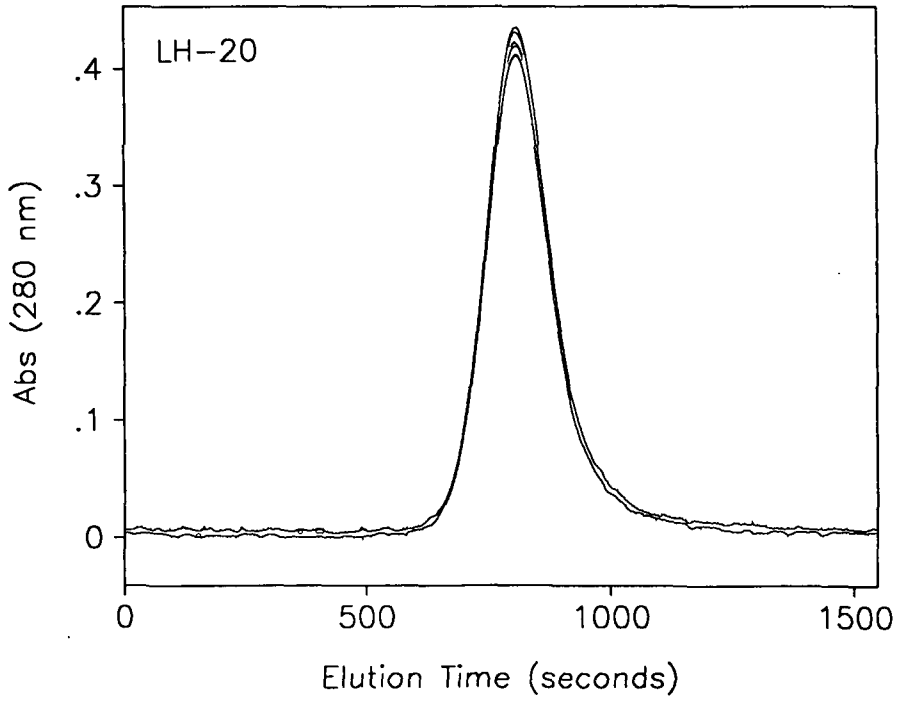

Figure 83. HPSEC profiles of reaction samples taken from the lignosulfonate control reaction. LH-20. Reaction conditions: 3.4 g/l lignosulfonate, pH 3.0 and 45°C. Sample times as indicated in Table 34.

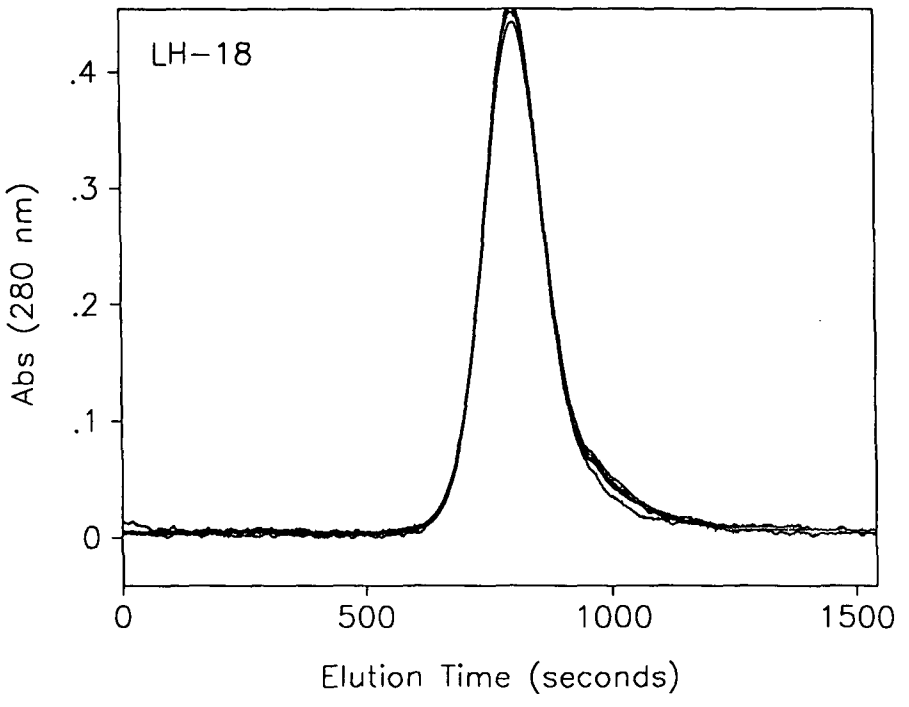

Figure 84. HPSEC profiles of reaction samples taken from the $FeSO_4$ control reaction. LH-18. Reaction conditions: 3.4 g/l lignosulfonate, 0.5 mM Fe-SO4, pH 3.0 and 45°C. Sample times as indicated in Table 36.

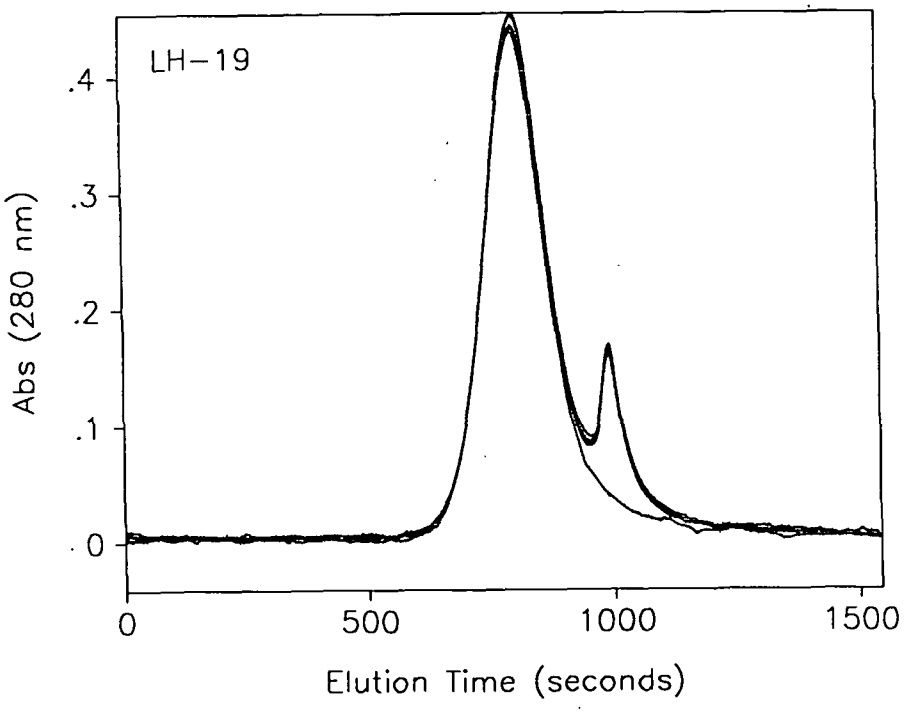

Figure 85. HPSEC profiles of reaction samples taken from the Fe-EDTA control reaction. LH-19. Reaction conditions: 3.4 g/l lignosulfonate, 0.5 mM Fe-EDTA, pH 3.0 and 45°C. Sample times as indicated in Table 38.

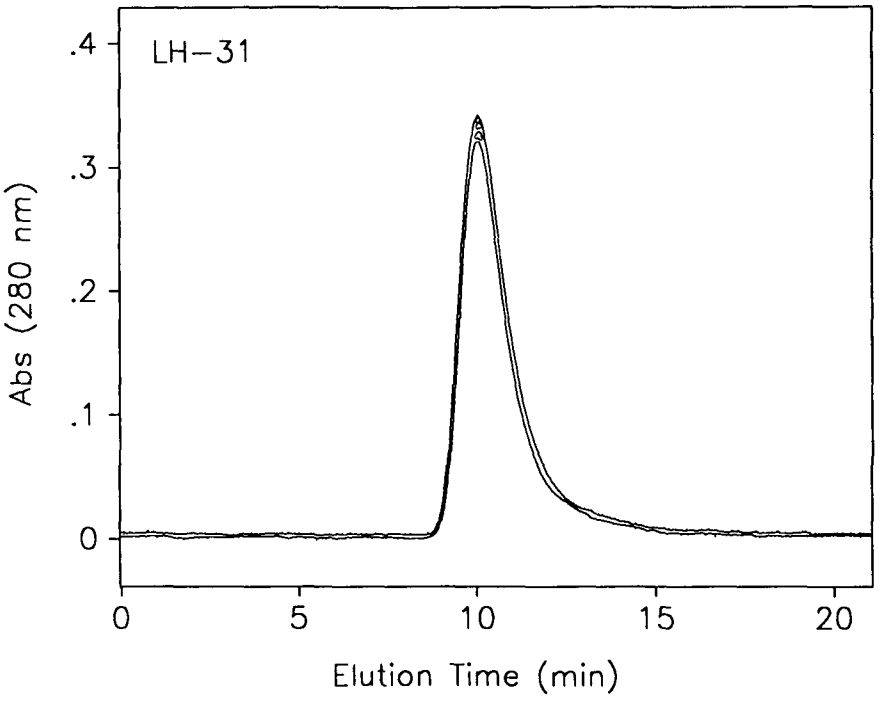

Figure 86. HPSEC profiles of reaction samples taken from the hemoglobin control reaction. LH-31. Reaction conditions: 3.4 g/l lignosulfonate, 1.0 g/l hemoglobin, pH 3.0 and 45°C. Sample times as indicated in Table 40.

APPENDIX IV

KINETIC DATA FROM LIGNOSULFONATE EXPERIMENTS

This appendix contains the kinetic data and plots used to determine the rate laws for the oxidation of lignosulfonate. Data are listed in Tables 41 - 46. Integral plots are shown in Figures 87 - 93.

Table 41. Kinetic data for the control reaction (LH-30). Differential plot shown in Figure 28; integral plot shown in Figures 87 and 88.

Time (min)	$[H_2O_2]$, mM	log $[H_2O_2]$	rate = - d [bonds] / dt (x 10^{-8})	log r
60	46.1	1.664	15.41	-6.812
120	44.0	1.643	7.33	-7.135
240	42.7	1.630	5.32	-7.274
480	39.2	1.593	3.53	-7.452
1535	33.7	1.528	2.70	-7.569
2918	28.3	1.451	1.90	-7.721
3273	28.0	1.447	—	—

Table 42. Kinetic data for the $FeSO_4$ reaction (LH-28). Differential plot shown in Figure 28; integral plot shown in Figures 89 and 90.

Time (min)	$[H_2O_2]$, mM	log $[H_2O_2]$	rate = - d [bonds] / dt (x 10^{-6})	log r
1	42.6	1.630	3.750	-5.426
10	33.9	1.530	1.428	-5.845
20	29.9	1.476	0.833	-6.079
40	24.5	1.390	0.526	-6.279
62	20.4	1.310	0.375	-6.426
90	16.5	1.217	0.333	-6.477
150	11.3	1.054	0.250	-6.602
240	6.52	0.814	0.142	-6.848

Table 43. Kinetic data for the Fe-EDTA reaction (LH-29). Differential plot shown in Figure 28; integral plot shown in Figures 91 and 92.

Time (min)	$[H_2O_2]$, mM	log $[H_2O_2]$	rate = - d [bonds] / dt (x 10^{-7})	log r
1	51.6	1.713	10.66	-5.972
15	44.6	1.650	4.25	-6.372
30	42.8	1.632	2.62	-6.582
45	41.7	1.620	2.06	-6.686
75	39.3	1.594	1.71	-6.767
120	35.9	1.556	1.50	-6.824
248	29.9	1.476	1.33	-6.876

Table 44. Kinetic data for the hemoglobin reaction (LH-27). Differential plot shown in Figure 28; integral plot shown in Figure 93.

Time (min)	$[H_2O_2]$, mM	log $[H_2O_2]$	rate = - d [bonds] / dt (x 10^{-8})	log r
30	43.8	1.642	40.9	-6.388
60	42.2	1.625	24.0	-6.620
120	37.4	1.572	13.3	-6.876
361	34.8	1.541	9.44	-7.025
602	31.6	1.500	8.17	-7.088
912	29.2	1.466	6.41	-7.193
3114	20.3	1.308	0.94	-8.027

Table 45. Kinetic data for the Fe-EDTA reaction at 0.06 mM Fe-EDTA (LH-32). Differential plot shown in Figure 29.

Time (min)	$[H_2O_2]$, mM	log $[H_2O_2]$	rate = - d [bonds] / dt (x 10^{-7})	log r
1	52.1	1.717	14.2	-5.849
30	45.7	1.660	2.22	-6.654
60	45.3	1.656	1.63	-6.785
120	43.9	1.643	1.14	-6.943
210	42.2	1.625	0.96	-7.017
391	39.4	1.595	0.43	-7.367
1437	30.1	1.479	0.36	-7.444
2915	21.8	1.338	0.11	-7.959

Table 46. Kinetic data for the disappearance of hydrogen peroxide.

Reaction	Time (min)	$[H_2O_2]$, mM	rate = - d $[H_2O_2]$ / dt
$FeSO_4$ (LH-28)	1	42.6	1.768
	10	33.9	0.556
	20	29.9	0.344
	40	24.5	0.214
	62	20.4	0.173
	90	16.5	0.123
	150	11.3	0.064
	240	6.52	0.057
(LH-24)	1	---	1.367
	16	---	0.336
	30	---	0.260
	60	---	0.156
	121	---	0.084
	180	---	0.060
	269	---	0.030
Fe-EDTA (LH-29)	15	44.6	0.155
	30	42.8	0.105
	45	41.7	0.085
(LH-25)	20	---	0.194
	42	---	0.117
	80	---	0.092
	120	---	0.077
	226	---	0.048

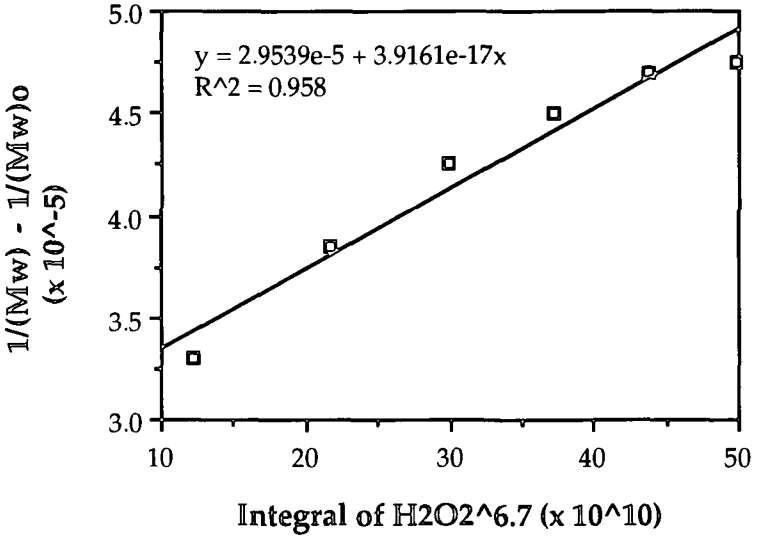

Figure 87. Integral plot for the control reaction (peroxide only) for H_2O_2 40 - 50 mM. LH-30.

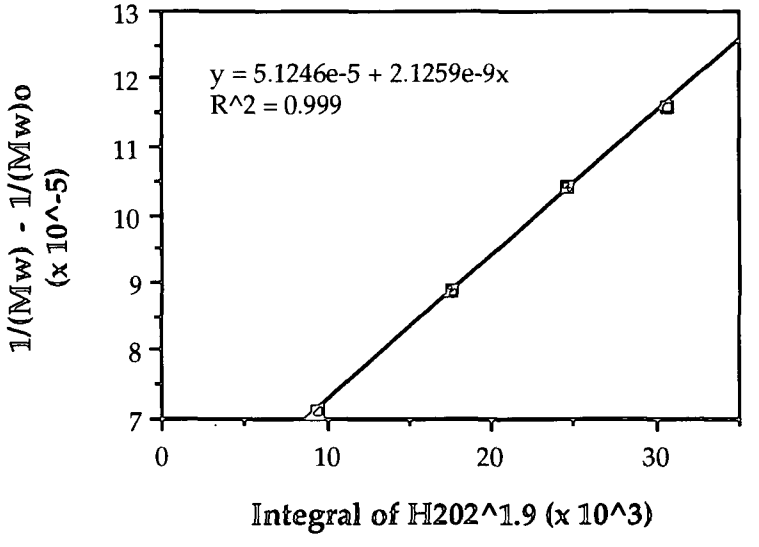

Figure 88. Integral plot for the control reaction (peroxide only) for H_2O_2 < 40 mM. LH-30.

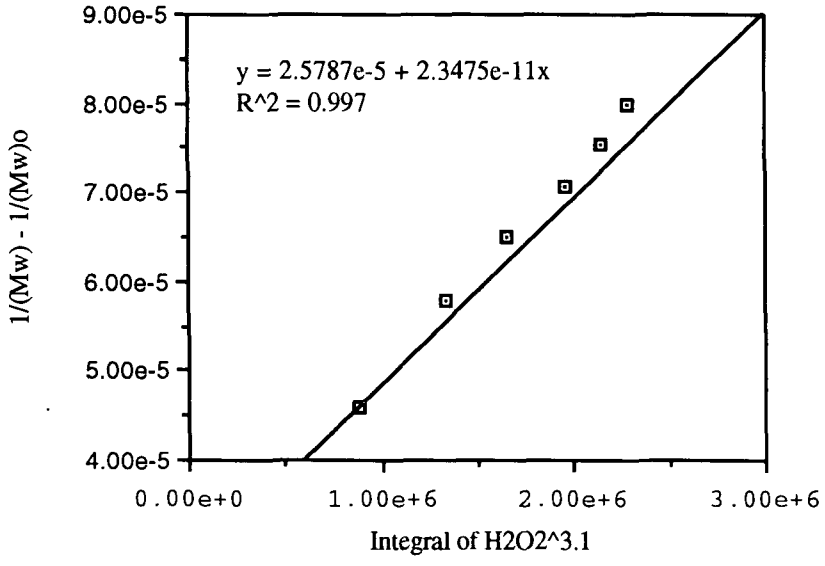

Figure 89. Integral plot for the $FeSO_4$ catalyzed reaction for H_2O_2 20 - 50 mM. LH-28.

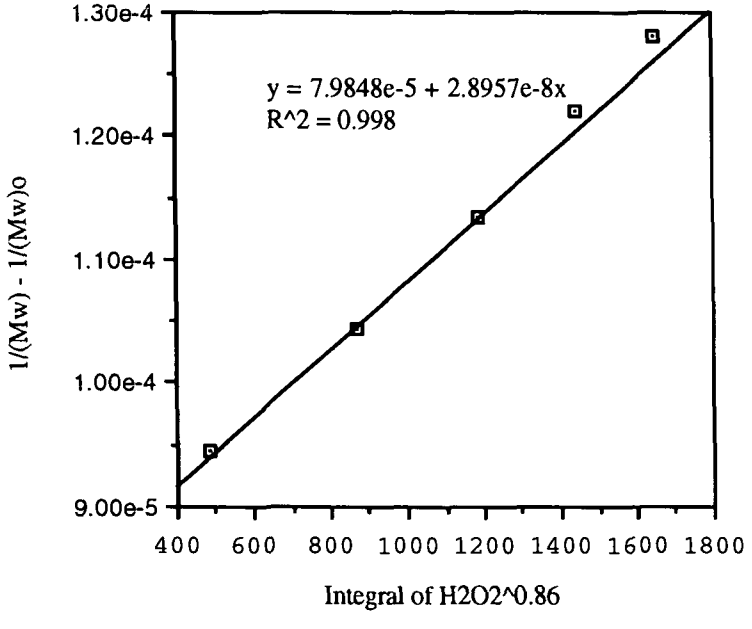

Figure 90. Integral plot for the $FeSO_4$ catalyzed reaction for H_2O_2 < 20 mM. LH-28.

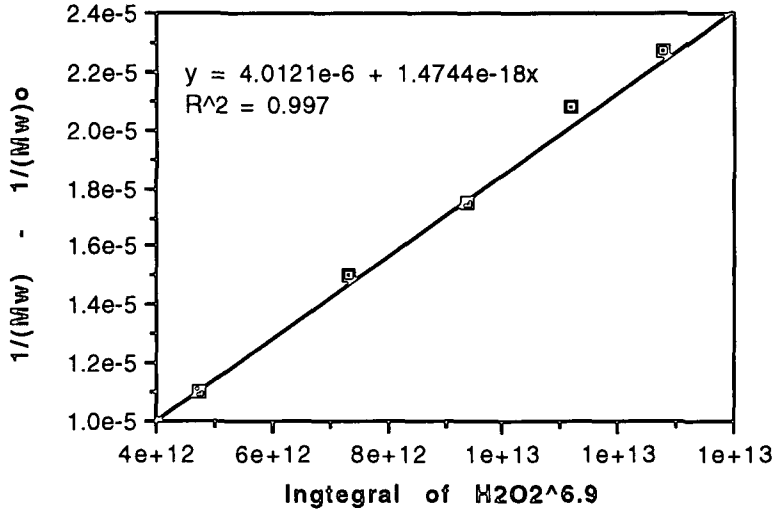

Figure 91. Integral plot for the Fe-EDTA catalyzed reaction for H_2O_2 40 - 50 mM. LH-29.

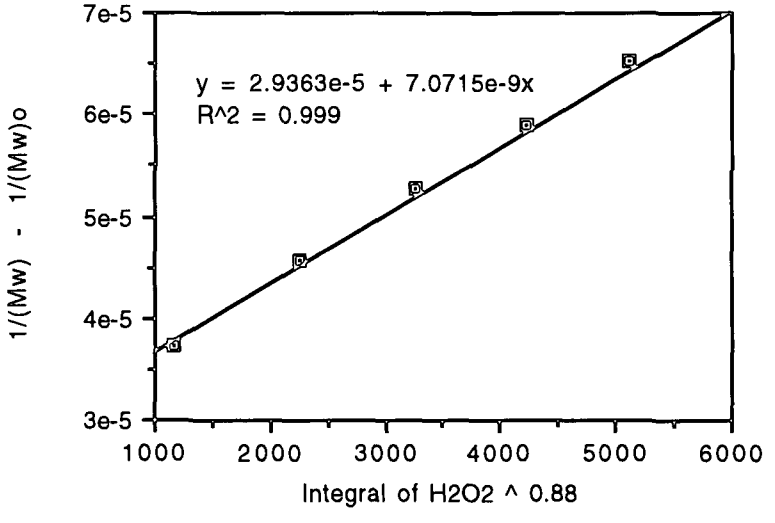

Figure 92. integral plot for the Fe-EDTA catalyzed reaction for $H_2O_2 < 40$ mM. LH-29.

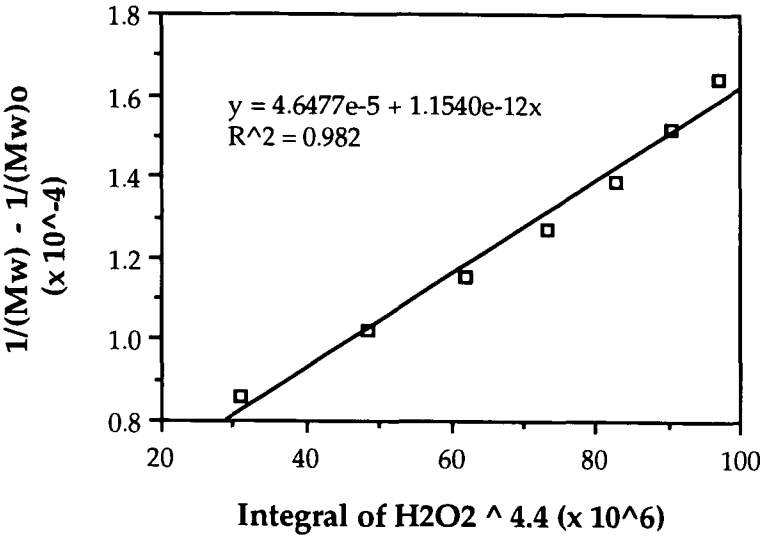

Figure 93. Integral plot for the hemoglobin catalyzed reaction. LH-27.

APPENDIX V

DATA FROM HEC EXPERIMENTS

This appendix contains all data from experiments with hydroxyethyl cellulose (HEC). Tables 47 - 54 are numerical values for data obtained. This appendix includes data from control experiments with no hydrogen peroxide (HEC alone and plus catalysts). In all cases, intrinsic viscosity measurements were made in duplicate.

Table 47. Data for the control reaction (no catalyst) at 20 mM H_2O_2. Reaction conditions: 3.0 g/l HEC, 20 mM H_2O_2, pH 3.0, 45°C. HH-16, Nbk. 4143, Pg. 132.

	Hydrogen Peroxide (mM)						Hydroxyethyl Cellulose		
Time (min)	Res.	Dec.	Cons.	pH	Chemi.	Std.	[η]	Mv	Std.
0	---	---	---	3.32	---	---	1.559	983,716	48,150
2	19.50	---	---	3.18	---	---	1.150	693,115	18,521
47	19.38	---	---	3.14	---	---	1.115	669,247	4,292
93	19.90	---	---	3.15	---	---	1.008	595,953	7,735
166	19.70	---	---	3.11	---	---	0.893	518,345	16,910
241	19.90	---	---	3.05	---	---	0.825	473,422	31,627

Table 48. Data for the control reaction (no catalyst) at 40 mM H_2O_2. Reaction conditions: 3.0 g/l HEC, 40 mM H_2O_2, pH 3.0, 45°C. HH-19, Nbk. 4201, Pg. 141.

	Hydrogen Peroxide (mM)						Hydroxyethyl Cellulose		
Time (min)	Res.	Dec.	Cons.	pH	Chemi.	Std.	[η]	Mv	Std.
0	--	---	---	3.14	---	---	1.435	894,011	2,431
3	37.92	---	---	3.07	---	---	1.140	686,627	8,173
33	36.46	---	---	2.97	---	---	1.045	621,405	28,259
91	36.67	---	---	2.88	---	---	0.954	559,155	596
180	36.92	---	---	2.83	---	---	0.849	489,414	11,253
307	37.33	---	---	2.78	---	---	0.712	399,350	3,526
445	37.75	---	---	2.75	---	---	0.604	330,742	3,244

Table 49. Data for the $FeSO_4$ reaction at 20 mM H_2O_2. Reaction conditions: 3.0 g/l HEC, 20 mM H_2O_2, 0.2 mM $FeSO_4$, pH 3.0, 45°C. HH-13, Nbk. 4143, Pg. 111.

Time (min)	Hydrogen Peroxide (mM)						Hydroxyethyl Cellulose		
	Res.	Dec.	Cons.	pH	Chemi.	Std.	[η]	Mv	Std.
0	—	—	—	2.87	5.08	3.27	1.399	869,107	142,454
2	21.12	—	—	2.83	242.88	38.46	0.225	106,217	242
25	20.12	—	—	2.71	749.18	86.91	0.079	31,978	3,740
50	19.40	—	—	2.97	913.80	55.77	0.058	22,494	2,775
77	18.60	—	—	3.08	964.01	82.70	0.043	15,769	265
120	18.10	—	—	3.05	1251.80	188.27	0.033	11,872	15
182	17.70	—	—	2.97	1263.70	63.04	0.030	10,631	2,277
242	17.40	—	—	2.99	1149.39	117.07	0.024	8,235	416

Table 50. Data for the $FeSO_4$ catalyzed reaction at 40 mM H_2O_2. Reaction conditions: 3.0 g/l HEC, 40 mM H_2O_2, 0.2 mM $FeSO_4$, pH 3.0, 45°C. HH-21, Nbk. 4201, Pg. 147.

Time (min)	Hydrogen Peroxide (mM)						Hydroxyethyl Cellulose		
	Res.	Dec.	Cons.	pH	Chemi.	Std.	[η]	Mv	Std.
0	—	—	—	3.16	9.86	5.92	1.406	873,332	26,003
2	37.38	—	—	3.12	355.95	3.04	0.289	141,943	1,830
11	36.50	—	—	3.10	1533.30	125.60	0.139	61,240	218
21	—	—	—	3.05	2239.51	129.55	0.080	32,522	2,533
31	—	—	—	3.03	2524.96	113.89	0.057	21,878	779

Table 51. Data for the Fe-EDTA catalyzed reaction at 20 mM H_2O_2. Reaction conditions: 3.0 g/l HEC, 20 mM H_2O_2, 0.2 mM Fe-EDTA, pH 3.0, 45°C. HH-12, Nbk. 4143, Pg. 106.

Time (min)	Hydrogen Peroxide (mM)						Hydroxyethyl Cellulose		
	Res.	Dec.	Cons.	pH	Chemi.	Std.	[η]	Mv	Std.
0	—	—	—	3.24	2.84	1.56	1.216	739,721	93,128
2	20.92	—	—	3.23	21.14	8.23	0.591	322,959	42,978
17	20.08	—	—	3.25	44.88	11.70	0.470	247,752	5,654
30	19.88	—	—	3.29	62.99	11.00	0.382	195,168	3,707
61	19.66	—	—	3.24	80.31	11.67	0.292	143,170	1,022
91	19.63	—	—	3.24	100.52	22.99	0.205	95,834	15,202
150	19.63	—	—	3.17	109.27	23.31	0.181	82,552	—
243	19.40	—	—	3.22	172.62	15.29	0.189	53,444	5,576

Table 52. Data for the Fe-EDTA catalyzed reaction at 40 mM H_2O_2. Reaction conditions: 3.0 g/l HEC, 40 mM H_2O_2, 0.2 mM Fe-EDTA, pH 3.0, 45°C. HH-20, Nbk. 4201, Pg. 144.

Time (min)	Hydrogen Peroxide (mM)						Hydroxyethyl Cellulose		
	Res.	Dec.	Cons.	pH	Chemi.	Std.	[η]	Mv	Std.
0	—	—	—	3.05	17.26	2.78	1.377	852,774	4,379
2	38.46	—	—	3.09	132.39	13.90	0.902	524,630	12,159
15	37.50	—	—	3.07	411.97	49.79	0.649	359,269	10,050
30	36.83	—	—	3.05	682.14	55.23	0.508	270,958	4,445
60	37.08	—	—	3.00	949.71	79.91	0.293	144,198	360
91	36.67	—	—	2.98	1359.16	98.73	0.201	93,237	1,208
135	37.25	—	—	2.96	2012.62	86.52	0.133	58,162	1,388
180	36.75	—	—	2.91	2362.17	198.69	0.102	42,693	2,295

Table 53. Data for the hemoglobin catalyzed reaction at 20 mM H_2O_2. Reaction conditions: 3.0 g/l HEC, 20 mM H_2O_2, 0.2 g/l hemoglobin, pH 3.0, 45°C. HH-17, Nbk. 4143, Pg. 164.

Time (min)	Hydrogen Peroxide (mM)						Hydroxyethyl Cellulose		
	Res.	Dec.	Cons.	pH	Chemi.	Std.	[η]	Mv	Std.
0	—	—	—	3.27	774.29	147.83	1.445	901,327	13,486
2	22.25	—	—	3.30	217.99	57.47	1.057	629,431	629
60	19.87	—	—	3.26	94.98	26.26	0.638	351,951	12,181
120	19.70	—	—	3.24	63.50	11.29	0.476	251,801	700
182	—	—	—	3.24	42.10	8.58	0.388	198,863	3,233
325	—	—	—	3.21	39.23	1.27	0.279	136,008	5,099

Table 54. Data for the hemoglobin catalyzed reaction at 40 mM H_2O_2. Reaction conditions: 3.0 g/l HEC, 40 mM H_2O_2, 0.2 g/l hemoglobin, pH 3.0, 45°C. HH-22, Nbk. 4201, Pg. 151.

Time (min)	Hydrogen Peroxide (mM)						Hydroxyethyl Cellulose		
	Res.	Dec.	Cons.	pH	Chemi.	Std.	[η]	Mv	Std.
0	—	—	—	3.10	2136.65	258.81	1.241	930,348	2,647
2	40.04	—	—	3.13	100.00	0.60	1.116	669,867	878
48	37.88	—	—	3.03	68.07	35.31	0.699	391,471	1,169
93	36.92	—	—	3.01	45.61	3.72	0.488	258,547	5,418
185	36.96	—	—	3.00	41.82	8.52	0.343	172,636	5,856
305	38.06	—	—	2.97	—	—	0.252	120,840	660
434	38.42	—	—	2.95	—	—	0.188	86,220	1,173

APPENDIX VI

DATA FROM COMBINED SUBSTRATE EXPERIMENTS

This appendix contains all data from experiments with lignosulfonate and hydroxyethyl cellulose (HEC). Tables 55 - 67 are numerical values for data obtained. This is followed by figures comparing various sets of experiments. This appendix also contains data for the control reactions where no hydrogen peroxide was added (substrates alone and plus catalysts).

Table 55. Data for the control reaction (no catalyst). Reaction conditions: 3.0 g/l HEC, 0.5 g/l lignosulfonate, 20 mM H_2O_2, pH 3.0, 45°C. S-8, Nbk. 4201, Pg. 26.

	Hydrogen Peroxide (mM)					
Time (min)	Res.	Dec.	Cons.	pH	Chemi.	Std.
0	---	---	---	3.17	18.41	3.03
2	20.30	0.00	0.00	3.16	12.18	8.63
30	18.87	2.26	-1.13	3.10	39.71	34.91
60	18.97	2.48	-1.45	3.08	11.03	6.35
105	18.48	2.61	-1.09	3.03	23.30	10.50
202	18.90	2.61	-1.51	3.00	19.13	12.93
349	18.60	2.40	-1.00	2.91	13.05	3.67

Table 56. Molecular weight data for reaction S-8 in Table 55.

Time (min)	by HPSEC Mw	Std.	Mn	Std.	Mw/Mn	by Viscometry [η]	Mv	Std.
0	3480	19.1	1842	31.8	1.89	1.274	780,330	77,266
20	657,876	24,426	77,495	4267	8.50	1.143	688,743	12,925
	3,548	112.4	2166	27.6	1.64	—	—	—
30	719,428	35,842	114,600	2668	6.28	0.591	322,416	208
	3,288	18.4	2034	1.4	1.62	—	—	—
60	701,405	19,170	113,104	404	6.21	0.434	226,342	46,398
	3214	46.0	1995	12.7	1.61	—	—	—
105	601,621	41,111	102,932	4578	5.84	0.346	174,038	3374
	2876	14.8	1520	24.8	1.89	—	—	—
202	471,584	31,382	88,018	728	5.36	0.240	114,454	209
	2732	14.8	1383	6.4	1.98	—	—	—
349	394,916	38,293	77,100	586	5.12	0.185	84,755	11,496
	2676	101	1339	22.6	2.00	—	—	—

Table 57. Data for the $FeSO_4$ catalyzed reaction. Reaction conditions: 3.0 g/l HEC, 0.5 g/l lignosulfonate, 20 mM H_2O_2, 0.2 mM $FeSO_4$, pH 3.0, 45°C. S-1, Nbk. 4143, Pg. 179.

Time (min)	Hydrogen Peroxide (mM) Res.	Dec.	Cons.	pH	Chemi.	Std.
0	—	—	—	3.16	9.23	4.59
2	19.98	0.00	0.03	3.09	16.23	13.54
15	17.40	2.12	0.48	3.05	12.42	16.46
29	16.40	2.22	1.38	3.01	32.76	8.78
59	14.83	2.35	2.82	2.98	41.44	17.59
105	13.53	1.98	4.49	2.93	33.18	10.31
174	12.35	0.83	6.82	2.88	70.45	9.97
255	11.15	-0.59	9.44	2.82	78.80	5.68

Table 58. Molecular weight data for reaction S-1 in Table 57.

	by HPSEC					by Viscometry		
Time (min)	Mw	Std.	Mn	Std.	Mw/Mn	[η]	Mv	Std.
0	6,646	—	3,035	—	2.19	1.418	881,846	4,550
2	725,677	—	85,679	—	8.47	0.173	78,767	757
15	444,150	—	34,923	—	12.7	0.066	25,740	1,119
29	308,878	—	28,777	—	10.7	0.047	17,612	—
59	195,765	—	18,629	—	10.5	0.032	11,092	—
105	108,128	—	14,938	—	7.24	0.020	6,547	—
174	62,825	—	11,735	—	5.35	0.016	2,505	3,542
255	38,896	—	9,484	—	4.10	0.010	2,977	211

Table 59. Data for the Fe-EDTA catalyzed reaction. Reaction conditions: 3.0 g/l HEC, 0.5 g/l lignosulfonate, 20 mM H_2O_2, 0.2 mM Fe-EDTA, pH 3.0, 45°C. S-2, Nbk. 4143, Pg. 183.

	Hydrogen Peroxide (mM)					
Time (min)	Res.	Dec.	Cons.	pH	Chemi.	Std.
0	—	—	—	3.20	46.52	9.02
0	—	—	—	3.13	13.14	4.22
2	20.52	0.00	-0.52	3.12	22.96	3.43
26	18.05	2.28	-0.33	3.09	38.03	2.94
50	16.73	2.41	0.87	3.08	44.66	9.12
95	15.18	2.44	2.38	3.04	45.15	7.34
155	13.50	2.18	4.32	3.00	43.94	7.35
240	11.55	1.48	6.97	2.95	49.47	13.68
388	9.62	-0.15	10.53	2.86	38.62	4.35

Table 60. Molecular weight data for reaction S-2 in Table 59.

Time (min)	by HPSEC Mw	Std.	Mn	Std.	Mw/Mn	by Viscometry [η]	Mv	Std.
0	—	—	—	—	—	1.358	839,582	—
2	551,771	—	75,258	—	7.14	0.304	150,418	—
26	399,329	—	52,903	—	7.55	0.106	45,000	—
50	277,972	—	39,013	—	7.13	0.067	26,421	—
95	146,344	—	23,323	—	6.27	0.043	15,751	—
155	85,866	—	18,748	—	4.58	0.027	9369	—
240	58,812	—	14,474	—	4.23	0.018	5595	—
388	27,705	—	10,008	—	2.76	0.005	1449	—

Table 61. Data for the hemoglobin catalyzed reaction. Reaction conditions: 3.0 g/l HEC, 0.5 g/l lignosulfonate, 20 mM H_2O_2, 0.4 g/l hemoglobin, pH 3.0, 45°C. S-12, Nbk. 4201, Pg. 158.

Time (min)	Hydrogen Peroxide (mM) Res.	Dec.	Cons.	pH	Chemi.	Std.
0	—	—	—	6.80	—	—
0	—	—	—	3.16	—	—
2	19.69	0.00	0.00	3.18	—	—
60	18.28	2.00	-0.28	3.06	—	—
121	17.38	1.87	0.75	3.02	—	—
240	16.60	1.70	1.70	2.95	—	—
360	16.28	1.66	2.06	2.89	—	—
477	15.83	1.75	2.42	2.83	—	—

Table 62. Molecular weight data for reaction S-12 in Table 61.

Time (min)	by HPSEC Mw	Std.	Mn	Std.	Mw/Mn	by Viscometry [η]	Mv	Std.
0	4709	12.7	2758	28.3	1.71	1.330	820,249	133,226
	2782	50.2	1830	74.2	1.53	—	—	—
2	2681	184	1532	11.3	1.75	1.020	603,702	433
60	644,640	29,266	74,101	3393	8.70	0.230	108,788	3586
	2144	50	1198	14.1	1.78	—	—	—
121	345,058	20,689	50,308	484	6.86	0.120	51,359	84
	2002	15.6	1120	9.2	1.79	—	—	—
240	415,697	289,611	44,128	6061	9.05	0.068	27,052	931
	2239	25.5	1144	5.7	1.96	—	—	—
360	135,005	24,999	32,444	1060	4.18	0.056	18,852	131
	2344	101	1177	32.5	1.99	—	—	—
477	110,932	—	28,594	—	3.88	0.042	15,534	—
	2406	—	1195	—	2.01	—	—	—

Table 63. Data for the $FeSO_4$ catalyzed reaction. Reaction conditions: 3.0 g/l HEC, 3.0 g/l lignosulfonate, 20 mM H_2O_2, 0.2 mM $FeSO_4$, pH 3.0, 45°C. S-9, Nbk. 4201, Pg. 45.

Time (min)	Hydrogen Peroxide (mM) Res.	Dec.	Cons.	pH	Chemi.	Std.
0	—	—	—	—	—	—
0	—	—	—	3.23	46.47	5.43
2	17.30	0.00	0.00	3.21	45.92	1.35
20	13.65	2.89	3.46	3.09	51.05	10.62
45	10.80	3.44	5.76	3.00	48.53	2.83
80	8.05	3.63	8.32	2.93	59.72	29.06
135	5.60	4.19	10.21	2.86	64.20	7.79
240	2.83	3.79	13.38	2.78	54.72	14.84

Table 64. Molecular weight data for reaction S-9 in Table 63.

Time (min)	by HPSEC Mw	Std.	Mn	Std.	Mw/Mn	[η]	by Viscometry Mv	Std.
0	—	—	—	—	—	—	—	—
0	—	—	—	—	—	—	—	—
2	—	—	—	—	—	—	—	—
60	—	—	—	—	—	—	—	—
121	—	—	—	—	—	—	—	—
240	—	—	—	—	—	—	—	—
360	—	—	—	—	—	—	—	—
477	—	—	—	—	—	—	—	—

Table 65. Data for the $FeSO_4$ catalyzed reaction. Reaction conditions: 0.2 g/l HEC, 0.5 g/l lignosulfonate, 20 mM H_2O_2, 0.2 mM $FeSO_4$, pH 3.0, 45°C. S-7, Nbk. 4201, Pg. 21.

Time (min)	Hydrogen Peroxide (mM) Res.	Dec.	Cons.	pH	Chemi.	Std.
0	—	—	—	3.18	—	—
0	—	—	—	3.17	36.50	4.19
2	17.33	0.00	0.00	3.09	115.03	12.48
20	14.20	2.52	3.28	2.98	352.57	19.63
41	15.50	2.83	4.67	2.88	336.71	17.42
70	10.40	3.28	6.32	2.80	298.59	13.02

Table 66. Molecular weight data for reaction S-7 in Table 65.

Time (min)	by HPSEC Mw	Std.	Mn	Std.	Mw/Mn	by Viscometry [η]	Mv	Std.
0	---	---	---	---	---	---	---	---
0	---	---	---	---	---	---	---	---
2	---	---	---	---	---	---	---	---
60	---	---	---	---	---	---	---	---
121	---	---	---	---	---	---	---	---
240	---	---	---	---	---	---	---	---
360	---	---	---	---	---	---	---	---
477	---	---	---	---	---	---	---	---

Table 67. Data for the control reaction at elevated pH. Reaction conditions: 3.0 g/l HEC, 0.5 g/l lignosulfonate, 20 mM H_2O_2, pH 11.0, 45°C. S-13, Nbk. 4201, Pg. 179.

Time (min)	Hydrogen Peroxide (mM) Res.	Dec.	Cons.	pH	Chemi.	Molecular Weight by HPSEC Mw	Mn	Mw/Mn
0	---	---	---	11.15	---	---	---	---
0	---	---	---	11.00	---	---	---	---
1	16.50	---	---	10.65	---	---	---	---
15	14.77	---	---	10.38	---	---	---	---
40	13.33	---	---	10.30	---	---	---	---
60	12.33	---	---	10.33	---	---	---	---
120	8.50	---	---	10.28	---	---	---	---
180	5.73	---	---	10.40	---	---	---	---

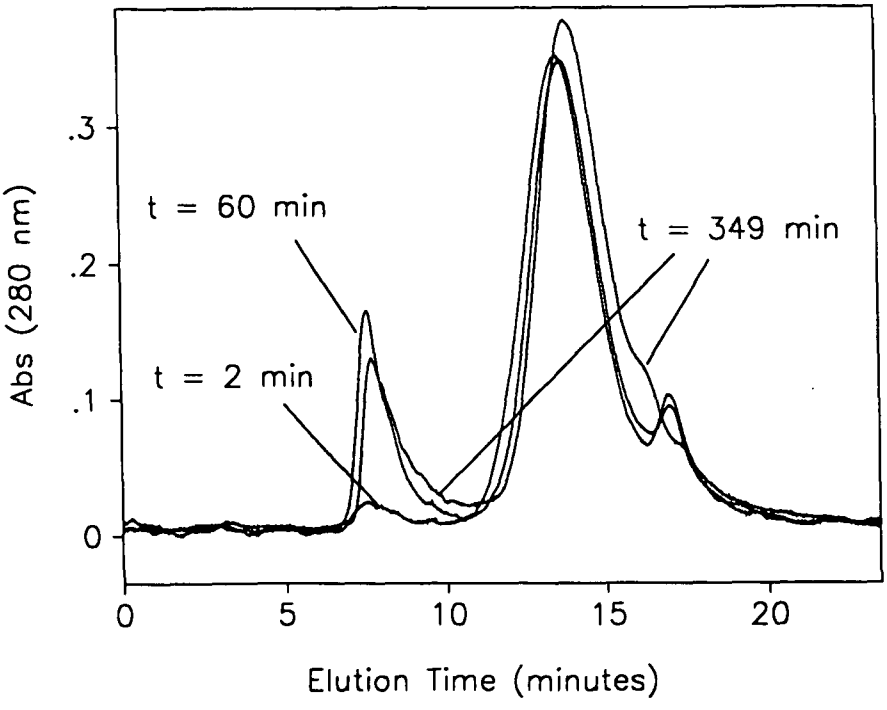

Figure 94. HPSEC profiles of reaction samples taken from the control reaction. S-8. Reaction conditions: 3.0 g/l HEC, 0.5 g/l lignosulfonate, 20 mM H_2O_2, pH 3.0 and 45°C.

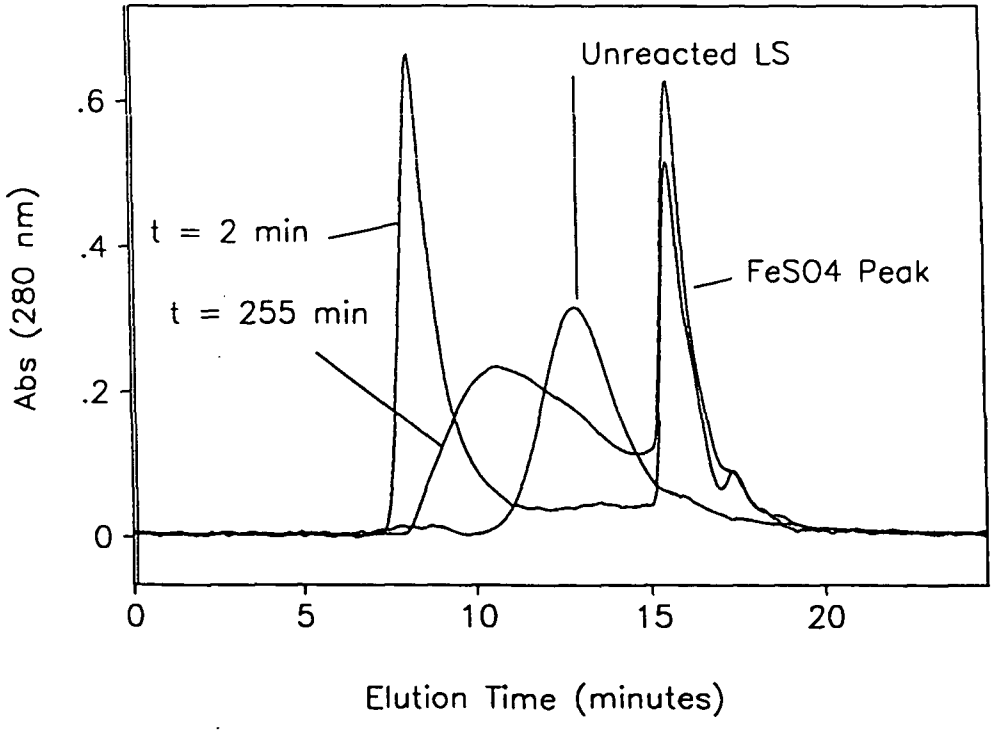

Figure 95. HPSEC profiles of reaction samples taken from the $FeSO_4$ catalyzed reaction. S-1. Reaction conditions: 3.0 g/l HEC, 0.5 g/l lignosulfonate, 20 mM H_2O_2, 0.2 mM $FeSO_4$, pH 3.0 and 45°C.

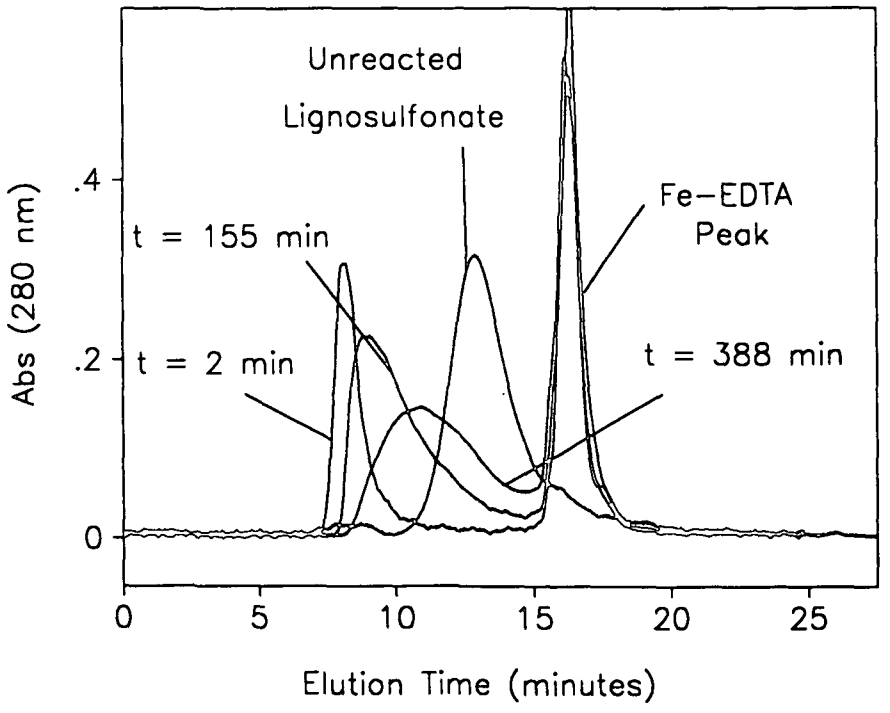

Figure 96. HPSEC profiles of reaction samples taken from the Fe-EDTA catalyzed reaction. S-2. Reaction conditions: 3.0 g/l HEC, 0.5 g/l lignosulfonate, 20 mM H_2O_2, 0.2 mM Fe-EDTA, pH 3.0 and 45°C.

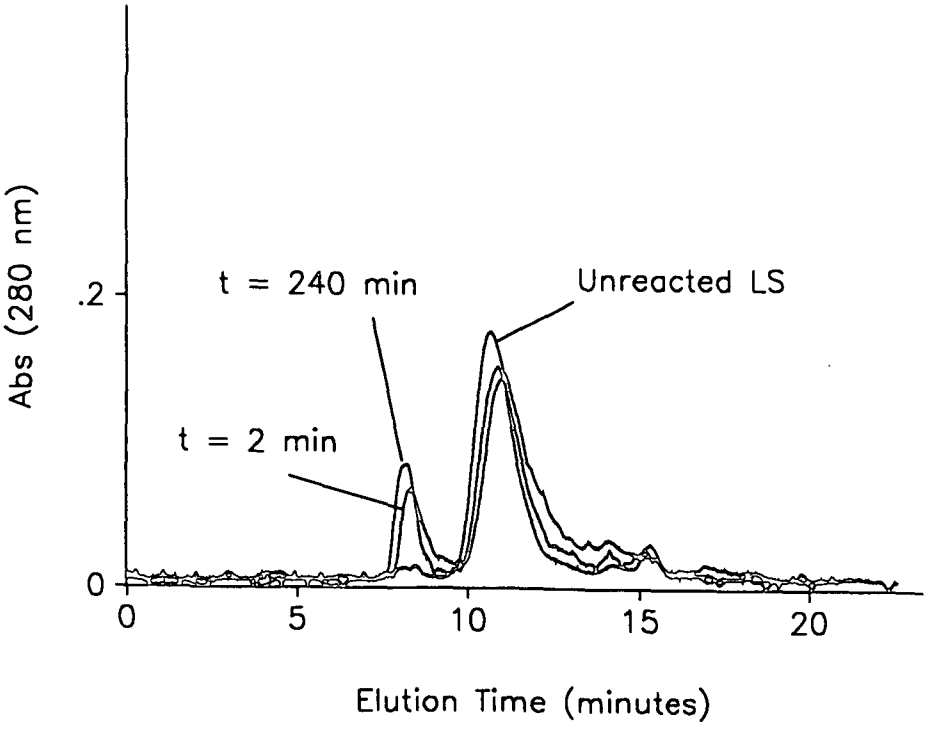

Figure 97. HPSEC profiles of reaction samples taken from the hemoglobin catalyzed reaction. S-12. Reaction conditions: 3.0 g/l HEC, 0.5 g/l lignosulfonate, 20 mM H_2O_2, 0.4 g/l hemoglobin, pH 3.0 and 45°C.

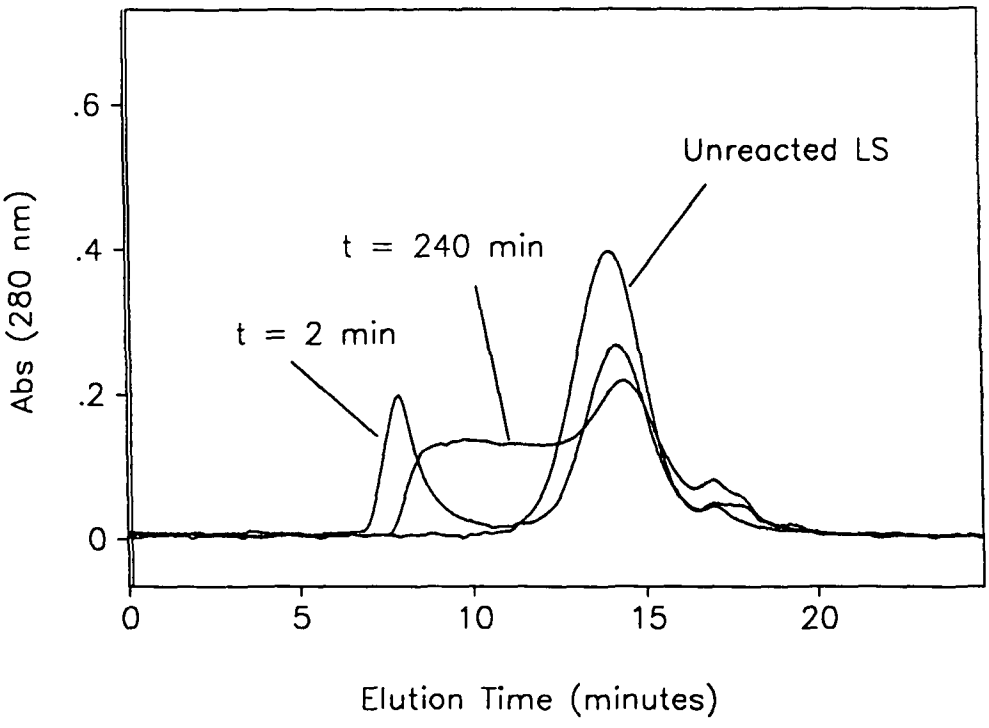

Figure 98. HPSEC profiles of reaction samples taken from the $FeSO_4$ catalyzed reaction. S-9. Reaction conditions: 3.0 g/l HEC, 3.0 g/l lignosulfonate, 20 mM H_2O_2, 0.2 mM $FeSO_4$, pH 3.0 and 45°C.

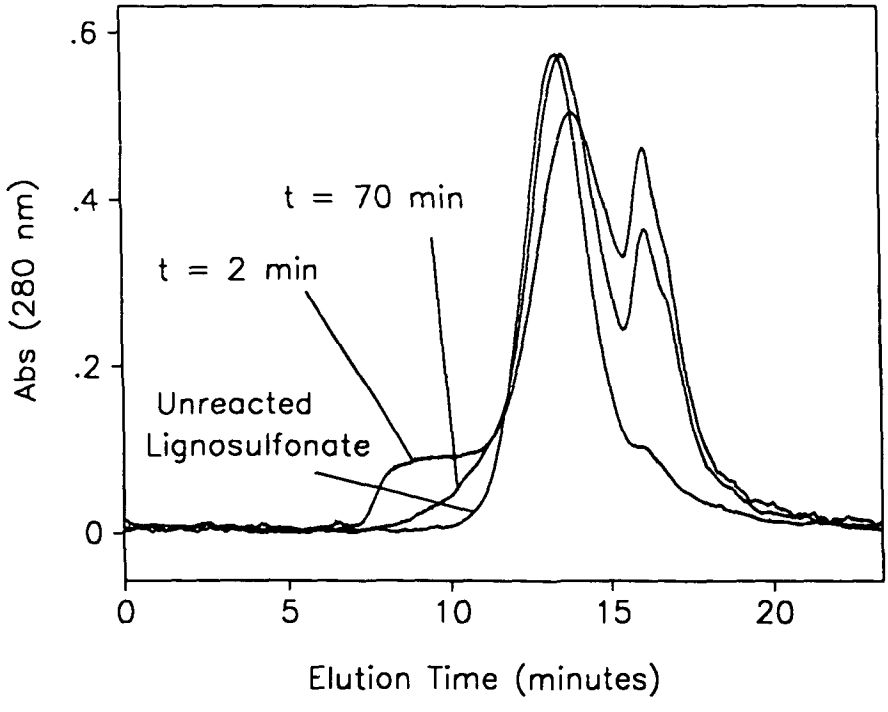

Figure 99. HPSEC profiles of reaction samples taken from the $FeSO_4$ catalyzed reaction. S-7. Reaction conditions: 0.2 g/l HEC, 0.5 g/l lignosulfonate, 20 mM H_2O_2, 0.4 g/l hemoglobin, pH 3.0 and 45°C.

APPENDIX VII

RESULTS FROM THE CHEMILUMINESCENCE ASSAY FOR THE HEMOGLOBIN CATALYZED EXPERIMENTS

Unfortunately, as noted by Reitberger and Gierer, the hemoglobin present in reaction samples interferes with the chemiluminescence assay. Figure 100 shows the chemiluminescent yield obtained from several samples taken from the hemoglobin catalyzed reaction.

The first sample, with lignosulfonate (LS) alone, was taken prior to addition of the hemoglobin to the reaction solution. The next sample, taken after hemoglobin was added to the reactor, shows a large chemiluminescent yield. As no hydroxyl radicals have been generated in the reaction solution, as hydrogen peroxide has not been added, this value is misleading. The next sample was taken 1 minute after the reaction was initiated by the addition of hydrogen peroxide. The large confidence limits of this sample are a result of the chemiluminescent yield decreasing with time. This is not typical of samples prepared for the chemiluminescence assay. The reason for the decay present in this sample may be due to the destruction of hemoglobin from the additional hydrogen peroxide present in the sample preparation.

The chemiluminescent yields obtained for the hemoglobin catalyzed degradation of lignosulfonate are therefore questionable. However, the chemiluminescent yields from the entire reaction are shown in Figure 101. After the initial increase, which is documented in detail in Figure 100, there is no substantial increase in the chemiluminescent yield during the entire reaction. The value obtained from 30 minutes onward is barely greater than the initial value.

Chemiluminescence data obtained from reactions with hemoglobin and HEC are shown in Figure 102. Data for both the 20 and 40 mM H_2O_2 reactions are shown.

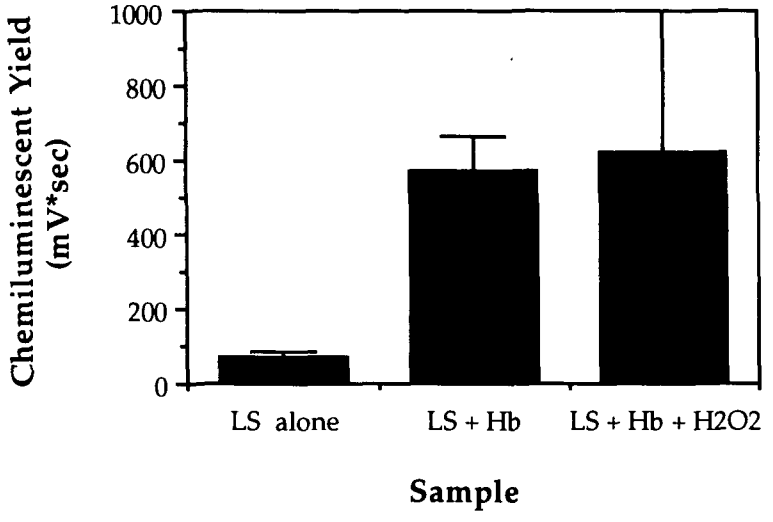

Figure 100. Chemiluminescent yields for three samples from the hemoglobin catalyzed reaction.

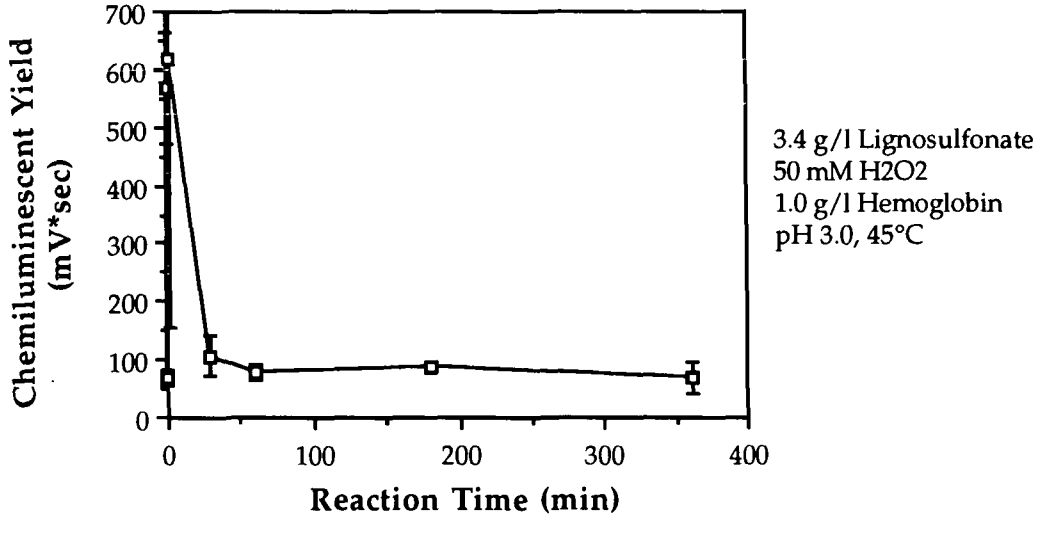

Figure 101. Chemiluminescent yield versus reaction time for the hemoglobin catalyzed reaction.

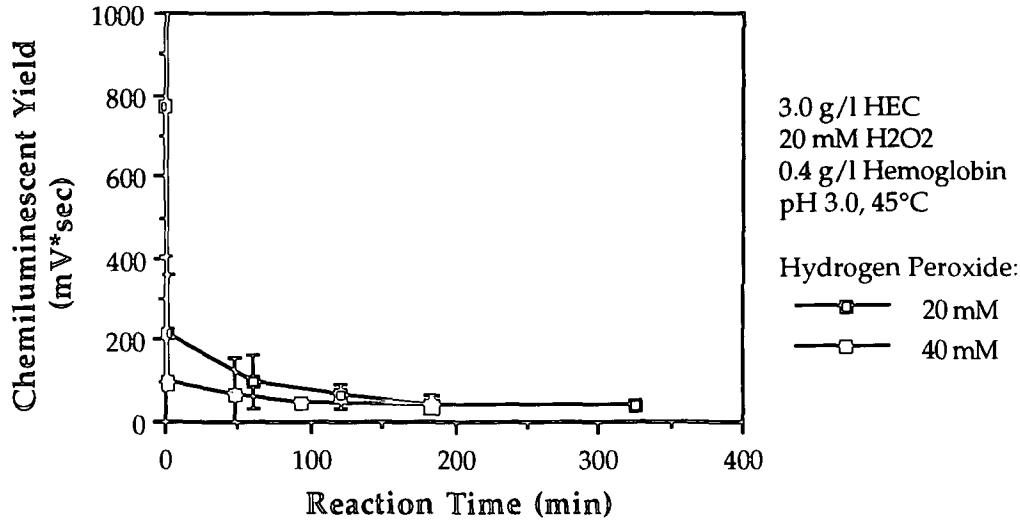

Figure 102. Chemiluminescence versus reaction time for the hemoglobin catalyzed degradation of HEC at 20 and 40 mM hydrogen peroxide.

APPENDIX VIII

PULP EXPERIMENTS

A comparison of the rate laws for lignosulfonate and HEC for their dependence on hydrogen peroxide indicated that at higher concentrations of hydrogen peroxide, the selectivity favored lignosulfonate degradation over HEC degradation. This was evident because the lignosulfonate rate laws exhibited a greater dependence on hydrogen peroxide concentration than those for HEC. This is true as long as the hydrogen peroxide concentration remains above the critical value, listed in Table 7 (usually 40 mM).

To verify these findings, pulp bleaching experiments were designed in which two concentrations of hydrogen peroxide were used. By measuring kappa number reductions (lignin degradation/removal) and viscosity (cellulose degradation) for these pulps, values for selectivity can be obtained.

Pulp bleaching was performed using reaction conditions similar to those used above for the model system. For the model system, two different concentrations of iron were used. These concentration (0.062 mM and 0.5 mM) correspond to 0.1 and 0.8 % of iron on lignin (or lignosulfonate), respectively.

Pulp bleaching was performed on an oxygen bleached softwood kraft pulp, starting Kappa = 15.7. After a chelation stage, 25 od grams of pulp were used to determine optimum conditions. The 0.8% iron on lignin caused too much hemoglobin to be present. This interfered with the Kappa number determination. Consequently, bleaching was done using the 0.1 % on lignin ratio. Results from a 24 hour bleach using two peroxide charges are shown in Table 68.

As the peroxide charge is increased from 2.0 to 4.0 %, the kappa number is reduced for the control and $FeSO_4$ treatments. The kappa number remains nearly the same for the

Fe-EDTA treatment, and it increases for the hemoglobin treatment. For this same increase in peroxide charge, a decrease in the viscosity is seen for only the control reaction.

Values for the selectivity of these treatments are shown in Table 69. Selectivities were determined by dividing the drop in kappa number by the decrease in viscosity. The $FeSO_4$ treatment is the only one which shows an increase in selectivity as the hydrogen peroxide charge is increased. For the control, Fe-EDTA and hemoglobin treatments, as the peroxide charge was increased, selectivity decreased. These results do not agree with those obtained in the model system.

These results are interesting, but additional work on the selectivity of hydroxyl radical-generating bleaching systems is needed. These experiments with pulp partially agree with the results obtained using the model system.

Table 68. Kappa numbers from hydrogen peroxide bleached pulp with the three catalysts. Bleaching conditions: 10% consistency, 2% H_2O_2, 0.1% Fe on lignin, 55°C for 24 hours. Starting Kappa = 15.7, Viscosity 19.0

CATALYST	H_2O_2 CHARGE (%)	VISCOSITY	KAPPA NUMBER
Control	2.0	13.2	13.6 ± 0.4
	4.0	8.9	12.6 ± 1.8
$FeSO_4$	2.0	4.3	12.0 ± 0.1
	4.0	4.7	11.3 ± 1.4
Fe-EDTA	2.0	4.0	12.4 ± 0.2
	4.0	5.0	12.8 ± 0.2
Hemoglobin	2.0	4.9	13.7 ± 0.1
	4.0	6.7	14.5 ± 0.3

Table 69. Selectivity (Δ kappa / Δ viscosity) of the three catalysts at two different hydrogen peroxide charges. Bleaching conditions are as stated in Table 68.

CATALYST	H_2O_2 CHARGE (%)	SELECTIVITY
Control	2.0	0.36
	4.0	0.31
$FeSO_4$	2.0	0.25
	4.0	0.31
Fe-EDTA	2.0	0.22
	4.0	0.21
Hemoglobin	2.0	0.14
	4.0	0.10